
UNIVERSITY OF
BIRMINGHAM

# PROTEIN EXTRACTION DURING SOYBASE PRODUCTION

## Enhancing yields using cavitational techniques

By

Katherine Elizabeth Preece

A thesis submitted to
The University of Birmingham
for the degree of
DOCTOR OF ENGINEERING

Department of Chemical Engineering
College of Physical and Engineering Sciences
The University of Birmingham
30th September 2016

# ABSTRACT

Soy-based products offers a dairy alternative for those seeking a healthier diet, suffering with lactose intolerance or those who simply enjoy the taste. The soybean offers a high concentration of complete protein. Soybase is the aqueous extract typically produced directly from whole soybeans. Milling disrupts cells and intracellular components become available for extraction. During separation, a high amount of the waste stream (okara) is produced, typically containing 80% moisture and a considerable fraction of protein. A novel extraction model is presented in this thesis that highlights this role of okara for the first time.

It is desirable to extract as much as possible from the raw material for sustainable processing. Primarily in this thesis, a microstructural assessment of the soybean processing materials, including an investigation of thermal processing identified the restraints of protein in more detail. Using confocal laser scanning microscopy (CLSM), various features of soy slurry, soybase and okara were localised within soybean processing materials that have not been previously reported. Oil, protein and intact cells were observed, in addition to aggregated protein bodies within the thermally treated samples (80 °C) located in the continuous phase and within intact cells. These findings are vital for identifying processing technologies for process intensification.

Ultrasound-assisted extraction (UAE) has been widely applied in lab-scale studies for the food industry. Ultrasound provides intensification via cavitational effects; imploding vapour cavities in a liquid result in increased mass transfer and cell disruption. During soybean processing at lab-scale, ultrasound improved oil, protein and solids extraction yields during slurry and okara treatment. Particle size data and CLSM confirmed that ultrasonic treatment disrupted aggregated protein outside of intact cells. Not only solubility was affected by ultrasound; separation efficiency was also slightly improved and effects were observed after 30 seconds of treatment. Once promising results were obtained at lab-scale, a pilot-scale study was performed to assess its scale-up potential. UAE significantly increased protein extraction from okara solution during pilot-scale studies; however, slurry treatment was unfeasible at this larger scale. Okara solution flow rate and okara concentration also significantly influenced the protein extraction yield. However, these improvements were limited in comparison to the lab-scale probe system. Considering the total extraction yield from the soybean, ultrasound was not considered effective for industrial examination.

High pressure homogenisation (HPH) offers an alternative to ultrasound, also based on cavitation phenomena. HPH (75-125 MPa) was applied at lab-scale to slurry and okara solution obtained from pilot scale with substantial increases in extraction yields. Reductions in particle sizes and CLSM confirmed the disruption of intact cells, providing protein that is more available. In comparison to ultrasound, HPH offers a better extraction assistance that should be explored at pilot-scale.

The results presented in this thesis provides the reader with an overview of challenges faced during aqueous protein extraction from soybeans, and offers potential routes for process intensification. It provides insights for other (plant protein) extraction processes with a considerable fraction of their desired component within the waste stream.

# ACKNOWLEDGEMENTS

During the course of my EngD project, I have experienced many new and exciting ventures in life and these would not have been possible without the help and support of the people around me. I have learnt many new skills and gained knowledge in areas much broader than just soy… I would like to take this opportunity to thank those people involved in my project, and for those who played a role in my personal life.

I would like to thank my academic supervisors Peter Fryer, Richard Greenwood and Phil Cox for their guidance and support during this project. I would especially like to thank Clive Marshman for his input in this project, including the tests on the structural composition of typical Dutch windmills and good wines. Thanks for the motivation, words of encouragement and tips for surviving in the Netherlands.

I would also like to thank those people at home, family and friends, who supported me during this chapter of my life. I have to thank my mum and dad for making me who I am today. Thank you Mum for supporting me; I am glad you were able to use FaceTime, mostly perfectly! An extra special thanks to my little brother, James, for offering words of encouragement when times were difficult and looking after things at home! A special mention to my extended family too! Thank you for those of you who we able to visit me during my time in Rotterdam: Ben, Grace, Harriet, Liz, Katie & co. and Nick. I know how easy it is to lose contact with friends, especially when some distance comes in between. I love how we cannot speak for several weeks, and then can pick up where things left off as if it were yesterday. A special mention to Grace Smith who also knows the struggles of the PhD life!

Having spent more than three years based in the Netherlands, I have enjoyed many experiences with this country, both in and outside of Unilever Research & Development Vlaardingen, as well as learning some of the Dutch language. Ik zou graag mijn industriële leidinggevende Ardjan Krijgsman en mijn dagelijkse begeleiders Klaas-Jan Zuidam en Nasim Hooshyar. Ik ben jullie dankbaar voor jullie bijdrage voor dit project, zonder jullie was het absoluut niet mogelijk om dit project te doen. Ik hoop dat dit project je geen ranzige smaak van soya achterlaat!

I cannot forget to thank the Vitality Runners Vlaardingen members for dragging me out of the office during unproductive moments and giving me a new expression to live life by: geen smoesjes! I am physically and mentally stronger as a result, and I must give a special mention to Kees and Randi.

Finally, I would like to thank those who I met in the Netherlands and put up with me! The many interns who stopped by in Unilever and the Labtap; I have many memories to cherish! A special mention to Francisco, Juliën and Viviana for keeping me sane throughout my time in Vlaardingen; a shoulder to cry on or a McDonalds was always available, when necessary! Last, but not least, the root to my tree, my moppie, Martin. Thank you for many happy times together. Here's to the next chapter!

# TABLE OF CONTENTS

# LIST OF FIGURES

# LIST OF TABLES

# NOMENCLATURE

## ABBREVIATIONS

| | |
|---|---|
| A | Artefacts |
| AFM | Atomic force microscopy |
| AM | Agglomerated material |
| ANOVA | Analysis of variance |
| CCD | Central composite design |
| CLSM | Confocal laser scanning microscopy |
| CW | Cell wall material |
| d.b. | Dry basis |
| EDX | Energy dispersive X-ray spectroscopy |
| HPH | High pressure homogenisation |
| ICC | Intact cotyledon cells |
| LOX | Lipoxygenase |
| $NaHCO_3$ | Sodium bicarbonate |
| OB | Oil bodies |
| PA | Phytic acid |
| PB | Protein bodies |
| PSD | Particle size distribution |
| R&D | Research & Development |
| RSM | Response surface methodology |
| SEM | Scanning electron microscopy |
| SPC | Soy protein concentrate |
| SPI | Soy protein isolate |
| TEM | Transmission electron microscopy |
| UAE | Ultrasound-assisted extraction |
| USLP | Unilever Sustainable Living Plan |
| w.b. | Wet basis |
| w/w | Weight per weight |

| | |
|---|---|
| w/v | Weight per volume |

## SYMBOLS

| | |
|---|---|
| $A$ | Cross-sectional area of the pipe |
| HPH | High pressure homogenisation |
| I | Primary extraction |
| II | Secondary extraction (Okara treatment) |
| $d$ | Particle diameter |
| $D_H$ | Hydraulic diameter of the pipe |
| $L$ | Liquid mass |
| $L_\infty$ | Total mass of liquid at the end of the extraction |
| $\eta$ | Kinematic viscosity |
| $O$ | Okara mass |
| $\rho_s$ | Particle density |
| $\rho_l$ | Liquid density |
| $Q$ | Volumetric flow rate |
| $Re$ | Reynolds number |
| $r_i$ | Radius of particle size $i$ |
| $r$ | Radial position of the particle |
| $S$ | Soybase mass |
| $S_\infty$ | Total mass of solid at the end of the extraction |
| $Slu$ | Slurry mass |
| $Sol$ | Solid mass |
| $v$ | Kinematic viscosity |
| $v_c$ | Sedimentation velocity in a centrifuge |
| $V_{I,i}$ | Volume of intact core of particles of size $i$ |
| $\omega$ | Angular viscosity of the rotor |
| $W$ | Water mass |

| | | |
|---|---|---|
| Y I | Primary extraction yield | |
| Y II | Secondary extraction yield, resulting from okara treatment | |
| $x_i$ | Mass fraction of component i | |
| $x_{i,j}$ | Mass fraction of component i in stream j | |
| i | o | Oil |
| | p | Protein |
| | s | Solids |
| | w | Water |
| j | S | Soybase |
| | O | Okara |

# CHAPTER 1

# INTRODUCTION AND BACKGROUND

## 1.1 BACKGROUND OF THESIS

Unilever is a British-Dutch multinational fast moving consumer goods company with an annual turnover of €53.3 billion in 2015 (Unilever Communications, 2015). The product portfolio of Unilever is vast, with more than 400 brands distributed to consumers all over the world. Every day, 2 billion people use Unilever products around the world, with some 13 brands responsible for sales of more than €1 billion each per year. Unilever's products are categorised into the following four sectors:

- Foods, e.g. savoury, cooking and spreads (margarine);
- Refreshments, i.e. ice cream, tea and soy beverages;
- Home Care, such as laundry, machine dish wash and house hold cleaning products;
- Personal Care, like shampoos, deodorants and skin or hand wash products.

The core to Unilever's business model focuses on sustainability whilst doubling the financial turnover, introduced by Chief Executive Officer (CEO) Paul Polman. Profitable growth should also be responsible growth. The business model is driven by the Unilever Sustainable Living Plan (USLP), which contains the following missions: improve health and well-being, reduce environmental impact and to enhance livelihoods through various targets. The focus on sustainability and on brands with a purpose has led to sales growth, showing that consumers support a business with an interest in the future generations.

Unilever's Refreshments sector was responsible for a turnover of €10.1 billion in 2015 (Unilever Communications, 2015), received from sales of ice cream and tea products from well-known brands such as Ben & Jerry's, PG tips and Wall's Ice Cream. One target attributed to the USLP is

that Unilever will be 'carbon positive' by 2030. This means all energy used across their operations will come from renewable sources and surplus will be available for externals. Sustainable sourcing of raw materials is also part of the USLP. Aims for responsible sourcing in the Refreshment category include tea to be 100% sustainably sourced by 2020 and Fairtrade status for Ben & Jerry's products. Ben & Jerry's has already been granted its status (January 2015), which ensures farmers receive a fair price and working standards (Unilever Sustainable Business & Communications, 2016).

Another Unilever brand in the refreshment category that supports the USLP through the sustainable sourcing of materials is AdeS, a soy-based drink brand manufactured and sold in Latin America. All soybeans used for soy beverages are now sustainably sourced (granted in 2015 by the Round Table for Responsible Soy). AdeS products range from soymilk to various soy-based fruit juices; a typical range of products can be seen in Figure 1.1. Soy protein is desirable to add to the diet as it is considered as a complete protein, meaning it contains all the essential amino acids, aiding to improve the health of consumers. Soymilk has a particular taste; therefore, the addition of fruit juice masks the beany flavour for those who want to increase their protein intake. AdeS sold 56.2 million unit cases of beverages during the year 2015 which equated to a net revenue of $284 million (Coca-Cola Journey Staff, 2016).


Figure 1.1. Example products of AdeS, the market leader of soy-based beverages in Latin America (Coca-Cola Journey Staff, 2016).

There is an increasing consumer trend to strive for a healthy diet and lifestyle, as well as a rising number of people with a lactose intolerance, with e.g. 50 to 80% of Latinos and 95 to 100% of Asians believed to lack a sufficient level of the enzyme lactase (Swagerty *et al.*, 2002). This has led to a welcomed increase in the desire for natural, health-promoting dairy alternatives. For example, in Europe the company Alpro offer a range of beverages, desserts, margarines, yoghurt and cream alternatives from plant-based sources. Firstly, these were only soy-based products but now also almond, hazelnut, coconut, rice, oat and cashew products are available from Alpro. Companies have to follow this consumer-driven trend for healthier products in order to remain a key competitor in the market. The recent acquisition of Alpro's mother company WhiteWave by the French dairy and water giant Danone highlights this trend to move towards dairy alternatives (Danone Press Release, 2016).

The Coca-Cola Company is well known for its carbonated soft drinks range, including products such as Coca-Cola, Sprite and Fanta. However, a shift towards a healthier product portfolio has

commenced. The Coca-Cola Company and Coca-Cola FEMSA recently acquired the AdeS brand for $575 million, announced June 2016 (Unilever Press Release, 2016). This is a further diversity push for the well-known fizzy drink giant towards a healthier product portfolio with juices, bottled water, teas and other plant-based beverages. This venture may provide the AdeS brand with access to new markets and distribution lines already part of the Coca-Cola Company in Asia and even Brazil.

The first generation of dairy alternatives has been led by soybean derivatives, such as soymilk and tofu. Production of these products initially involves the extraction of protein and other desirable components, such as oil and isoflavones, to provide an aqueous extract called soybase. Additional ingredients are then added to the soybase, such as sugars, flavours and gums, to prepare soymilk or coagulating agents for tofu production. The extraction includes the mechanical disruption of the soybeans in water, typically at an alkali pH to enhance protein extraction yield. Elevated temperatures aid with the solubilisation of protein and other components and in the inactivation of lipoxygenase and trypsin inhibitors, which cause detrimental effects to the final product. After milling, the soy slurry is fed to a separation unit, where insoluble materials are separated from soybase. The insoluble fibrous by-product is typically referred to as okara, and is mainly utilised as animal feed. Figure 1.2 shows a typical extraction process for the production of soybase, the precursor for soymilk and tofu production.

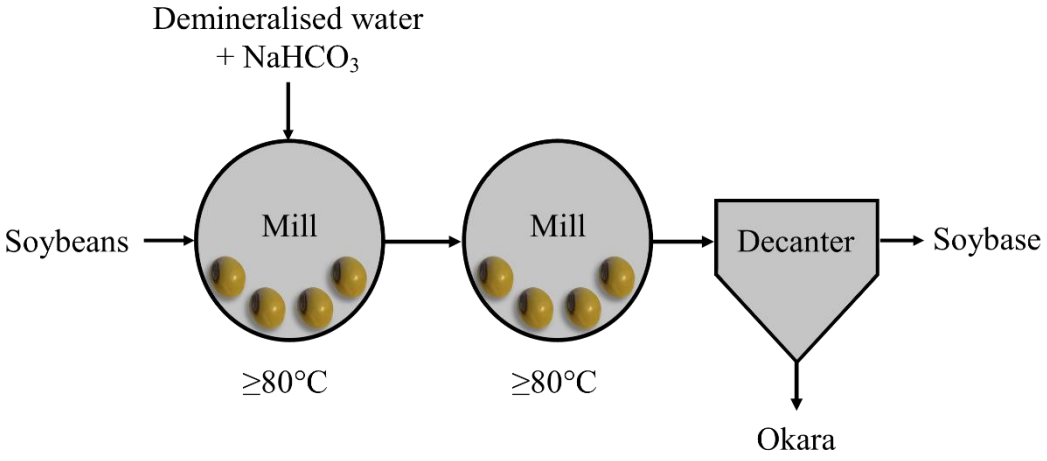


Figure 1.2. Typical aqueous extraction of water-soluble components from soybeans.

During current production processes, the okara stream contains a considerable amount of protein and other desirable components. It has been found that 30% or more of total protein found within the soybean ends up in the waste stream (Ma *et al.*, 1996). In terms of sustainability, this has an environmental impact; extracting more of the valuable and health promoting components from soybeans would reduce the amount of raw materials for a given unit of product. This will become increasingly necessary with the ever-increasing human population; we will need to do more with less, to ensure a nutritionally balanced diet is available for all. There is also a financial initiative for business, such as Unilever, to reduce production costs.

There are a few possibilities for enhancing the protein extraction yield directly from soybeans. A number of parameters influence the extraction of protein from soybeans, such as particle size and temperature, and these will be discussed in detail in the following chapter. These processing parameters are commonly a compromise between reducing the effects of anti-nutritional factors and achieving the greatest extraction yield of protein. The process has already been extensively optimised using the current unit operations for milling and separation. Therefore, to improve

extraction yields further, the addition of a new processing technology is required. This can be approached by gaining a superior understanding of the microstructure of the soybean during processing. There has been some investigations previously that deal with the exploration of the microstructure of soybeans (Rosenthal *et al.*, 1998; Campbell & Glatz, 2009). Gathering information on the processing materials can also provide useful information on the localisation of components of interest, such as protein in this instance. However, this has not been reported. With knowledge of the physical constraints, a new technology can be chosen which enhances the disruption of the raw materials microstructure to aid the extraction of protein and other health promoting factors. The aim is to manage improving protein yields without increasing the extraction of off-flavours and anti-nutritional components to an undesirable level.

The insights presented in this thesis focus on extraction directly from soybeans; this information is also useful for other plant-based protein extraction processes. In recent years, different sources such as oat, almond, lupin and pea have begun entering the market as milk alternatives (Sethi *et al.*, 2016). Many other extraction systems will also find this thesis of great importance when dealing with a high concentration of desirable component within the waste stream.

## 1.2 OBJECTIVES OF THESIS

The objective of this work was initially to gain a fundamental understanding of the current soybase production limitations, particularly by examining the microstructure of soybean processing materials. With this information, innovative processing technologies for enhancing the extraction of protein and other health promoting factors were identified and evaluated for implementation, including pilot-scale studies.

## 1.3 THESIS OUTLINE

Each chapter of this thesis is based on a publication in a peer-reviewed journal; therefore, some overlap in the text is present. The details of the publication are located on the front page of each chapter. **Chapter 2** of this thesis gives a review of the literature in the area of soybean processing, more specifically soy protein extraction from whole soybeans. The important processing parameters for extraction of protein have been described, as well as a new model highlighting okara as the main factor in yield loss. This chapter was adapted from the journal publication of Preece *et al.* (2016).

Localisation of protein and other nutritive components are detailed in **chapter 3**. Confocal laser scanning microscopy (CLSM) was employed to visualise features within soybean processing materials that had not been seen previously within the literature (Figure 1.3 is one such example). This information is vital for improving current protein extraction processes, and elucidate why the protein yield was higher when processed at room temperature than at 80 °C. This chapter was based on a publication in a peer-reviewed journal by Preece *et al.* (2015).

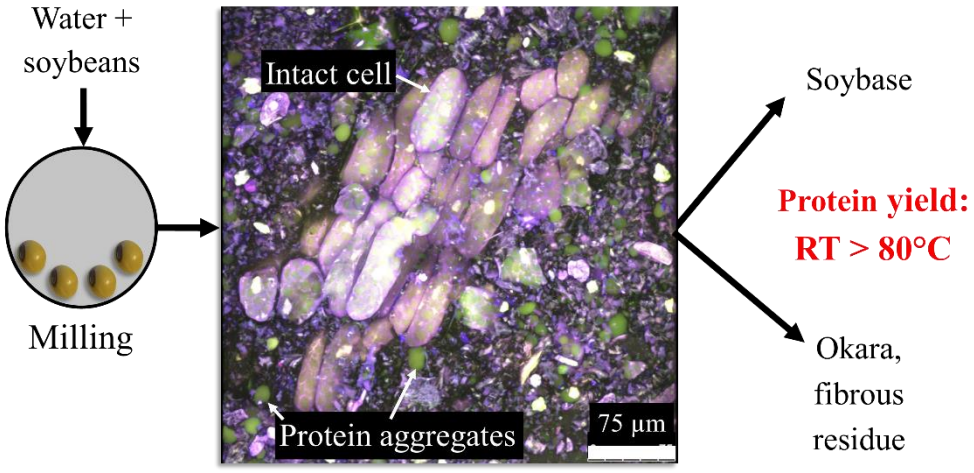


Figure 1.3. Graphical representation of contents of **chapter 3.**

**Chapter 4** introduces a technology at lab-scale that aids in the solubilisation of aggregated protein located in the continuous phase of soy slurry. This chapter includes the use of CLSM to provide information of the microstructure of ultrasound-assisted extracted materials, and those without treatment (see Figure 1.4). Other techniques for analysis were employed to calculate extraction yields, availability of protein and separation efficiencies and to measure particle size distributions. The chapter has been published in a journal by Preece *et al.* (2017b).

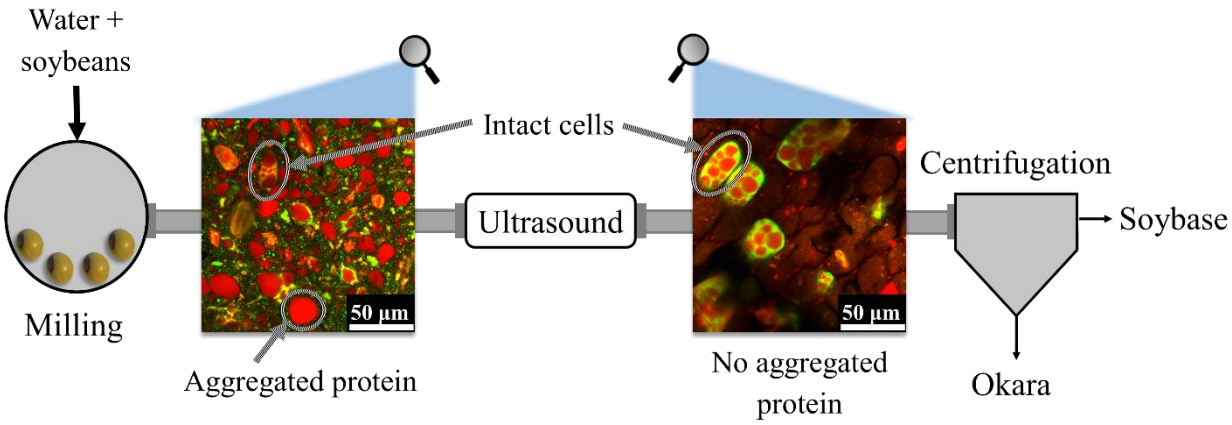


Figure 1.4. Graphical representation of the main content of **chapter 4.**

Once the effects had been studied at lab-scale, a comparison to a pilot-scale probe system was made in **chapter 5** (see also Figure 1.5). In this chapter, a response surface methodology was employed to study the effects of temperature, okara concentration and okara solution flow rate through the ultrasonic field for comparison to a control sample (without ultrasonic treatment). In contrast to lab-scale, ultrasound treatment of slurry was found to be infeasible at pilot scale. This chapter has been published in a peer-reviewed journal by Preece *et al.* (2017c).

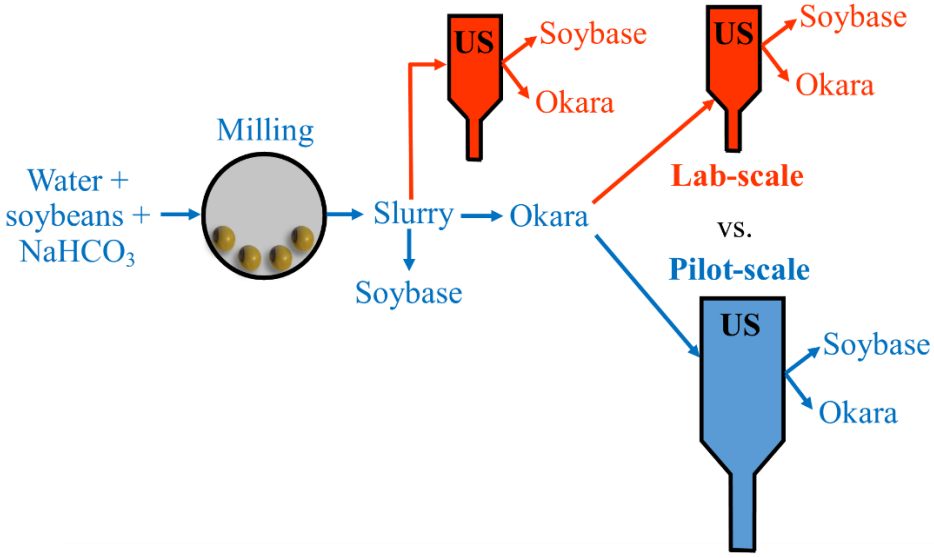


Figure 1.5. Pictorial representation of the content of **chapter 5.**

Another technology based on the phenomena of cavitation, is high pressure homogenisation (HPH). Hydrodynamic cavitation is a technique widely employed at industrial scale for the production of fine emulsions. **Chapter 6** investigates the application of HPH as an aid for extraction during soybase production (see Figure 1.6). A comparison to ultrasound-assisted extraction is made in this investigation. Work from this chapter has been published peer-reviewed journal by Preece *et al.* (2017a).

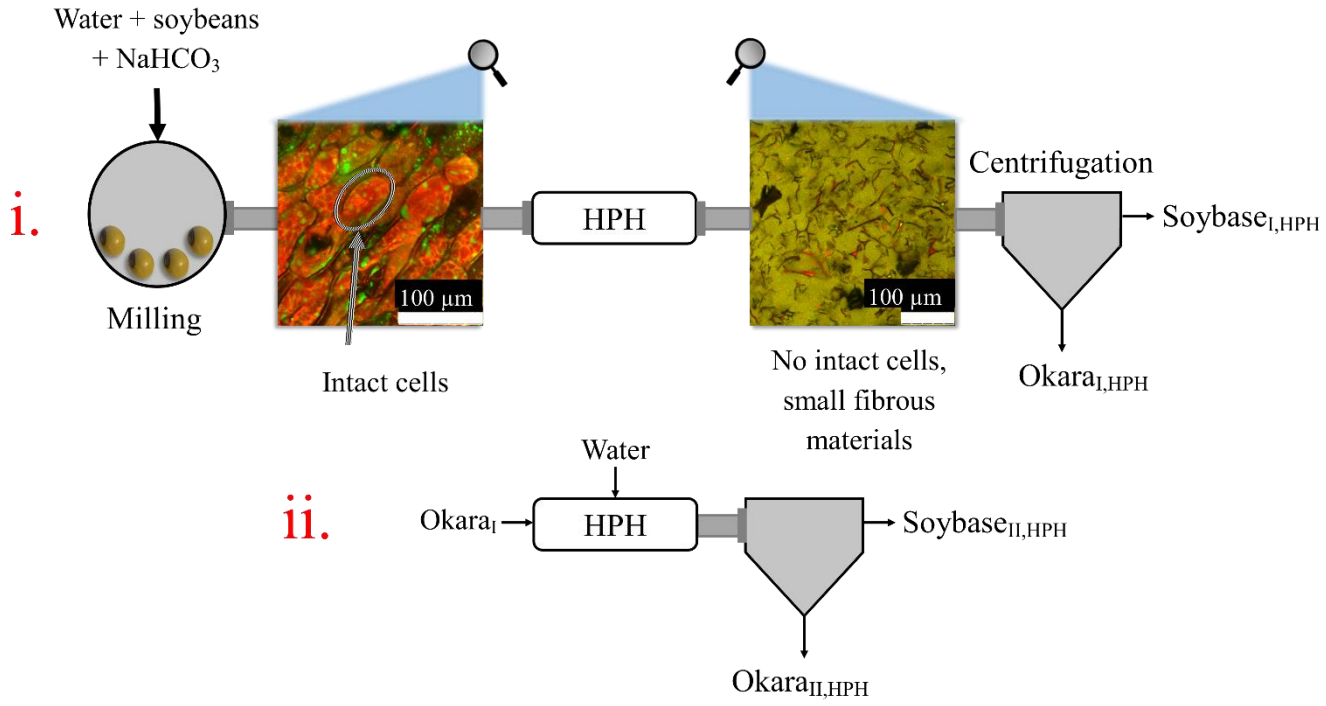


Figure 1.6. Summary of high pressure homogeniser (HPH) treatments on soy slurry and okara solution samples.

**Chapter 7** presents overall conclusions and suggested recommendations for future work.

## 1.4 CONTRIBUTION OF CO-AUTHORS AND ANALYTICAL SUPPORT

Research presented within this thesis was performed and written by the main author, Katherine Preece. This thesis includes the main authors' ideas and laboratory work was carried out almost exclusively by Katherine Preece. All co-authors mentioned on the cover page of each chapter of this thesis were involved with the proof reading and discussion of ideas for each manuscript prior to publication. Exceptions are limited to:

- Caroline Remijn (Unilever Research & Development, Vlaardingen) performed scanning electron microscopy (SEM) for this project. Caroline produced Figures 2.4 & 4.7. Discussions were held between Caroline and Katherine to interpret the micrographs.
- Aldo Ziere (Unilever Research & Development, Vlaardingen) carried out gas chromatography – mass spectrometry analysis (GC–MS) presented in **chapter 5**.
- Bas Domburg, Marco Karreman and Nico de Jong (Unilever Research & Development, Vlaardingen) performed trials in the pilot plant to investigate the role of the water-to-solid ratio in protein extraction. This data is shown in Figure 2.12.
- Juliën Boelhouwer (Unilever Research & Development, Vlaardingen) analysed samples for moisture, oil and protein contents in **chapters 5 & 6**.

## 1.5 REFERENCES

Campbell, K. A., Glatz, C. E. (2009). Mechanisms of aqueous extraction of soybean oil. *J Agric Food Chem, 57,* 10904-10912.

Danone Press Release. (2016). Danone to acquire WhiteWave, a USD 4 bn sales Global Leader in Organic Foods, Plant-based Milks and related products. Retrieved from http://www.danone.com/fileadmin/user_upload/PR_Danone_WhiteWave.pdf

Coca-Cola Journey Staff. (2016). The Coca-Cola Company and Coca-Cola FEMSA to acquire AdeS soy-based beverage business from Unilever. Retrieved from http://www.coca-colacompany.com/coca-cola-unbottled/the-coca-cola-company-and-coca-cola-femsa-to-acquire-ades-soy-based-beverage-business-from-unilever

Ma, C. Y., Liu, W. S., Kwok, K. C., Kwok, F. (1996). Isolation and characterization of proteins from soymilk residue (okara). *Food Res Int, 29,* 799-805.

Preece, K. E., Drost, E., Hooshyar, N., Krijgsman, A., Cox, P. W., Zuidam, N. J. (2015). Confocal imaging to reveal the microstructure of soybean processing materials. *J Food Eng, 147,* 8-13.

Preece, K. E., Hooshyar, N., Krijgsman, A. J., Fryer, P. J., Zuidam, N. J. (2017a). Intensification of protein extraction from soybean processing materials using hydrodynamic cavitation. *Innov Food Sci Emerg Technol., 41, 47-55.*

Preece, K. E., Hooshyar, N., Krijgsman, A., Fryer, P. J., Zuidam, N. J. (2017b). Intensified soy protein extraction by ultrasound. *Chem Eng Process, 113*, 94-101.

Preece, K. E., Hooshyar, N., Krijgsman, A. J., Fryer, P. J., Zuidam, N. J. (2017c). Pilot-scale ultrasound-assisted extraction of protein from soybean processing materials shows it is not recommended for industrial usage. *J Food Eng, 206*, 1-12.

Preece, K. E., Hooshyar, N., Zuidam, N. J. (2016). Whole soybean protein extraction processes: A review. *Manuscript submitted for publication in Innov Food Sci Emerg Technol.*

Rosenthal, A., Pyle, D. L., Niranjan, K. (1998). Simultaneous aqueous extraction of oil and protein from soybean: Mechanisms for process design. *Food Bioprod Process: Trans IChemE, Part C, 76*, 224-230.

Sethi, S., Tyagi, S. K., Anurag, R. K. (2016). Plant-based milk alternatives an emerging segment of functional beverages: a review. *J Food Sci Technol*, 1-16.

Swagerty, D. L., Walling, A., Klein, R. M. (2002). Lactose intolerance. *Am Fam Physician, 65*, 1845-1856.

Unilever Communications. (2015). Unilever Financial Report. 35-39. Retrieved from https://www.unilever.com/Images/annual_report_and_accounts_ar15_tcm244-478426_en.pdf

Unilever Press Release. (2016). Unilever to sell AdeS soy beverage business in Latin America to Coca Cola FEMSA and The Coca Cola Company. Retrieved from

https://www.unilever.com/news/press-releases/2016/unilever-to-sell-ades-soy-beverage-business-in-latin-america-to-coca-cola-femsa-and-the-coca-cola-company.html

Unilever Sustainable Business & Communications. (2016). Unilever Sustainable Living Plan, Mobilising Collective Action: Summary of progress 2015. Retrieved from https://www.unilever.com/sustainable-living/the-sustainable-living-plan/our-strategy/

# CHAPTER 2

# WHOLE SOYBEAN PROTEIN EXTRACTION PROCESSES: A REVIEW

This chapter is based on a manuscript submitted for publication:

Preece, K. E., Hooshyar, N., & Zuidam, N. J. (2016). Whole soybean protein extraction processes: A review. *Manuscript submitted for publication in Innov Food Sci Emerg Technol.*

## ABSTRACT

Soybeans are an important raw material for those seeking vegan, lactose-free products, such as soymilk and tofu. The aim of this review article is to provide an overview of aqueous extraction of protein and other desirable components from whole soybeans. Firstly, a discussion of the microstructure of the soybean is held, including a summary of protein localisation and properties. A detailed review of common whole soybean extraction process is then given, along with extraction process parameters and process intensification steps that can improve yield. A novel extraction model is presented, which reveals separation as the main limitation for protein extraction during aqueous soy protein extraction due to high amount of okara waste stream and its high moisture content.

## 2.1 INTRODUCTION

Plant-based protein is more sustainable than animal-based protein when comparing fossil fuel usage, land use and water consumption (González *et al.*, 2011). With the human population projected to increase to 9.5 billion by the year 2050 (Reynolds *et al.*, 2015), a greater portion of the nutrients required for human nutrition will be supplied by plant-based sources. The first generation plant-based protein source for human consumption has been the soybean. Reportedly the consumption of soybeans can be dated back as early as 3$^{rd}$ century BC in China (Huang *et al.*, 2008). The consumption of soy has gained popularity in the western world over recent decades due to:

- increased knowledge of the consumer and drive for a healthier lifestyle
- increased prevalence of lactose intolerance
- improved processing of soybeans with reduced off-flavour (Debruyne, 2006)

The increased consumption of soy-based products leads to the incentive for more sustainable soybean processing. Not only is sustainability a motivation for industry, but financial gain is also made possible through improved utilisation of the raw material. Table 2.1 shows an overview of the typical oil and protein contents of soybean and the main soy-derived commercially available ingredients. The summarised production methods for these soy-ingredients can be seen in Figure 2.1.

Table 2.1: Typical variations in protein and oil contents on a wet basis (w.b.) for soybean and some of its commercial ingredients. *Values derived from Riaz (2006) and own observations.

| Product | Typical protein content (w.b. %) | Typical oil content (w.b. %) |
|---|---|---|
| **Soybean** | 20-40 | 40-20 |
| **Soybase** | 4-5 | 2 |
| **Soy flour** | 40 | 20 |
| **Defatted soy flour/flakes** | 44-54* | 0.5-1* |
| **Soy protein isolate (SPI)** | 85-90* | Trace* |
| **Soy protein concentrate (SPC)** | 65-70* | Trace* |

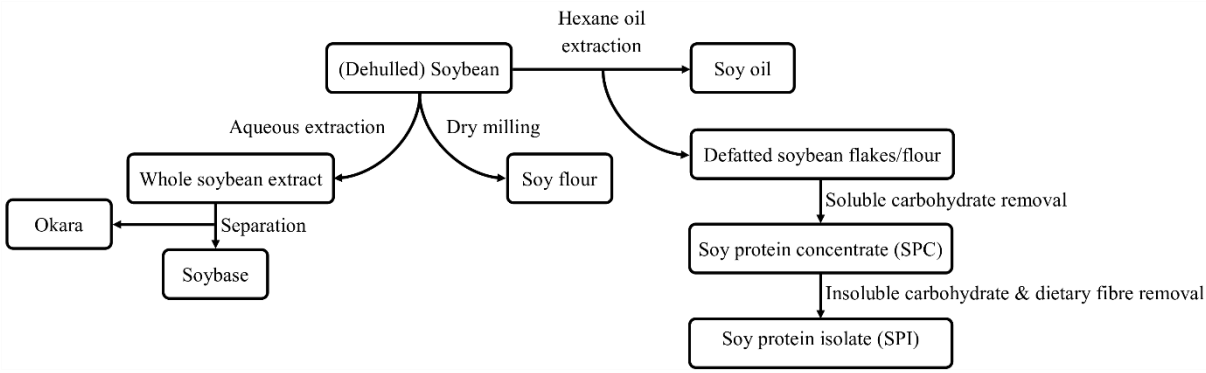


Figure 2.1. Simplified scheme of processes applied to soybeans to produce common soy ingredients.

Defatted soybean flakes are common by-products from oil extraction, the most common component utilised from the oilseed. Soybeans are crushed in a roller mill and then the oil is extracted using a solvent, typically hexane. The remaining solvent within the soybean matrix is removed via heat evaporation. Mechanical extraction can also be employed; however, compared to solvent extraction, the oil yield is not as lucrative. Defatted soy flour refers to the same material, but with a finer particle size. It can be used as a feed, yet more value can be created when the proteins are extracted from it. To produce soy protein concentrate (SPC), defatted soybean flakes are added to alcohol or water to remove carbohydrates. Soy protein isolate (SPI) contains a higher

protein content than SPC due to the removal of insoluble carbohydrate and dietary fibres via an intermediate, acidic precipitation step.

A less commonly used extraction route is the whole soybean extraction (far left process in Figure 2.1). The aqueous extract of whole soybean extraction is called soybase and it is mainly used for making consumer products containing both soy protein and soybean oil. Products like soymilk, soy-fruit beverages and tofu are produced by adding various ingredients to the soybase, such as flavours, gums, stabilisers, minerals, vitamins, sugars, fruit juices and/or coagulating agents in case of tofu. At industrial scale, the use of soybase may result in products with better sensory properties and might be a commercially more attractive route than first isolating soy protein and soybean oil separately and then blending them together at a later stage. However, a large quantity of protein, oil and other components exit the process in the waste stream (30-40% of total protein, depending on the exact conditions). The waste stream, referred to as okara in the field, is typically utilised as animal feed (Li *et al.*, 2012).

This review article provides an overview of the latest insights in whole soybean extraction processing and the emerging technologies employed to aid especially protein extraction. Firstly, the soybean composition and microstructure is discussed, as insights from these can be gained into extraction processes. Then an overview of these most common processes is given, as well as a more detailed discussion of the challenges and opportunities of each extraction step. Finally, a novel extraction model will highlight the location of greatest losses of protein during soybean processing. Findings in this area of research are also beneficial for the advancing generations of other plant-based protein sources, such as pea, canola and lupin, as well as many other extraction systems that contain components of interest in high amounts of waste stream.

## 2.2 SOYBEAN COMPOSITION AND MICROSTRUCTURE

The composition of soybeans can vary; for the production of soy-based products, such as soymilk and tofu, a strain of soybean containing relatively high amounts of proteins should be selected. Other criteria for soybean selection include the colour and sensory properties of its extract in the final consumer product. The composition of a typical soybean for producing soymilk on a wet and dry basis can be seen in Figure 2.2 (Imram *et al.*, 2003). Soybeans used for soybean oil production are commonly richer in oil and lower in proteins (about 40 and 20%, respectively). Soybeans are considered as the most important legume as they are one of few vegetal materials containing all of the essential amino acids required for human development. Dairy alternative products prepared from soybeans are not only selected for their high protein content, but also for their lack of cholesterol and lactose.

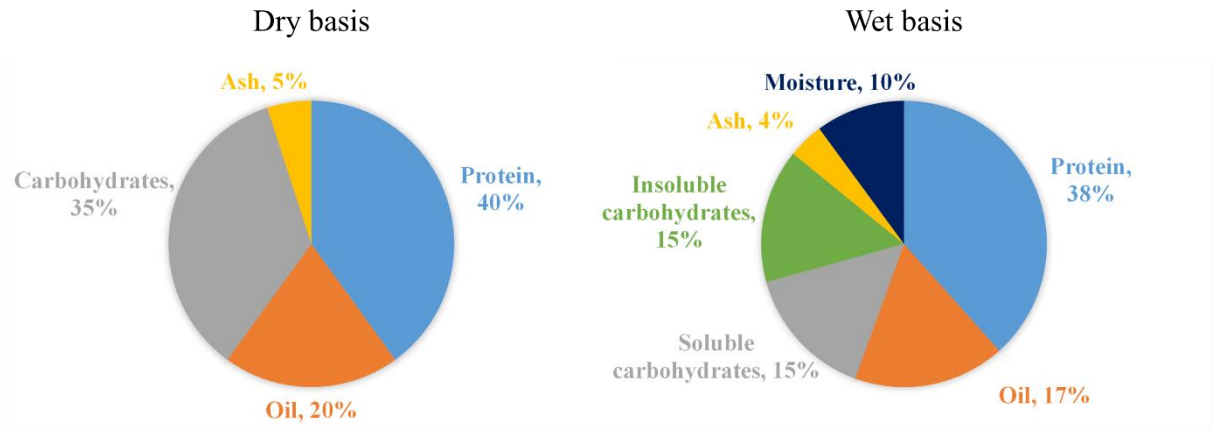


Figure 2.2. Composition of a soybean preferably chosen for soymilk production on a dry and wet basis. Data from Imram *et al.* (2003).

For optimal extraction of components from soybeans, it is vital to understand the structure located within the soybean. There are a number of structures which make up the soybean: the hull, the

hypocotyl axis and predominantly cotyledon cells (Campbell *et al.*, 2011). Figure 2.3 shows an image of soybeans and their microstructure after pre-soaking. The main constituent of the soybean, cotyledon cells, are organised within the bulk in a space-filling arrangement. Cotyledon cells are 70-80 µm in length and 15-30 µm in width (Campbell & Glatz, 2009; Rosenthal *et al.*, 1998). Hydration may cause the cells volume to increase.

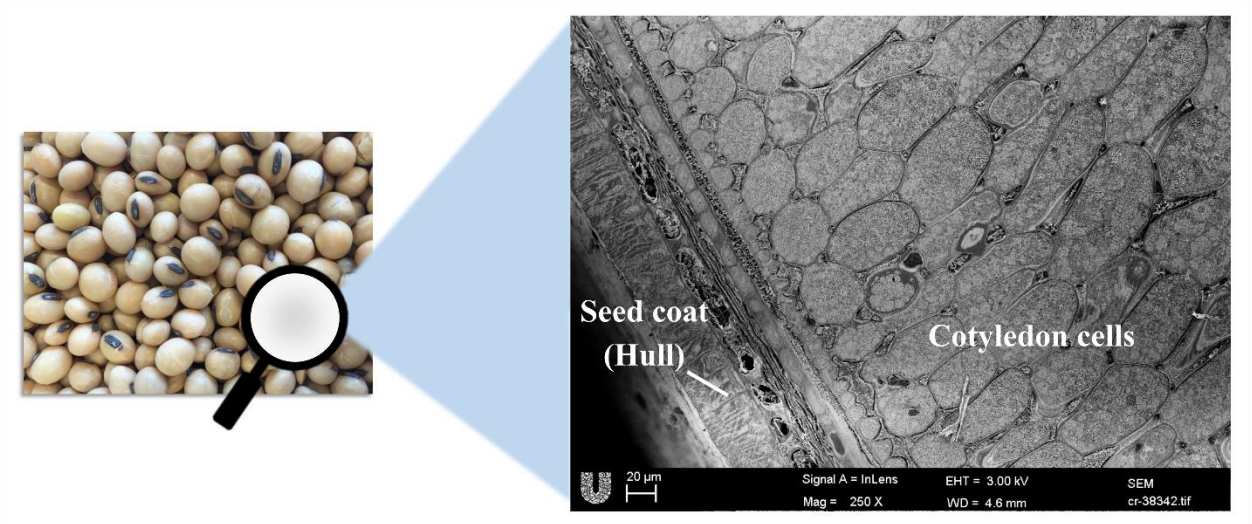


Figure 2.3. Image of soybeans (about 5 mm in size) and scanning electron microscopy (SEM) image of a pre-soaked soybean, work of Unilever R&D Vlaardingen. Within this micrograph, the seed coat (hull) and swollen cotyledon cells containing protein bodies can be observed.

The cell wall of the soybean cotyledon is comprised of a series of polysaccharides, which are often cross-linked with proteins and phenolic compounds (lignin) (Ouhida *et al.*, 2002). The primary cotyledon cell wall contains pectins, hemicelluloses and microfibrils of cellulose cross-linked with proteins (Campbell *et al.*, 2011). There is a secondary cell wall within the primary wall containing cellulose and hemicelluloses also capable of binding to proteins. Cells are held together by adhesive substances found in the middle lamella, the extracellular space between cells, and contain pectins, glycine and hydroxyproline-rich proteins (Campbell *et al.*, 2011; Kasai *et al.*, 2003).

### 2.2.1 Soybean oil

Oil consists of approximately 88.1% triglycerides, 9.8% phospholipids, 1.6% unsaponifiable components and 0.5% free fatty acids (Salunkhe *et al.*, 1992).The majority of oil is located in oil bodies (oleosomes) within the cotyledon cells (Waschatko *et al.*, 2012). Oil bodies are found within the cytoplasmic network of the cells and are stabilised by small molecular weight proteins termed oleosins (Rosenthal *et al.*, 1998), which make them more hydrophilic and easy to extract aqueously. The oil bodies typically vary in size from 0.2-0.5 µm (Campbell & Glatz, 2009). Figure 2.4 shows a SEM image of a dry soybean. Oil bodies are observed in this micrograph, as well as other components of interest, most notably protein bodies and phytic acid (Preece *et al.*, 2017b; **chapter 4**).

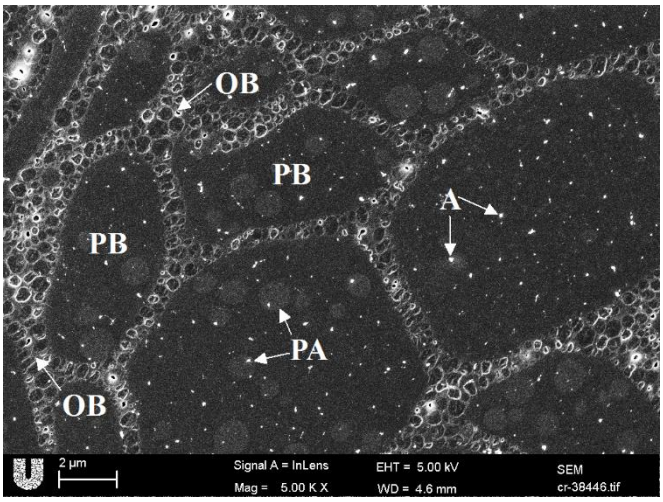


Figure 2.4. SEM micrograph of soybean cell without prior pre-soaking (Preece *et al.*, 2017b; **chapter 4**). Various components are labelled on the image: oil bodies (OB), protein bodies (PB), phytic acid (PA; spherical structures) and artefacts (A; white dots) can be seen. Scale bar represents 2 microns.

### 2.2.2 Soybean proteins

The majority of proteins are organised in protein bodies of the cotyledon cells, labelled in Figure 2.4. According to Preece *et al.* (2017b; **chapter 4**), the protein bodies within the cotyledon cells were found to be in the size range 2.4 to 13.5 μm when examined using SEM without sample hydration. These values fell on the low side when compared to values recorded from TEM of 2 to 20 μm on hydrated soybeans (Rosenthal *et al.*, 1998). It has been reported previously (White *et al.*, 2013) that protein bodies swell upon hydration with water at neutral pH to double their original size, confirming these findings.

There are two major storage proteins that account for typically 60-80% of the total soybean protein: the globulins glycinin (11S) and β-conglycinin (7S) (Murphy, 2008). At neutral pH and ambient temperature, glycinin (11S) is a hexameric complex comprised of acidic and basic polypeptides linked by disulphide bridges to provide a molecular weight in the range 320-375 kDa (Lakemond *et al.*, 2000). β-conglycinin (7S) contains three major subunits (β, α and α') reportedly with sizes of 50, 67 and 71 kDa, respectively (Maruyama *et al.*, 1999). Globulins are, by definition, only 100% water soluble in a salt solution (Kapchie *et al.*, 2012).

Other metabolic protein sources within the soybean include oleosins (8-20% of the total protein) for oil body stabilisation, trypsin inhibitors (0-1.7% of the total protein) and enzymes such as lipoxygenase (LOX) (Murphy, 2008). Trypsin inhibitors are a group of proteins present within the soybean that cause negative effects on human digestion. Trypsin and chymotrypsin are digestive enzymes located within the gastrointestinal tract with which trypsin inhibitors form very stable complexes with (Savage, 2003). Trypsin inhibitors are commonly denatured by heat inactivation during the extraction process ((Kwok *et al.*, 2002; Van Der Ven *et al.*, 2005); e.g., 90% inactivation

after 5-10 min at 121 °C at pH 6.5). High temperature treatment may also denature LOX, an enzyme activating the oxidation of polyunsaturated fatty acids and formation of fatty acid hydroperoxides, which are turned into volatile off-flavours. A balance is recommended between the inactivation of trypsin inhibitors and LOX and the detrimental effects of heat treatment, especially as protein denaturation will cause a reduction in the protein extraction yield (Rosenthal *et al.*, 1998). As soy protein is a complex mixture containing various proteins, it has different denaturation temperatures. β-conglycinin and glycinin, the main storage proteins, possess denaturation temperatures of about 68 °C and 86 °C, respectively (Peng *et al.*, 2016).

Within its native state, protein is aggregated within intact cells. Protein folds to bury the hydrophobic side chains in the core of the aggregate, with hydrophilic groups covering the exterior of the protein in the aqueous cell environment. Solubilisation is a process that occurs once the cell wall has been disrupted. Solubility is a function of the distribution of hydrophilic and hydrophobic amino acids at the surface of a folded protein, dependent on the nature of the solvent (Weiss *et al.*, 2011). In its native form, protein is stabilised by various interactions: charge-charge interactions, salt bridges, hydrogen bonding and polar group burial (Pace *et al.*, 2004). These interactions need to be overcome in order to migrate from insoluble to a soluble state; the driving force for this is conformational entropy (Pace *et al.*, 2004). Protein can be described as soluble when protein molecules have diffused as single units in a homogeneous manner. Protein unfolding due to heating may lead to exposure of the more hydrophobic inner sites to the outside, and this results in aggregation. Protein unfolding and thus aggregation also depends on charge, as it will result in a more hydrophilic amino acid. In general, the isoelectric points (pI) of the majority of soy proteins is at pH 4.5 (Campbell *et al.*, 2011; Kinsella, 1979), and then the soy proteins are least soluble due

to their total zero charge. Soy proteins are more soluble at pH values below 3 and above 6, as protonation or deprotonation results in more surface charges.

## 2.3 WHOLE SOYBEAN EXTRACTION PROCESSES

### 2.3.1 Common processes

The traditional process for soybase preparation used in the Orient, which is still used for the preparation of soybase in the home or by street vendors today, includes the following steps (Kwok & Niranjan, 1995):

- Soaking of the soybeans
- Grinding in cold water
- Filtering
- Cooking at 93-100°C for 30 min

This method could be modified by grinding in hot water, which has the advantage of LOX inactivation. Today such processes are adapted to make soybase at larger scale, either in a batch or continuously. As illustrative examples, some of these processes are shown in Figure 2.5. Process 1 is also known as the Tetra Pak Alwin™ process (Imram *et al.*, 2003) and is shown in more detail in Figure 2.6. Soybeans are ground at about 85 °C and pH 8 in order to solubilise compounds, and then the okara is removed by decanting and the soybase is further heated to 141 °C and vacuum treated. The classic Illinois process developed through research at the University of Illinois is similar to process 1; the significant difference between the two processes is the overnight pre-soaking of soybeans prior to milling (Nelson *et al.*, 1976). Process 2 is a process in which the soybeans are first dehulled and the soybean slurry is heated to 141 °C and vacuum treated prior to decanting. Although a limited amount of protein is lost due to dehulling, it has the advantage that less okara will be produced during the extraction process and therefore slightly higher extraction yields can be achieved in comparison to process 1 (see Section 2.4). Another advantage of process

2 is that the okara has more exposure to heat, and it is therefore more microbiologically stable and useful for other food applications after immediate drying. Process 3 is an example of grinding soybeans at ambient temperature, in contrast to the other processes. This is commonly utilised by ProSoya, for example (Gupta, 2014). An advantage of cold grinding is that the proteins are not denatured at this stage and can solubilise well into the aqueous phase (see also Section 2.3.3). However, the oxygen levels should be kept low otherwise LOX may cause off-flavours. An alternative is to use LOX-free soybeans, but these are more expensive than standard soybeans. Heat treatment is still necessary at a later stage in Process 3 to denature trypsin inhibitors and create some microbiological stability of the soybase until further usage. Please note that these three processes are used here as examples and that some elements of one process can be used in one of the other process as well.

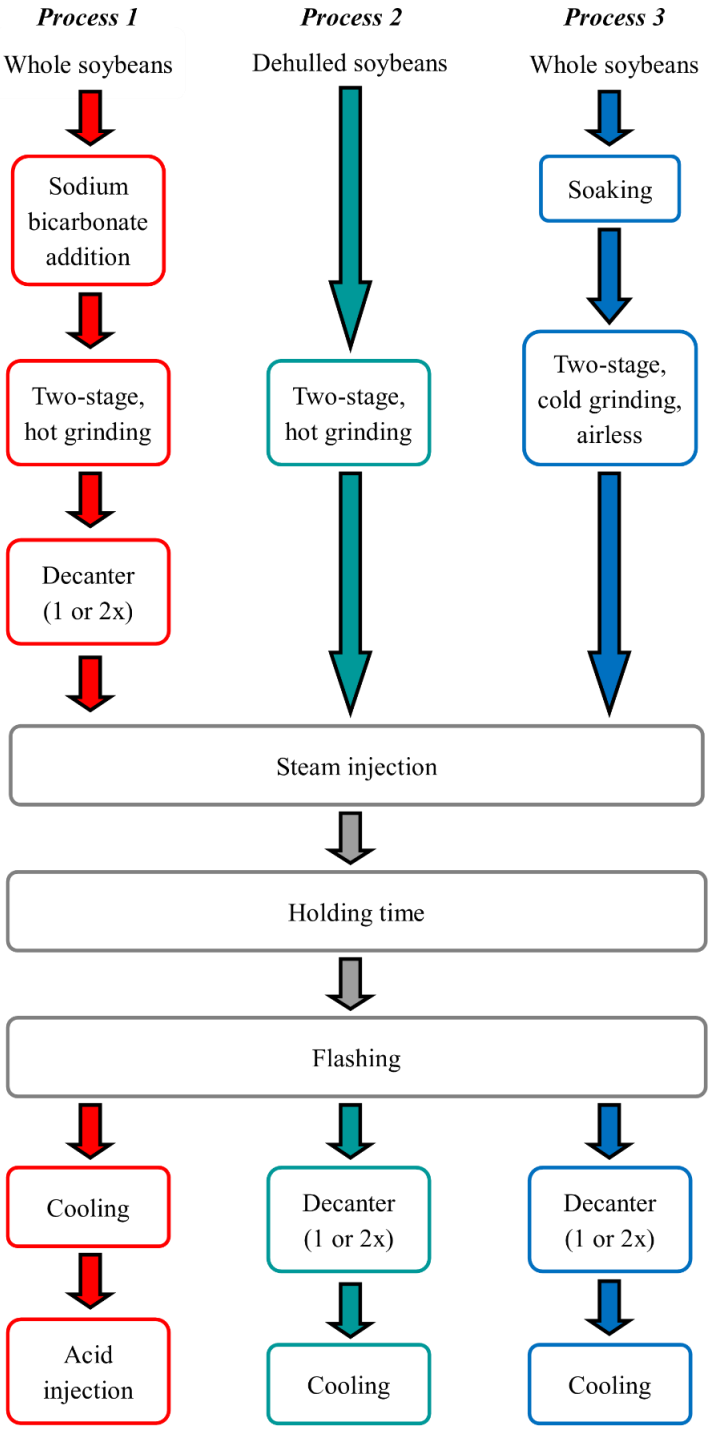


Figure 2.5. Examples of common, large-scale processes for soybase preparation. Typically, soybeans are dry cleaned first to remove dirt and damaged soybeans. Process 1 describes the Tetra Alwin process from Tetra Pak (Imram *et al.*, 2003, see also Figure 2.6); process 2 shows a variation in the order of processing with steam injection prior to the decanter; and process 3 is an example of an airless, cold grinding extraction process, utilised by ProSoya (Gupta, 2014).

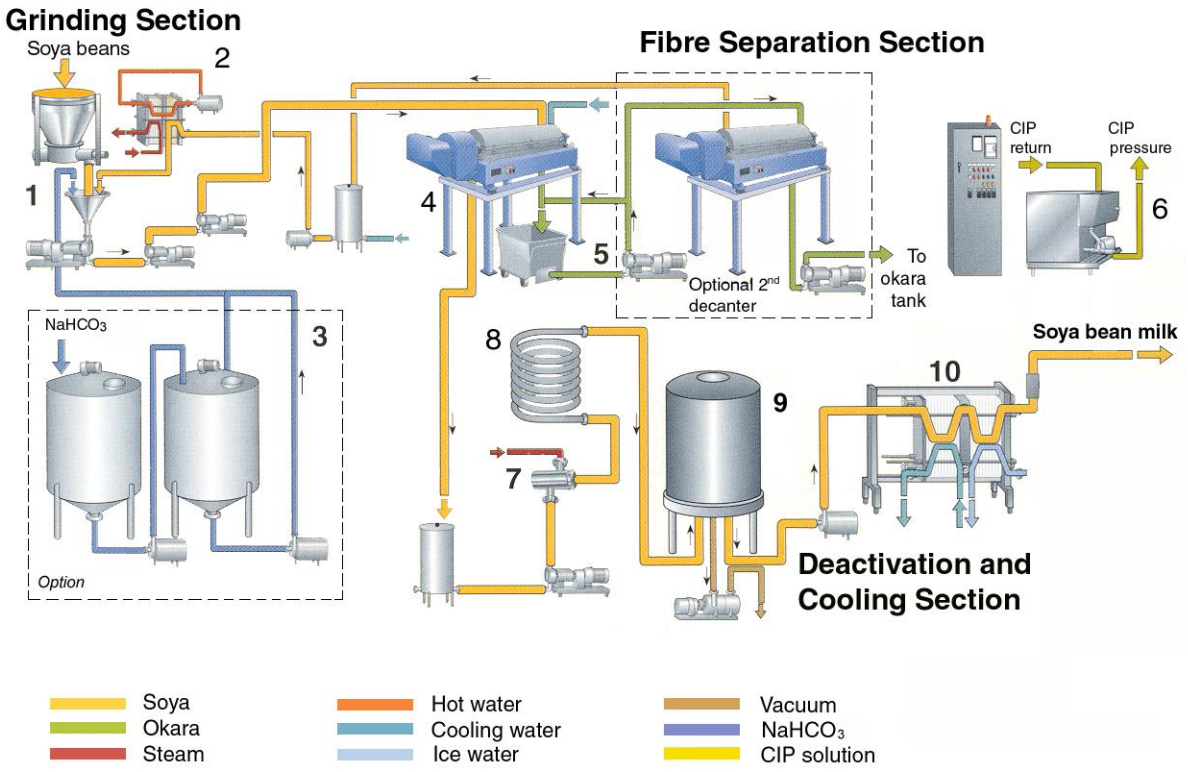


Figure 2.6. Tetra Alwin® Soy process line (courtesy of Tetra Pak; published with their permission) is an example of a commercially available line for the continuous production of soybase directly from soybeans (Imram *et al.*, 2003). It is the same as Process 1 in Figure 2.5. Optionally, sodium bicarbonate can be added to bring the pH to 8 and increase the ionic strength.

The sections below discuss each extraction step and important process parameters in more detail.

### 2.3.2 Mechanical disruption of soybean cells

Traditional methods for producing homemade soymilk, such as 'nama-shibori', include pre-soaking of the soybeans prior to mechanical disruption (Toda *et al.*, 2007). Yet in most industrial processing plants, this is not employed due to the generation of off-flavours (Kwok & Niranjan, 1995). Blanching of soybeans is sometimes utilised by manufacturers to eliminate off-flavours in the final product (Peng *et al.*, 2017); however, this causes denaturation and aggregation of the protein.

Soybeans are ground by either dry or wet milling to disrupt intact cotyledon cells to make protein and other components available for extraction via mechanical forces. The cell wall is a physical barrier to intrusion from external sources, but also needs to be mechanically strong to withstand external pressures generated by the extracellular matrix surrounding a cell (Tomas, 2000). A number of techniques have been utilised to measure the force required to break the cell walls and yield the intracellular components from various cell types (Zhang *et al.*, 2009). Dry milling can be achieved with, e.g., six-roller mill equipped with proper cooling, in which three sets of two rolls are used with one roll in each pair rotating faster than the other. For optimal dry milling, the particle size of the flour should be smaller than that of intact cells (see Section 2.3.3.1). Wet milling is often done at elevated temperatures (≥80 °C) to eliminate the effects of the LOX. Two to three mills might be used in sequence, such as disk mill, colloid mill and/or high pressure homogeniser. Swelling of soybean cells occurs upon hydration, therefore the maximal particle size for optimal extraction is greater for wet milling than for dry milling. New mills are grinding better than ones that have worn, and this affects the final yield of the extraction process directly.

### 2.3.3 Solubilisation of compounds

The solubilisation of compounds can be split further into a number of steps: diffusion of the solvent into the plant matrix, solubilisation of cellular components, transport of the solutes to the exterior of the solid matrix and transport of the solutes from the matrix surface to the bulk medium. The rate determining step for mass transfer is most likely the solubilisation of intracellular components and their transfer to the surface (Jung *et al.*, 2011). Solubilisation of protein is influenced by several processing parameters, which impact the extraction of intracellular components into the bulk phase:

- particle size of the matrix (milling efficiency)
- pH of the solvent
- ionic strength of the solvent
- temperature of the solvent
- solubilisation time
- protein concentration of the resultant soybase

In the following sections, these main parameters are discussed in more detail.

#### *2.3.3.1 Particle size*

Lower particle sizes of the plant matrix results in high extraction yields of protein and oil from flour (Rosenthal *et al.*, 1998; Russin *et al.*, 2007; Vishwanathan *et al.*, 2011a, 2011b). This is related to the available surface area for interaction with the solvent, or the fact that more cell walls were then disrupted by the milling, favouring cell content release. Decreasing the average particle diameter of soy flour from 223.4 to 89.5 μm, increased the protein recovery from 40 to 52% (Russin *et al.*, 2007). The maximum recovery of protein by extraction was achieved from a fine fraction of

particles with a particle size below 75 μm; 97% and 93% from soybean flour and okara flour respectively (Vishwanathan *et al.*, 2011a). The effects of particle size during wet milling of soybeans to produce soybase has also been reported (Vishwanathan *et al.*, 2011b). Particle size (364 to 182 μm) was found to have an inverse relationship with protein recovery (78.8 to 89.3%) (Vishwanathan *et al.*, 2011b). Similar results were also obtained using a stone grinder and a colloidal mill (Vishwanathan *et al.*, 2011b). These sizes quoted are slightly greater than those discussed previously relating to the size of intact cotyledon cells in Section 2.2 and to those measured during dry processing. This can be attributed to the particles swelling to larger sizes when in contact with water compared to the dry milling counterpart. Laser diffraction techniques to measure the particle size can also overestimate the size of structures; the technique cannot differentiate between a mass of intact cells and a cage-like structure of cell walls with the contents extracted. Campbell and Glatz (2009) argued that only broken soybean cells in the outer layer of soybean particles can release their content. Their model assumes a spherical cotyledon cell of 55 μm (average of 30 and 80 μm) and spherical flour or ground soybean particles. So one may estimate a minimal particle diameter for full release from soybean particles of 110 μm (= 2 broken cells × 55 μm), although the structures of processed soybean microstructures we observed by confocal laser scanning microscopy (CLSM) did not fit with this model (Preece *et al.*, 2015; **chapter 3**).

A comparison of the particle size distributions across different scales of soybean processing materials can be seen in Figure 2.7. The production of these materials can be found in the literature for lab-scale (**chapter 3**, Preece *et al.*, 2015) and pilot-scale processes (**chapter 5**, Preece *et al.*, 2017c). Focusing on the slurry data, it is possible to see a peak in the material prepared at lab-scale in the size range of 2-35 μm that is not present in the pilot-scale equivalent. This is believed to

correspond to intact protein bodies found outside of intact cells, which were found as a result of thermal treatment (ca. 80 °C) for a prolonged period of time (30 min) (**chapter 3**, Preece *et al.*, 2015).The overall size range is similar for both of the slurry samples, independent of scale. Focusing on the okara samples, a similar range of particle sizes of 0.3-3000 µm was observed for both lab-scale and pilot-scale versions. The okara prepared at lab-scale contains the intact protein bodies, and not the soybase, confirmed by CLSM (**chapter 3**, Preece *et al.*, 2015). A larger volume of particles in the size range 0.3-3 µm were found in the soybase prepared at pilot-scale (Figure 2.7B) in comparison to lab-scale (Figure 2.7A). This could correspond to soluble proteins or stabilised oil droplets, as the extraction yield was much greater at pilot-scale compared to the lab-scale extraction procedure. It can be concluded that the separation efficiencies are comparable when focusing on the particle size distributions. However, the milling at pilot-scale is much more efficient than at lab-scale as the milling process occurs within seconds compared to the lab-scale milling process of 30 min. The greater time period at elevated temperature for the lab-scale process results in the formation of a peak in the particle size range 2-35 µm in the slurry and okara samples, which corresponds to aggregated protein.

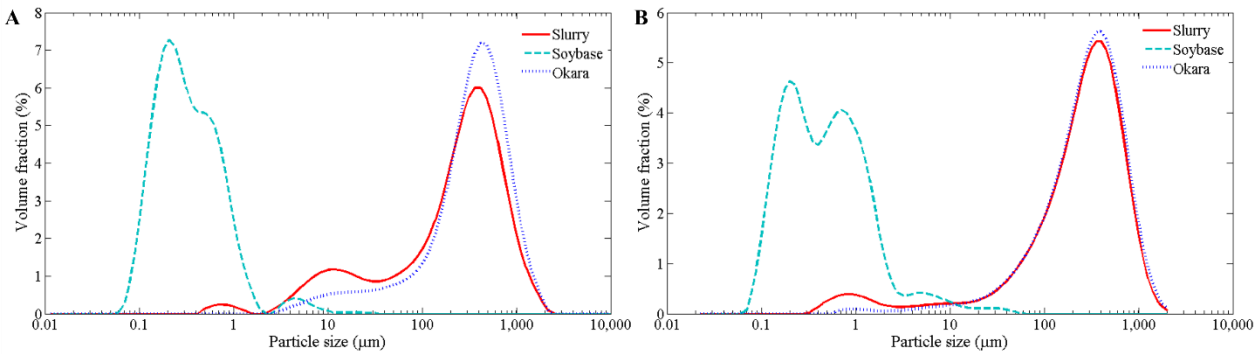


Figure 2.7. Particle size distributions for soy slurry, soybase and okara produced at lab-scale (A) and pilot-scale (B) at Unilever R&D, Vlaardingen.

#### *2.3.3.2 Effect of pH and ionic strength*

There is a good correlation between extraction yield and solubility (see Section 2.2.2) of soy protein as function of pH. The highest extraction yields from either milled soybeans or okara are observed at either low or high pH values (<3 and >6), and the lowest around the pI of the majority of soy proteins at 4.5 (Ma *et al.*, 1996; Rosenthal *et al.*, 1998; Vishwanathan *et al.*, 2011a). Interestingly, oil extraction yields follow the same pH correlation as the protein extraction yields, although oil itself cannot be (de)protonated. This can be explained by the properties of the surface active proteins that stabilise oil droplets within the aqueous extract. In general a pH of about 8 – 8.5 is chosen for extraction. Although the solubility may be improved at higher pH values, the functional properties of the proteins may then be impaired because of disaggregation and hydrolysis of the proteins. The extraction medium can be alkalised using sodium bicarbonate ($NaHCO_3$). This also increases the ionic strength, which also contributes to the solubility of soy protein (see Section 2.2.2).

#### *2.3.3.3 Effect of temperature*

Proteins in their native state are more soluble than those that have been denatured. Therefore, the extraction temperature should ideally be kept below the soy protein denaturation temperature (<70°C, see also Section 2.2.2) (Deak & Johnson, 2007; Rosenthal *et al.*, 1998). However, increasing the temperatures aids in breaking the protein-carbohydrate complex, leading to an improved protein yield (Kasai & Ikehara, 2005). Other benefits of thermal treatments also include the inactivation of LOX and trypsin inhibitors. Thus, a sacrifice must be made for improved solubility versus denaturation of certain protein components.

Preece *et al.* (2015, **chapter 3**) visualised the effect of thermal treatment at 80 °C and compared it to wet, ambient extraction (<42 °C) at lab scale. Upon 30 min wet, ambient milling of soybeans, it was possible to extract 26% more protein (absolute value) in comparison to the thermal equivalent (80 °C, 30 min). CLSM (Figure 2.7) confirmed aggregation of protein bodies (depicted in green) in- and outside of intact cotyledon cells (appear purple) upon extraction at 80 °C. Interestingly, we could not visualise such aggregated protein bodies when the soybean extraction was performed at pilot plant scale, which might be caused by its much shorter milling time (Preece, *et al.*, 2017c; **chapter 5**).

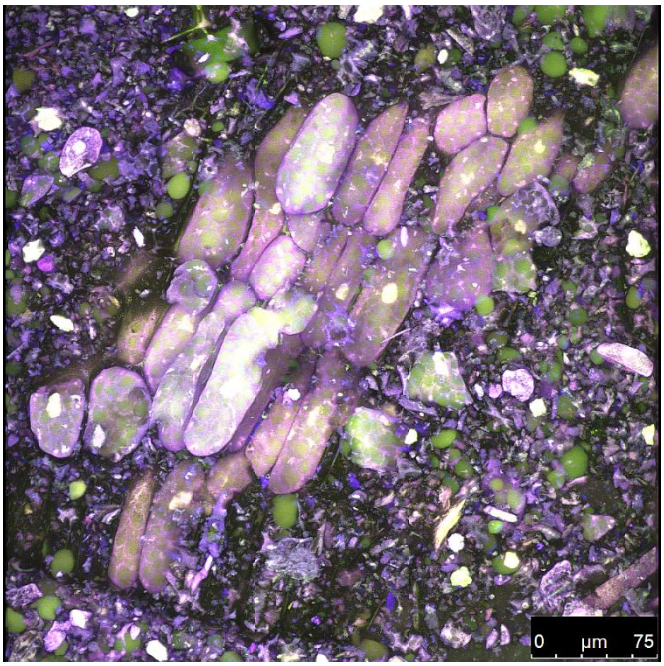


Figure 2.7. CLSM image of soy slurry visualised using acridine orange after grinding soybeans at 80 °C, work of author. The green colour of the protein bodies indicates that these are relatively hydrophobic and thus denatured, as protein bodies inside cotyledon cells after grinding at ambient temperature are purple and not seen outside these cells.

The release of protein from okara was found to be more sensitive to temperature in comparison to flour and wet milling of soybean (Ma *et al.*, 1996). Increasing the temperature from 25 to 90°C resulted in a progressive increase in the extraction of protein. This can be explained through the thermal processing previously experienced by the okara proteins during soybase production, leading to their denaturation and retarded release.

#### *2.3.3.4 Effect of solubilisation time*

The effect of incubation time of soy flour on protein extraction yield has been studied previously at lab-scale (Rosenthal *et al.*, 1998). After a period of approximately 10 min and 50 °C, the protein yield plateaued at 75% for non-heat treated flour and 25% for heat treated samples. The rapid release rate of protein can be attributed to a short diffusion path offered by the fine flour, and

follows first-order kinetics (unpublished Unilever results). Higher temperatures and smaller particles will result in faster release rates.

#### *2.3.3.5 Protein concentration*

Proteins above a concentration of 5-6% (w/w) in soybase tend to aggregate and sediment (unpublished Unilever results), and therefore the liquid-to-solid ratio commonly used for whole soybeans is often around 6:1 or 7:1 w/w (40% protein in soybean / 7 = 5.7%). Although higher amounts of water may result in relatively more yield (see Section 2.4), both the protein throughput and the protein concentration will be lower. The latter is important for further product formulation; e.g., one needs a soybase with a concentration well above 4% if one would like to make a soymilk with 3% protein as other ingredients need to be incorporated as well.

### 2.3.4 Separation and effect of solid-to-liquid ratio

For the removal of insoluble ingredients, typically filtration or centrifugal separation techniques are employed, with decanting the more frequent choice due to its continuous operation. A schematic diagram of a decanter centrifuge can be seen in Figure 2.8, which is commonly utilised in industry for solid-liquid separation driven by density differences between solids and the liquid phase. The soy slurry is fed into the centrifuge through an Archimedean screw inside a rotating bowl. Both the screw and bowl are rotating at slightly different speeds, scraping the okara towards the solid exit whilst soybase is discharged from the other end of the bowl. A small bank is present to reduce the moisture content of the okara stream as much as possible as it scrolls above the soybase layer. Successive extraction like double decanting, using a water-to-okara ratio of about 1:3 (w/w), achieve higher yields (about 10-15%, depending on exact conditions). Please note that insolubility is here defined as ingredients that do not end up in the soybase, as some small and/or

light solids can still end up in the soybase (e.g. denatured proteins, oil droplets, etc.). Insoluble ingredients are separated based on their density compared to the solvent in a decanter, resulting in a 'milky' soybase and the waste material okara.

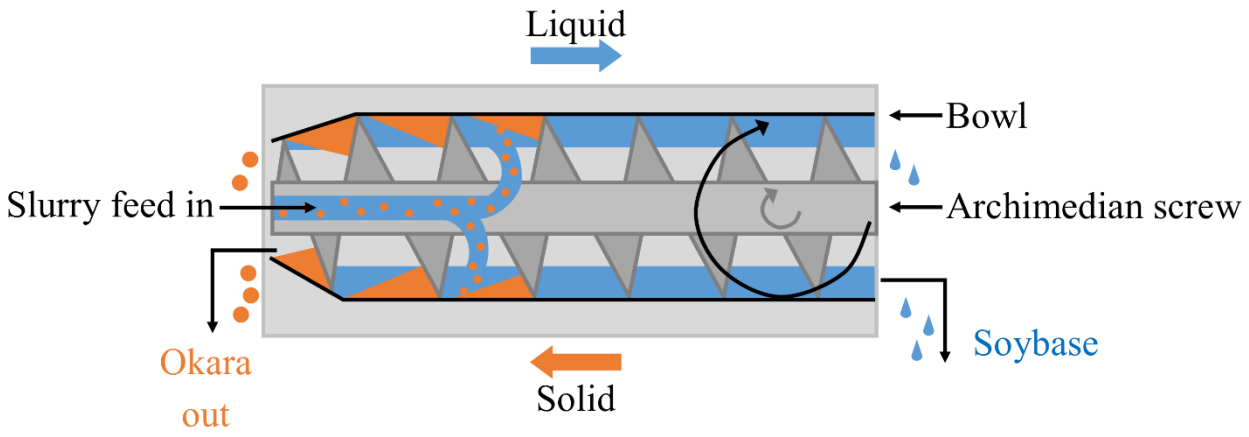


Figure 2.8. Schematic diagram of a decanter centrifuge for the separation of okara from soybase.

Filtration is a mechanical process used to separate and retain particulates from a liquid via a 'filter media', whilst the liquid passes through. During filtration, a layer of okara builds on the filter media, which is often referred to as a 'cake'. The cake retains a significant amount of product (soybase) and as the okara cake layer increases in volume; it becomes increasingly difficult to deliquor the soy slurry as clogging of the filer media can occur due to a high concentration of fibrous material.

Okara (see Figure 2.9) has a surprisingly high moisture content of approximately 80% (Preece *et al.*, 2015; **chapter 3**). We believe that this high moisture content is responsible for most of the protein losses during whole soybean extraction, especially as the amount of okara produced is quite high. It is about two times more in weight than hulled soybeans in a process similar to the one shown in Figure 2.6, and for tofu production a soybean/okara ratio of 1:1.2 (w/w) has been reported (Li *et al.*, 2012). Surprisingly, others have not reported this cause for the low yield. We also

hypothesise that the efficiency of the separation step is highly dependent on the liquid-to-solid ratio (also called water-to-bean ratio) because of the presence of okara. This is in contrast to what has been reported before by others, who argue that the use of more water results in more protein solubilisation (see below and Rosenthal *et al.* (1998), Vishwanathan *et al.* (2011a) and Ma *et al.* (1996). However, we propose that, after a certain minimum needed to solubilise soy ingredients, the use of more water results in better separation efficiency as relatively less water stays in the okara. Therefore, we propose a new model in Section 2.4.

Figure 2.9. Photograph of okara produced at Unilever Research & Development facilities, Vlaardingen. It contains a surprisingly high water content of about 80%, most likely due to remaining, although most often broken, cell wall structures (see also the CLSM image of okara shown by Preece *et al.* (2015); Figure 3.6, **chapter 3**).

### 2.3.5 Ensuring sensorial quality and a safe product

Soybase is heated to denature LOX and to hinder the effects of trypsin inhibitors (Section 2.2.2), which cause digestive problems, if left untreated. Either steam injection or steam infusion can be used to increase the temperature to 121°C or higher. This unit operation may cause some denaturation or dissociation of proteins (Johnson & Synder, 1978), browning of the product by Maillard reactions, and cooked flavours (Kwok & Niranjan, 1995). Afterwards the soybase enters a vacuum tank for deodorising. The drop in pressure (from about 2 to 0.6 bar) and temperature (from about 121 to 80 °C) facilitates off-flavour removal by flashing. The thermal and vacuum treatment can be carried out before or after separation of insoluble materials, which influences the properties of both soybase and okara.

The obtained soybase is then chilled but not sterile, although the microorganisms that survived the steam injection process are unlikely to grow during short-term storage. Furthermore, oxidation may take place when exposed to air in the processing facility and this is the main reason that soybase should be processed quickly.

### 2.3.6 Process intensification options

To aid in the extraction of protein and other components from soy, a number of other unit operations can be employed. An overview of studied techniques can be seen in Table 2.2.

Table 2.2 Processing intensification options, including tested experimental conditions, effects of protein yield and the drawbacks of each technique.

| **Process intensification option** | **Soybean source** | **Conditions** | **Drawbacks** | **Protein yield (Intensified vs. control)** | **Reference** |
|---|---|---|---|---|---|
| **Enzyme-assisted extraction** | Full-fat extruded flakes | Protease (0.5%), pH 5, 50 °C, 1 h, S/L: 0.17 | pH similar to pI for the majority of soy proteins, costly enzymes and processing, require investigation at pilot-scale. | 49% vs. 61% | de Almeida *et al.*, 2014 |
| | Full-fat extruded flakes | Protease (0.5%), pH 5, 50 °C, 1 h, S/L: 0.17 | | 66% vs. 96% | de Moura *et al.*, 2011 |
| | Soy flour | Protease (0.45%), pH 5, 50 °C, 1 h, S/L: 0.125 | | 60% vs. 57% | Rosenthal *et al.*, 2001 |
| | Dried & powdered okara | Cellulase (1%), 40 °C, 15 h, S/L: 0.15 | Long incubation times, costly enzymes and processing, requires investigation at pilot-scale. | Up to 85% | Kasai *et al.*,2004; |
| | Soy flour | Cellulase (0.45%), pH 5, 50 °C, 1 h, S/L: 0.125 | Lower yield than control sample, pH similar to pI of the majority of soy proteins. | 55% vs. 57% | Rosenthal *et al.*, 2001 |
| | Defatted soy flour | Carbohydrolase (30 FBG), pH 9, 60 °C, 0.5 h, S/L: 0.05 | Costly enzymes and processing, require investigation at pilot-scale. | 56% vs. 33% | Rosset *et al.*, 2014 |
| **Ultrasound-assisted extraction** | Direct from soybean | Lab-scale probe, 20 kHz, 400 W, 1 min, 80 °C, S/L: 0.17 | - | 48 vs. 37% | **Chapter 4,** Preece *et al.*, 2017b |
| | Okara solution | Pilot-scale probe, 20 kHz, 2000 W, 2.85% solid solution, 50 °C | Requires 2nd separation process, costly. | 4.2% improvement (absolute) | **Chapter 5,** Preece et al., 2017c |

Table 2.2 continued. Processing intensification options, including tested experimental conditions, effects of protein yield and the drawbacks of each technique.

| **Process intensification option** | **Soybean source** | **Conditions** | **Drawbacks** | **Protein yield (Intensified vs. control)** | **Reference** |
|---|---|---|---|---|---|
| **High pressure homogenisation** | Direct from soybean | Lab-scale, 9 L $h^{-1}$, 100 MPa, single pass | Requires investigation at pilot-scale, slow flow rate, blockages could become an issue | 82% vs. 66% | **Chapter 6,** Preece *et al.*, 2017a |
| **Double decanting** | Washing of okara | Industrial scale | Requires 2nd separation process, costly | 10% or more improvement | Debruyne (2006) |
| **Belt press** | Deliquoring of okara | Reducing moisture content of okara from 80% to 65-70% | Open design (hygiene issues), theoretical value | Up to 18% improvement (theoretical) | - |

Enzyme-assisted extraction using protease was found to improve both the extraction of oil and protein from soy flour (Rosenthal *et al.*, 2001). The effects of protease were also studied with positive effects in combination with membrane recovery by de Moura *et al.* (2011) and enhanced protein solubility from full fat extruded flakes (de Almeida *et al.*, 2014). Protease may improve the solubility of soy proteins, especially when they are denatured and/or aggregated. In general the smaller the proteins, the better their solubility. In addition, protease may cleave proteins from cell wall materials. Cellulases have also been used in an attempt to degrade cell walls, although the results were limited (Kasai *et al.*, 2003, 2004; Rosenthal *et al.*, 2001). The main issue with cellulases is that these enzymes are most active at pH 5; at this pH soy proteins tend to aggregate since their pI is 4.5 (see Section 2.2.2). Enzyme treatment times are usually long, and expenses of both enzyme and process are relatively high. One should realise that optimal conditions for enzyme activity might not be similar to the optimal conditions of protein extraction (see above). More detail can be found on enzyme-assisted extraction can be found for plant protein recovery by Sari *et al.* (2015).

Cavitation is a phenomenon which has been widely studied within the food industry (Knorr *et al.*, 2004), with improvements attributed to enhanced mass and heat transfer and cell disruption. Cavitation is defined as the generation of microbubbles, their subsequent growth and sudden collapse resulting in local regions of very high temperatures and pressures Gogate *et al.* (2006). Several means can be used to introduce cavitation into a liquid system:

- Acoustic cavitation (ultrasound)
- Hydrodynamic cavitation (high pressure homogenisation)
- Optic cavitation

- Particle cavitation

Upon microbubble implosion, localised short-lived temperatures and pressures of up to 5000 K and approximately 50 MPa have been reported (Tiwari & Mason, 2012). As a result of microbubble collapse, shear energy waves are produced causing turbulence in the cavitation zone leading to improved mass transfer (Patist & Bates, 2008). Microjet impacts and shock-wave-induced damages also occur as a result of microbubble collapse; the potential energy of the expanding microbubble is converted into mechanical energy by means of a liquid jet that enters the bubble on one side and penetrates the opposite bubble wall (Esclapez *et al.,* 2011). Improvements in extraction of vegetal components have been attributed to the disruption of cell walls caused by the liquid jetting by previous reports in the literature (Li *et al.,* 2004; Shirsath *et al.* 2012).

Ultrasound refers to sound waves that are present at frequencies inaudible to humans from 20 kHz up to the GHz range. Within the food industry, ultrasound is typically applied at frequencies in the range 16-100 kHz to bring changes to the food material (Soria *et al.,* 2010). Upon application of ultrasound, sound waves are transmitted through a series of compression and rarefaction cycles (Tiwari & Mason, 2012). Upon a sufficiently negative pressure value applied to a liquid sample, the intermolecular distance exceeds a critical value, causing microbubbles to form and potentially violently collapse after a series of cycles (Tiwari & Mason, 2012). Ultrasound-assisted extraction has been studied at lab (Preece *et al.,* 2017b; **chapter 4**) and pilot scale (Preece *et al.,* 2017c; **chapter 5**) for enhancing the extraction of protein from soybeans, based on cavitation. Improvements in extraction yields from soy slurry and okara were found for materials prepared at lab-scale due to improved solubility, confirmed by CLSM (Preece *et al.,* 2017b; **chapter 4**). When

okara was prepared at pilot-scale, the improvement in protein extraction yield was less significant, therefore was not recommended for industrial scale-up.

High pressure homogenisation (HPH) is another unit operation based on hydrodynamic cavitation which can improve extraction yields from soybean processing materials (Preece *et al.*, 2017a; **chapter 6**). Within a high pressure homogeniser, high pressure is exerted on the liquid sample in a matter of seconds prior to forcing through a small orifice, typically several microns in width (Dumay *et al.*, 2013). As a result the sample experiences a pressure drop, leading to intense mechanical forces and cavitation. Improvements in yields were found to be a result of disruption of all intact storage cells, with a maximum total protein yield of 94% reported for okara solution with a single pass through a homogeniser at 100 MPa (Preece *et al.*, 2017a; **chapter 6**). Debruyne (2006) mentioned that homogenisation can cause a negative effect on the separation efficiency. However, this was only the case after multiple passes of soy slurry through the homogeniser at 100 MPa (Preece *et al.*, 2017a; **chapter 6**). Additional investigations are required to assess the scalability of this promising result obtained using a lab-scale homogeniser as well as the sensory and physico-chemical properties of the final soy-based product.

Another approach to improve protein extraction yield from whole soybeans is to target the separation of fibrous materials, termed okara. Industrial separation is most commonly performed using a decanter centrifuge, achieving a moisture content of approximately 80% for the okara stream (see Section 2.3.4). Decreasing the moisture content of okara will improve the separation yields (see also next section). Options to get drier okara may include the use of centrifugal separation techniques using a higher *g*-time than the standard decanter (e.g. using a Sedicanter® (Flottweg Separation Technology, 2016)).

The addition of a belt press (also available from Flottweg or other companies) at the end of the current process may be another option, which may reduce the water content of okara from 80 to 65-70%. Please note that this is equal to an about 40% weight reduction. Direct treatment of okara is desirable versus re-diluting the waste stream. One such design can be seen in Figure 2.10. In this example filter press, okara is fed between two belts, the press belt and filter belt. The drive rollers cause these belts to turn, feeding the okara in between the press rollers that apply pressure to the okara. The filter belt contains holes that are designed to allow the filtrate to squeeze out into the collection area. The hole size will require investigation to achieve a similar solid content as the soybase, as well as being sufficiently large enough to not be frequently blocked with solids. If necessary, a vacuum can be applied to the filter bed to draw through more of the filtrate. This new soybase should be analysed for composition and sensory perception, in comparison to decanted soybase. Unfortunately, the design of the belt press is quite open to air in the processing facility and therefore hygienic control may not be easy.

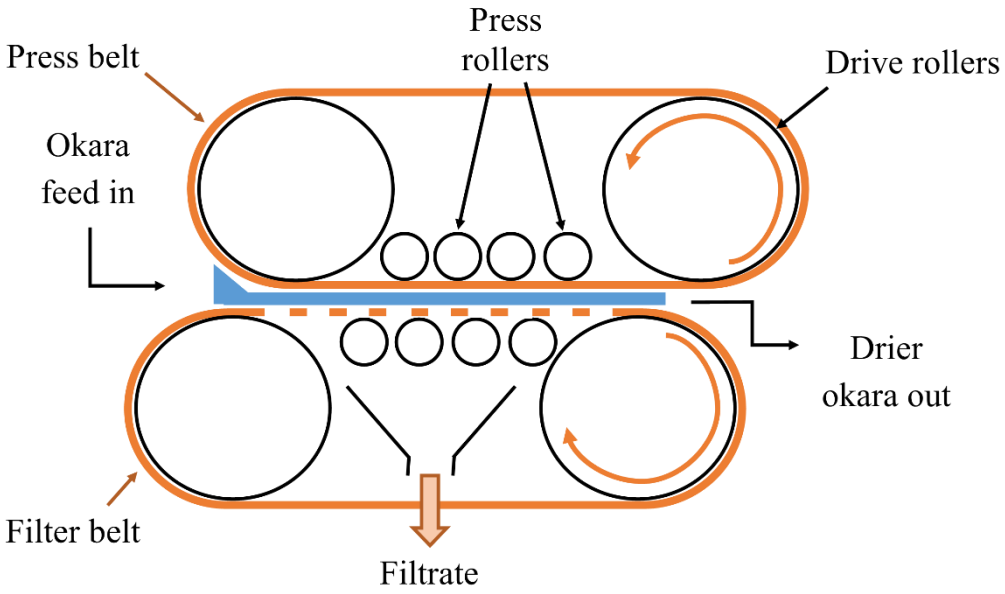


Figure 2.10. Illustration of a horizontal belt press. This example utilizes mechanical pressure to remove filtrate (soybase) from the cake (okara), thereby increasing its solid content from approximately 20 to 30-35%. Filter pressing is commonly utilised during wastewater treatment; e.g. raw sludge slurry containing 55% solids has been dewatered to 95% solids in previous reports (Chen, *et al.*, 2002).

## 2.4 A NOVEL MODEL FOR EXTRACTION

Previously a model was derived by Rosenthal *et al.* (1998), which described their results very well, relating the yield to the concentration in the 'solid' phase using a partition coefficient:

$$1/Yield = 6.52\left(S_\infty/L_\infty\right) + 1 \quad (2.1)$$

where:

$S_\infty$ Total mass of solid at the end of the extraction

$L_\infty$ Total mass of liquid at the end of the extraction

The use of more water (higher liquid-to-solid ratio) results in more protein dissolution and therefore higher extraction yields. Some of our own data could also be fitted well to their model, especially when performed at ambient temperature when protein aggregation did not happen (see Preece *et al.* (2015; **chapter 3**) for more information). The protein extraction yield could also be predicted well using another mechanistic model developed by Campbell and Glatz (2009) and measured D[4,3] values (see Section 2.3.3.1):

$$V_{I,i} = 4/3\,\pi(r_i - 55\ \mu\text{m})^3 \quad (2.2)$$

where:

$r_i$ Radius of particle size *i*

$V_{I,i}$ Volume of intact core of particles of size *i*

However, this model did not fit with the processed soybean microstructures we observed by CLSM (Preece *et al.*, 2015; **chapter 3**). We believe that, after a certain minimum of water needed to solubilise soy ingredients, protein dissolution in the aqueous phase is not the limiting factor in most cases, and it is also hard to see how extracted protein is going back to the solid phase in beans (as is suggested in the equilibrium model by Rosenthal *et al.* (1998)). Moreover, especially at high temperature of 80 °C and above at which whole bean extraction is commonly performed, soy proteins are mainly present (75-100%) in an aggregated, dispersed form with a particle size of about 0.1-1 micron in the liquid phase (soybase) (unpublished Unilever data).

Therefore, we would like to propose a new model. The protein extraction yield can be defined by the amount of protein in the soybase divided by the total amount of protein in both the soybase and okara; this yield is a function of both protein availability and separation efficiency as well:

$$Yield\ (\%) = \left[\frac{S \cdot x_{\mathrm{p,s}}}{(S \cdot x_{\mathrm{p,s}} + O \cdot x_{\mathrm{p,o}})}\right] \times 100\%$$

$$= Protein\ availability\ (\%) \times Separation\ efficiency\ (\%) \qquad (2.3)$$

where:

$S$ mass of soybase

$O$ mass of okara

$x_{\mathrm{p,s}}$ mass fraction of protein in soybase

$x_{\mathrm{p,o}}$ mass fraction of protein in okara

Protein availability is here defined as the percentage of proteins that can be solubilised or dispersed in the extraction medium, here water. It is affected by the mechanical disruption of cells and

solubilisation of compounds, whereas separation efficiency deals directly with the removal of solid materials. These two phenomenon can be observed pictorially in Figure 2.11. Within the slurry, it is possible to observe intact cells containing intact protein bodies, insoluble protein and solvent containing solubilised protein. Protein is classed as unavailable if it is insoluble, or still remains in intact cells, which both reside in the okara phase. Separation efficiency refers to the amount of solvent containing soluble protein that still remains in the okara feed. The moisture retained in the okara is believed to have the same concentration of protein as the soybase.

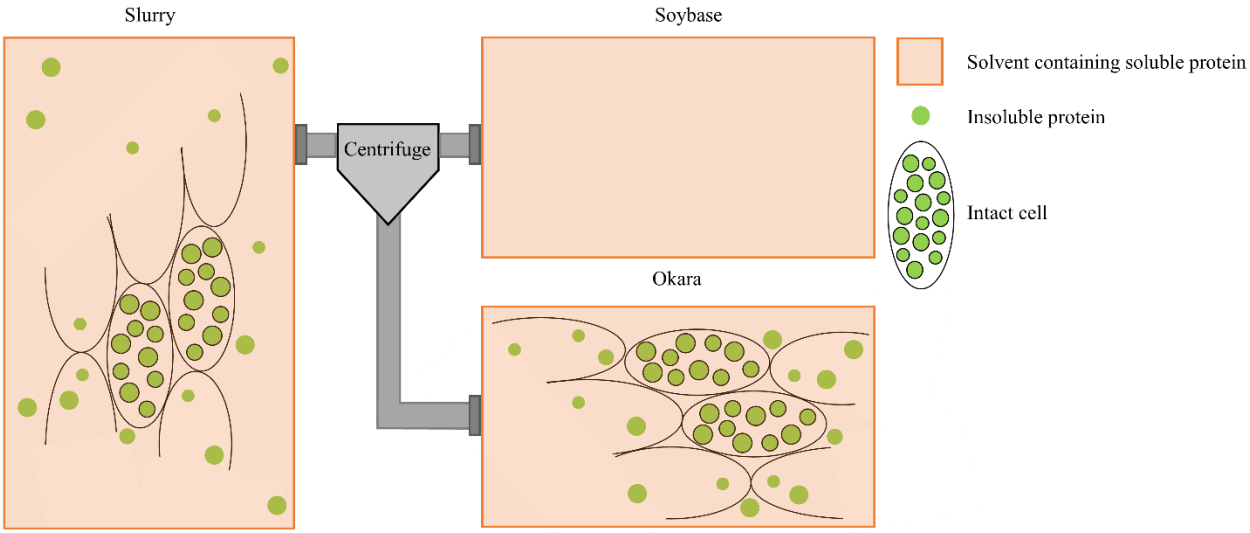


Figure 2.11. Pictorial representation to define accessibility of protein and separation efficiency during soybase production.

We hypothesise that the main losses in soy protein extraction yield are especially due to the high amount of okara and its water content, containing available proteins. Often the separation efficiency is not optimal. Of course, losses may also occur if the milling step is not optimal. After separation, okara still contains a large volume of water (about 80% w/w, see Figure 2.9) and commonly about 1-2 times more okara is produced than soybeans used in whole soybean extraction

(see Section 2.3.4). We propose that this high amount of water and the large amount of okara to be separated are the fundamental reasons why separation is more efficient at a higher liquid-to-solid ratio. This is illustrated by the equations and figure below.

The masses of soybean slurry (*Slu*) and soybase (*S*) can be expressed as:

$$Slu = B + W = S + O \tag{2.4}$$

where:

*Slu* mass of soy slurry

*B* dry mass of soybeans

*W* mass of water (either added or already present in the soybeans)

The mass here or below can be in weight (kg or ton), and can also be expressed per time (mass flow rate) when using a continuous set-up, without accumulation. Equation 2.4 can be rewritten as:

$$S = B + W - O \tag{2.5}$$

Assuming that the available proteins are equally distributed over the aqueous phase of soybase and the aqueous phase of okara, the separation efficiency can then be calculated by taking the ratio of the water phase in the soybase and the total water phase (in both soybase and okara):

$$\text{Separation efficiency (\%)} = \left[\frac{S \cdot x_{w,s}}{(S \cdot x_{w,s} + O \cdot x_{w,o})}\right] \times 100\% \tag{2.6}$$

where $x_{w,s}$ and $x_{w,o}$ are the fractions of water in the soybase and okara, respectively. Please note that the protein concentration is not present in equation 2.6, so it is applicable to soybeans with different protein contents as well as to partly solubilised protein conditions.

The liquid (*L*)-to-solid (*Sol*) ratio can be expressed as:

$$\frac{L}{Sol} = \frac{W}{B} \tag{2.7a}$$

which can be re-written as:

$$W = \frac{L}{Sol} \times B \tag{2.7b}$$

Addition of equation 2.7b into equation 2.5 and then 2.6 results into:

$$\text{Separation efficiency } (\%) = \frac{\frac{L}{Sol} \times B - O}{\frac{L}{Sol} \times B + B - O + \left(O \times \frac{x_{w,o}}{x_{w,s}}\right)} \times 100\% \tag{2.8}$$

Figure 2.12 shows that the separation efficiency becomes more efficient when more water is used. Again, this is not due to high protein solubility, but there is simply more aqueous soybase compared to (the water in) the okara phase at relatively higher water contents.

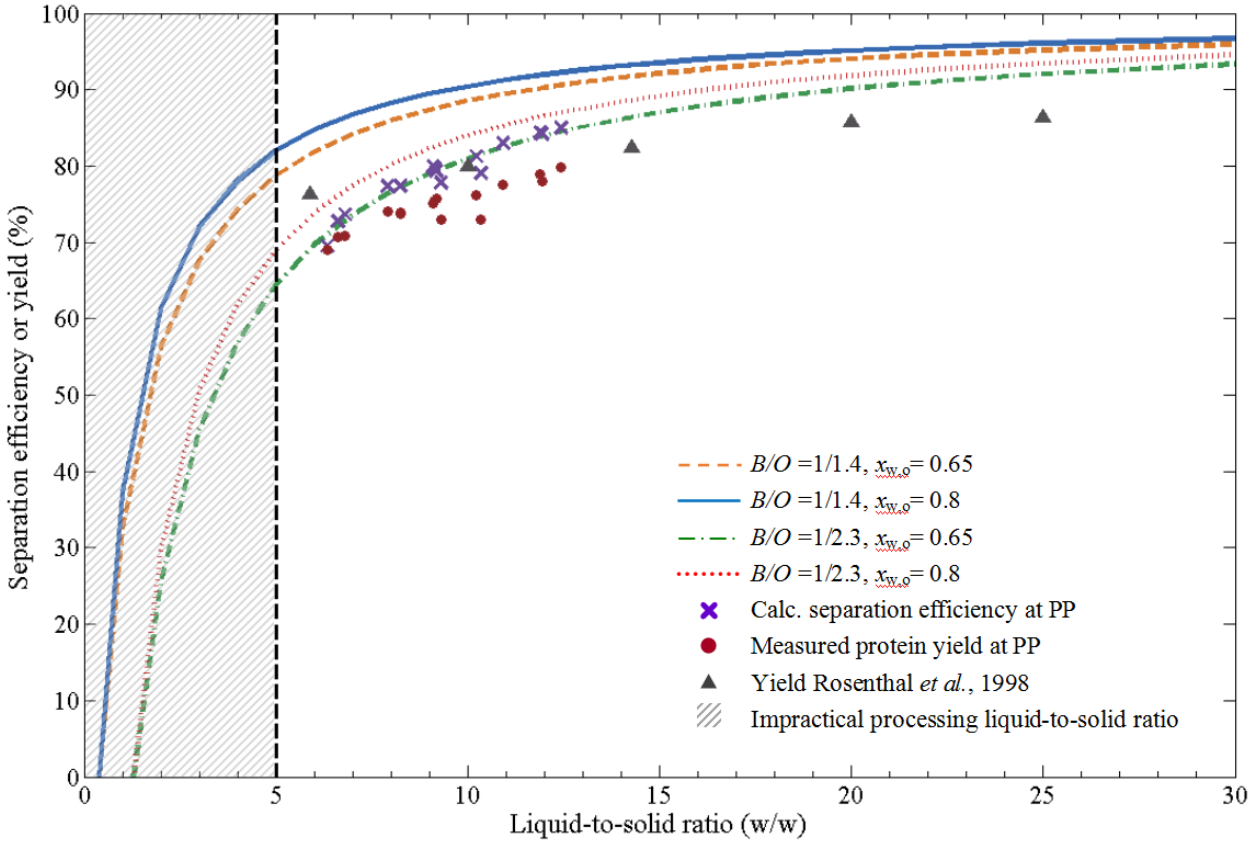


Figure 2.12. Separation efficiency or yield as a function of liquid-to-solid ratio. The separation efficiency lines were calculated using equation 2.8, assuming a mass of okara is either 1.4 or 2.3 times the mass of soybeans used. Also plotted in this figure are measured protein yields from a continuous soybean extraction process (like Process 1, see Figure 2.5 or Figure 2.6) at pilot scale at Unilever R&D Vlaardingen (●). Separation efficiencies were also calculated using equation 2.8 and real data, i.e. measured flow rates of soybeans (corrected for their moisture content), water and okara (**X**). On average the okara to dry bean flow rate ratio during the pilot plant experiments was 2.3 and the $x_{w,o}$ was approximately 0.8. Finally, the yields as obtained from Rosenthal *et al.* (1998) are also plotted here (▲).

The model above assumes that the protein or other ingredient concentration is equal in all phases, especially in soybase phase and the okara phase. This may not completely be true. If desired, one may introduce a correlation factor in the equations:

$$\frac{x_{\mathrm{p,o}}}{x_{\mathrm{p,s}}} = \omega \qquad (2.9)$$

And the *O* in the equations above needs to be multiplied with ω. E.g. equation 2.6 becomes then:

$$\text{Separation efficiency (\%)} = \left[\frac{S \cdot x_{w,s}}{(S \cdot x_{w,s} + \omega \cdot O \cdot x_{w,o})}\right] \times 100\% \qquad (2.10)$$

In Figure 2.12 we have also plotted the measured protein yields of whole soybean extraction performed at our pilot plant in Unilever Research & Development facilities, Vlaardingen, as well as the separation efficiency calculated using equation 2.8 (no correlation factor used here). The experimental data agrees very well with the theoretical lines: an $R^2$ value of 0.9442 was found for the pilot plant separation efficiencies shown in Figure 2.12. Interestingly, the calculated separation efficiencies using real flow rate data of the different masses from pilot-scale experiments are most often just slightly above the measured protein yield data (0.5-6% greater, see Figure 2.12). This indicates that very little protein was unavailable for extraction in our pilot-scale experiments; about 92-99% was available (see equation 2.3). Indeed we have found by CLSM that the milling process in the pilot plant was very efficient as no aggregated protein bodies outside cells and not many intact cells were found during soybean experiments at pilot plant, in contrast to soybean extraction performed at lab scale (Preece *et al.*, 2017c; **chapter 5**). During our lab scale extraction from whole soybeans (Preece *et al.*, 2015; **chapter 3**), the yields were lower due to observed protein aggregation or inefficient milling. However, a similar trend in yields as a function of liquid-to-solid ratio can still be observed and one may then calculate the yield by multiplying the separation efficiency with the amount of protein that is available for extraction (from 0-100%) according to equation 2.3. Unfortunately, such high yields as shown in Figure 2.12 are not common at factory scale, probably due to quick wear of the mills resulting in lower percentage of available protein.

Despite this very good agreement between theory and experimental data, we have measured that the protein content was often greater in okara during this pilot study ($\omega = 0.96$ at L/Sol of 6:1 to $\omega = 1.3$ times at L/Sol at 11:1 or higher). Both the protein concentration in the soybase ($x_{p,s}$) and in

the okara ($x_{p,o}$) decreased with higher L/Sol ratio, but not with the same magnitude. When studying the liquid-to-solid ratio, there is a limitation of parameter extremes due to processing equipment. It is impractical to study the process at L/Sol ratio below 5:1 due to difficulties with pumping the resultant wet solid and wear of the mills.

We also derived yield data from the study by Rosenthal *et al.* (1998) and plotted these in Figure 2.12 as well. Again, the theory and practical data agree very well with each other, although Rosenthal *et al.* (1998) obtained these with a very different system, with extraction from soybean flour at 50 °C and pH 8 at lab scale for 15 min whilst stirring at 200 rpm. They did not report amounts of okara and did not explain with their model the lower yield obtained at 80 °C.

The effects of okara mass ($O$) and okara moisture content ($x_{w,o}$) are also shown in Figure 2.12. Reducing the moisture content from 80%, typically achieved using a decanter centrifuge, to 65% improved the separation efficiency. A higher separation efficiency is also achieved if a mass reduction of okara production is attained. In Section 2.3.6 we discussed the use of belt press, which can reduce $x_{w,o}$ from 80 to 65% and $O$ by 40% (e.g. soybean/okara ratio ($B/O$) from 2.3 to 1/1.4, w/w). Figure 2.12 shows that an improvement of yield by 13-18% might then be achieved at L/Sol values of 7-5, respectively.

Please note that equation 2.7 can also be expressed with a solid-to-liquid ratio (instead of liquid-to-solid ratio) in a similar way, and this will give an almost linear plot that is very comparable to the results published by Rosenthal *et al.* (1998). Please also note that the extraction yield of oil and solids follow a similar dependency as function of liquid-to-solid ratio, although their values are not the same as the protein yield (Preece *et al.*, 2017a; **chapter 6**; 2017b; **chapter 4**; Rosenthal *et al.*, 1998).

As we argued above, a good fit with theory and experimental data is not a full proof of our model. The model is simple but not perfect, as shown by the measured difference in protein concentration in soybase and okara. However, we based our model on the soybean microstructures seen upon processing (see Figure 2.7 and previous article (Preece *et al.*, 2015; **chapter 3**)) and highlight for the first time (as far as we know) that the well-known L/Sol ratio effect on protein extraction yield is caused by the amount of okara and its moisture content.

## 2.5 CONCLUSIONS

In this review, aqueous extraction from whole soybeans has been detailed, with a focus on protein extraction. Soybeans commonly used for products like soymilk and tofu consist of about 40% proteins and 20% oil. Most of the soybean is build up by cotyledon cells which are 70-80 μm in length and 30-50 μm in width. The majority of the proteins are within 2-14 μm protein bodies surrounded by smaller oil bodies in these cotyledon cells. During a whole soybean extraction process, soybeans are first ground, and the intracellular components are then extracted into the medium followed by separation of the okara waste stream. The availability of a component depends on particle size of the plant matrix after grinding, the properties of the aqueous medium used (pH, ionic strength, temperature) and the incubation time. High temperature is needed to inactivate LOX and trypsin inhibitors, so a sacrifice is required when considering processing conditions for soybean processing between protein solubility and inactivation of anti-nutritional proteins. A sufficient amount of water needs to be used in the extraction process to ensure protein concentration in the soybase is below 5-6%, preventing aggregation and sedimentation. The amount of water used also influences the separation efficiency. At higher L/Sol ratio there is better separation than at lower L/Sol, as relatively less water containing protein stays in okara. This better separation results in higher yield. A novel model presented for the first time in this article explain this effect and agrees very well with experimental data. Unfortunately, the use of too much water will lower protein throughput and does not allow for product formulations with high protein content. The best process intensification options to consider might be the use of high pressure homogenisation and ways to obtain drier okara (e.g. decanters with higher centrifugal force, belt press). Less promising options seems to be the use of enzymes or ultrasound. The best, total extraction process for obtaining the

final product might be a compromise between the optimal conditions of each individual step. Both microstructural control and process science should play a role in the design of an optimal process. Aspects like sensorial quality and throughput (which affect costs) should be taken into account as well.

The current review focuses on whole soybean extraction processes, but we believe that some of these insights and also the model can be utilised for the study of other soy protein extraction processes (like SPC or SPI, see Figure 2.1). Extraction of other plant protein (such as pea, canola and lupin) and many other extraction processes in which the moisture content of the waste stream is high and entraps a notable amount of the desired component can also benefit from understanding the discussed information.

## 2.6 REFERENCES

Campbell, K. A., Glatz, C. E. (2009). Mechanisms of aqueous extraction of soybean oil. *J Agric Food Chem, 57,* 10904-10912.

Campbell, K. A., Glatz, C. E., Johnson, L. A., Jung, S., de Moura, J. M. N., Kapchie, V., Murphy, P. (2011). Advances in aqueous extraction processing of soybeans. *J Am Oil Chem Soc, 88,* 449-465.

Chen, G., Yue, P. L., Mujumdar A. S. (2002) Sludge dewatering and drying. *Drying Technol, 20:4-5,* 883-916.

de Almeida, N. M., de Moura Bell, J. M. L. N., Johnson, L. A. (2014). Properties of soy protein produced by countercurrent, two-stage, enzyme-assisted aqueous extraction. *J Am Oil Chem Soc, 91,* 1077-1085.

de Moura, J. M. L. N., Campbell, K., De Almeida, N. M., Glatz, C. E., Johnson, L. A. (2011). Protein extraction and membrane recovery in enzyme-assisted aqueous extraction processing of soybeans. *J Am Oil Chem Soc, 88,* 877-889.

Deak, N. A., Johnson, L. A. (2007). Effects of extraction temperature and preservation method on functionality of soy protein. *J Am Oil Chem Soc, 84,* 259-268.

Debruyne, I. (2006). Soy base extract: soymilk and dairy alternatives. In Riaz M.N. (Ed.), *Soy Applications in Food* (pp. 111-134). London: CRC Press.

Dumay, E., Chevalier-Lucia, D., Picart-Palmade, L., Benzaria, A., Gràcia-Julià, A., Blayo, C. (2013). Technological aspects and potential applications of (ultra) high-pressure homogenisation. *Trends in Food Science & Technology*, *31*(1), 13-26.

Esclapez, M. D., García-Pérez, J. V., Mulet, A., Cárcel, J. A. (2011). Ultrasound-assisted extraction of natural products. *Food Engineering Reviews*, *3*(2), 108.

Flottweg Separation Technology (2016). *Flottweg Sedicanter: Discover New Potentials.* Retrieved from: https://www.flottweg.com/fileadmin/user_upload/data/pdf-downloads/Sedicanter_EN.pdf

Gogate, P. R., Tayal, R. K., Pandit, A. B. (2006). Cavitation: a technology on the horizon. *Current Science*, *91*(1), 35-46.

González, A. D., Frostell, B., Carlsson-Kanyama, A. (2011). Protein efficiency per unit energy and per unit greenhouse gas emissions: potential contribution of diet choices to climate change mitigation. *Food Policy*, *36*(5), 562-570.

Gupta, R. P. (2014). *Taming of the Golden Bean*. Retrieved from: http://prosoya.com/wp-content/uploads/2014/03/taming.pdf

Huang, H. T., DuBois, C. M., Tan, C. B., Mintz, S. W. (2008). Early uses of soybean in Chinese history. *CM Du Bois, C.-B.Tan u.SW Mintz (Hg.), The World of Soy, Urbana/Chicago,* 45-55.

Imram, N., Gomez, I., Soh, V. (2003). Soya Handbook. *Tetra Pak, Singapore*.

Johnson, K. W., Synder, H. E. (1978). Soymilk: A comparison of processing methods on yields and composition. *J Food Sci, 43,* 349-353.

Kapchie, V. N., Towa, L. T., Hauck, C. C., Murphy, P. A. (2012). Recovery and functional properties of soy storage proteins from lab-and pilot-plant scale oleosome production. *J Am Oil Chem Soc, 89,* 947-956.

Kasai, N., Ikehara, H. (2005). Stepwise extraction of proteins and carbohydrates from soybean seed. *J Agric Food Chem, 53,* 4245-4252.

Kasai, N., Imashiro, Y., Morita, N. (2003). Extraction of soybean oil from single cells. *J Agric Food Chem, 51,* 6217-6222.

Kasai, N., Murata, A., Inui, H., Sakamoto, T., Kahn, R. I. (2004). Enzymatic high digestion of soybean milk residue (okara). *J Agric Food Chem, 52,* 5709-5716.

Kinsella, J. (1979). Functional properties of soy proteins. *J Am Oil Chem Soc, 56,* 242-258.

Knorr, D., Zenker, M., Heinz, V., Lee, D. U. (2004). Applications and potential of ultrasonics in food processing. *Trends Food Sci Tech, 15,* 261-266.

Kwok, K. C., Liang, H. H., Niranjan, K. (2002). Optimizing conditions for thermal processes of soy milk. *J Agric Food Chem, 50,* 4834-4838.

Kwok, K. C., Niranjan, K. (1995). Review: Effect of thermal processing on soymilk. *Int J Food Sci Tech, 30,* 263-295.

Lakemond, C. M., de Jongh, H. H., Hessing, M., Gruppen, H., Voragen, A. G. (2000). Heat denaturation of soy glycinin: influence of pH and ionic strength on molecular structure. *J Agric Food Chem, 48,* 1991-1995.

Li, H., Pordesimo, L., Weiss, J. (2004). High intensity ultrasound-assisted extraction of oil from soybeans. *Food research international*, *37*(7), 731-738.

Li, B., Qiao, M., Lu, F. (2012). Composition, nutrition, and utilization of okara (Soybean Residue). *Food Rev Int, 28*, 231-252.

Ma, C. Y., Liu, W. S., Kwok, K. C., Kwok, F. (1996). Isolation and characterization of proteins from soymilk residue (okara). *Food Res Int, 29,* 799-805.

Maruyama, N., Sato, R., Wada, Y., Matsumura, Y., Goto, H., Okuda, E., Nakagawa, S., Utsumi, S. (1999). Structure–physicochemical function relationships of soybean β–conglycinin constituent subunits. *J Agric Food Chem, 47*, 5278-5284.

Murphy, P. A. (2008). Soybean proteins. In L.A. Johnson, P. J. White, R. Galloway (Eds.), *Soybeans - Chemistry, production, processing and utilization* (pp. 229-267). Urbana: AOCS Press.

Ouhida, I., Perez, J. F., Gasa, J. (2002). Soybean (Glycine max) cell wall composition and availability to feed enzymes. *J Agric Food Chem, 50,* 1933-1938.

Pace, C. N., Trevino, S., Prabhakaran, E., Scholtz, J. M. (2004). Protein structure, stability and solubility in water and other solvents. *Philosophical Transactions of the Royal Society of London B: Biological Sciences*, *359*(1448), 1225-1235.

Patist, A., Bates, D. (2008). Ultrasonic innovations in the food industry: From the laboratory to commercial production. *Innovative food science & emerging technologies, 9*(2), 147-154.

Peng, X., Ren, C., Guo, S. (2016). Particle formation and gelation of soymilk: Effect of heat. *Trends Food Sci Tech, 54,* 138-147.

Peng, X., Wang, Y., Xing, J., Wang, R., Shi, X., Guo, S. (2017). Characterization of particles in soymilks prepared by blanching soybeans and traditional method: A comparative study focusing on lipid-protein interaction. *Food Hydrocolloids*. *63,* 1-7.

Preece, K. E., Drost, E., Hooshyar, N., Krijgsman, A., Cox, P. W., Zuidam, N. J. (2015). Confocal imaging to reveal the microstructure of soybean processing materials. *J Food Eng, 147,* 8-13.

Preece, K. E., Hooshyar, N., Krijgsman, A. J., Fryer, P. J., Zuidam, N. J. (2017a). Intensification of protein extraction from soybean processing materials using hydrodynamic cavitation. *Innov Food Sci Emerg Technol., 41, 47-55.*

Preece, K. E., Hooshyar, N., Krijgsman, A., Fryer, P. J., Zuidam, N. J. (2017b). Intensified soy protein extraction by ultrasound. *Chem Eng Process, 113,* 94-101.

Preece, K. E., Hooshyar, N., Krijgsman, A. J., Fryer, P. J., Zuidam, N. J. (2017c). Pilot-scale ultrasound-assisted extraction of protein from soybean processing materials shows it is not recommended for industrial usage. *J Food Eng, 206,* 1-12.

Reynolds, L. P., Wulster-Radcliffe, M. C., Aaron, D. K., Davis, T. A. (2015). Importance of animals in agricultural sustainability and food security. *J Nutr, 145,* 1377-1379.

Riaz M.N. (2006). Processing of soybeans into ingredients. In *Soy Applications in Food* (pp. 39-63). London: CRC Press,Taylor & Francis Group.

Rosenthal, A., Pyle, D. L., Niranjan, K. (1998). Simultaneous aqueous extraction of oil and protein from soybean: Mechanisms for process design. *Trans IChemE, Part C, 76,* 224-230.

Rosenthal, A., Pyle, D. L., Niranjan, K., Gilmour, S., Trinca, L. (2001). Combined effect of operational variables and enzyme activity on aqueous enzymatic extraction of oil and protein from soybean. *Enzyme and Microb Technol, 28,* 499-509.

Rosenthal, A., Deliza, R., Cabral, L. M., Cabral, L. C., Farias, C. A., Domingues, A. M. (2003). Effect of enzymatic treatment and filtration on sensory characteristics and physical stability of soymilk. *Food Control, 14,* 187-192.

Rosset, M., Acquaro, V. R., Beléia, A. D. P. (2014). Protein extraction from defatted soybean flour with Viscozyme L pretreatment. *J Food Process Preserv, 38*(3), 784-790.

Russin, T. A., Arcand, Y., Boye, J. I. (2007). Particle size effect on soy protein isolate extraction. *J Food Process Pres, 31,* 308-319.

Salunkhe, D. K., Chavan, J. K., Adsule, R. N., Kadam, S. S. (1992). *World oilseeds: Chemistry, technology and utilization*. New York: AVI.

Sari, Y. W., Mulder, W. J., Sanders, J. P., Bruins, M. E. (2015). Towards plant protein refinery: review on protein extraction using alkali and potential enzymatic assistance. *Biotechnol J, 10*(8), 1138-1157.

Savage, G. P. (2003). Trypsin inhibitors. In *Encylopedia of food sciences and nutrition* (2nd ed). (pp. 5878-5884). Cambridge: Academic Press.

Shirsath, S. R., Sonawane, S. H., Gogate, P. R. (2012). Intensification of extraction of natural products using ultrasonic irradiations—a review of current status. *Chemical Engineering and Processing: Process Intensification, 53,* 10-23.

Tiwari, B. K., Mason, T. J. (2012). Chapter 6 - Ultrasound Processing of Fluid Foods. In P.J.Cullen, K. T. Brijesh, V. Vasilis, & V. Vasilis (Eds.), *Novel Thermal and Non-Thermal Technologies for Fluid Foods* (pp. 135-165). San Diego: Academic Press.

Toda, K., Chiba, K., Ono, T. (2007). Effect of components extracted from okara on the physicochemical properties of soymilk and tofu texture. *J Food Sci, 72,* C108-C113.

Tomos, D. (2000). The plant cell pressure probe. *Biotechnology letters*, *22*(6), 437-442.

Van Der Ven, C., Matser, A. M., Van den Berg, R. W. (2005). Inactivation of soybean trypsin inhibitors and lipoxygenase by high-pressure processing. *J Agric Food Chem, 53,* 1087-1092.

Vishwanathan, K. H., Singh, V., Subramanian, R. (2011a). Influence of particle size on protein extractability from soybean and okara. *J Food Eng, 102,* 240-246.

Vishwanathan, K. H., Singh, V., Subramanian, R. (2011b). Wet grinding characteristics of soybean for soymilk extraction. *J Food Eng, 106,* 28-34.

Waschatko, G., Junghans, A., Vilgis, T. A. (2012). Soy milk oleosome behaviour at the air-water interface. *Faraday discuss, 158,* 157-169.

Weiss, J., Kristbergsson, K., Kjartansson, G. T. (2011). Engineering food ingredients with high-intensity ultrasound. In *Ultrasound technologies for food and bioprocessing* (pp. 239-285). New York: Springer.

White, J., Welsby, D., Kolar, C. (23-5-2013). *Neutral beverage and other compositions and process for making same*. Publication no. US20130129879.

Zhang, Z., Stenson, J. D., Thomas, C. R. (2009). Micromanipulation in mechanical characterisation of single particles. *Advances in Chemical Engineering, 37,* 29-85.

# CHAPTER 3

# CONFOCAL IMAGING TO REVEAL THE MICROSTRUCTURE OF SOYBEAN PROCESSING MATERIALS

This chapter is based on a published manuscript:

Preece, K.E., Drost, E., Hooshyar, N., Krijgsman, A.J., Cox, P.W., & Zuidam, N.J. (2015). Confocal imaging to reveal the microstructure of soybean processing materials. *J Food Eng, 147*, 8-13.

## ABSTRACT

Sustainable production of food products for human consumption is required to reduce negative impacts on the environment and to consumer's health. Soybeans are an excellent source of nutritive plant proteins; aqueous extraction yields part of the available oil and protein from the legume. Many studies have been conducted which detail the various processing parameters and their effects on the extraction yields, however there is little data on the localisation of nutritive components such as oil and protein in the fibrous unextracted by-product. Here we show a novel confocal laser scanning microscopy investigation of soybean processing materials and the physical effects of thermal treatment on the materials microstructure upon aqueous extraction. Various features, more specifically oil, protein (including protein aggregation) and cell wall structures, are visualised in the fibrous by-product, soy slurry and soybase, with their presence both in the continuous phase and within intact cotyledon cells. Thermal treatment reduced the protein extraction yield; this is shown to be a result of aggregated protein bodies in the continuous phase and within intact cotyledons cells. Knowledge of the processing material microstructures can be applied to improve extraction yields and reduce waste production.

## 3.1 INTRODUCTION

In recent years, sustainable food supply has become a prevalent topic for consumers, industry and the scientific community (Adams and Demmig-Adams, 2013; Aiking, 2011; Cakmak, 2001; Leiserowitz *et al.*, 2006; Pimentel and Pimentel, 2003). With the world population projected to increase by 2.3 billion inhabitants by 2050, the need to address uncertain food supplies is required at this moment to prevent malnutrition in coming years (Bruinsma, 2014). Adams and Demmig-Adams (2013) approach the topic by considering it not a question of plant- versus meat-based diets causing the most undesirable environmental and health issues, but more the methods chosen for animal rearing or crop production which makes a greater contribution to sustainability. However, no consideration is given for the post-processing during food manufacture. Processing of food sources requires examination to yield the most value from land available for agriculture, which will be limited by urbanisation and water required for their production in the near future. To maximise the availability of nourishment for human consumption, the extraction of health-promoting components also requires optimisation.

Used for a broad range of products, the soybean crop is versatile, and produces good quality protein for human consumption (Masuda and Goldsmith, 2009). Aqueous extraction of components from soybeans is currently undertaken for the production of some soy-based products, such as soymilk and tofu. The most frequent aqueous extraction protocol involves the grinding of dried soybeans with hot aqueous solution prior to the removal of insoluble fibrous material, termed okara (Giri and Mangaraj, 2012). The protein extraction yield of the described process is less than desirable, with a large fraction, typically 25-40% (dry basis) of soy proteins being separated into the fibrous by-product, termed okara (Campbell *et al.*, 2011; Kasai and Ikehara, 2005; O'Toole, 1999; Rosenthal

*et al.*, 1998). Most commonly usage of the by-product is not widely employed due to the uneconomical resale value of soy fibre products. More sustainable processing for food production could result in nutritious material being used for human sustenance (Jankowiak *et al.*, 2014), rather than exiting the process within a waste stream, not limited just to soy milk and tofu preparation.

The microstructure of the starting material for extraction, the soybean, has been well studied (Bair and Snyder, 1980; Horisberger *et al.*, 1986; Lili *et al.*, 2013; Rosenthal *et al.*, 1998; Tombs, 1967). The soybean is mainly comprised of cotyledon cells; oval in shape, 15-20 μm in diameter and 70-80 μm long, and consisting of lipid and protein bodies, in the size ranges of 0.2-0.5 μm and 8-20 μm respectively (Rosenthal *et al.*, 1998). The protein bodies account for 60-80% of the total soybean protein content, consisting of storage proteins glycinin and β-conglycinin, confirmed using an immunogold method (Horisberger *et al.*, 1986). Techniques used to deduce the microstructure of soybeans, including electron microscopy and fluorescence microscopy, possess limiting factors ranging from laborious sample preparation prior to visualisation and/or poor resolution, which prevent their routine use.

Previously studies to investigate ways to increase the extraction yields of health-promoting components from soybeans have been conducted (Giri *et al.*, 2012; Rosenthal *et al.*, 1998; Vishwanathan *et al.*, 2011). Yet there is a lack of understanding of the microstructure of processing materials which is crucial for achieving greater extraction yields. With this information, processing which targets the exposed restraints can be employed to improve their extraction yields. In this paper we show the location of oil and protein in soybase, soy slurry and okara, alongside the effects of heat treatment using confocal laser scanning microscopy (CLSM).

## 3.2 MATERIALS AND METHODS

### 3.2.1 Materials

All extractions and microstructural investigations were carried out using commercially available soybeans from the same batch. Soybeans were stored in an airtight container prior to processing. All extractions were carried out using demineralised water, and resulting samples were stored at 4°C before analysis. Fluorescent dyes for confocal laser scanning microscopy were purchased from various suppliers; acridine orange (Polysciences Inc., Warrington, PA), nile blue A (Janssen Chimica, Belgium) and rhodamine B (Merck, Germany) were investigated. All materials utilised for the SDS-PAGE were purchased from Bio-Rad Laboratories, California, USA.

### 3.2.2 Sample preparation

This methodology has been adapted from a previous method in a patent (Wijngaard & Zuidam, WO14154472, 2014). To prepare soy processing materials, dried soybeans were coarsely ground in demineralised water at a soybean:water ratio of 1:6 (w/w) with a commercial blender (Varoma Thermomix, Vorwerk, Germany) (10 min, 80 °C (final temperature approximately 85 °C)), levels 2-8 stepwise) and ground finely using a high shear mixer (Silverson L4RT, Silverson Machines International, UK) (20 min, 3000-6500 rpm stepwise (final temperature approximately 70 °C)) to produce a soy slurry. The resultant soy slurry (pH 6.45) was immediately centrifuged at 4249×$g$ for 10 min to separate the soybase (pH 6.39) from the fibrous insoluble okara. This is presented in a process flow diagram in Figure 3.1.

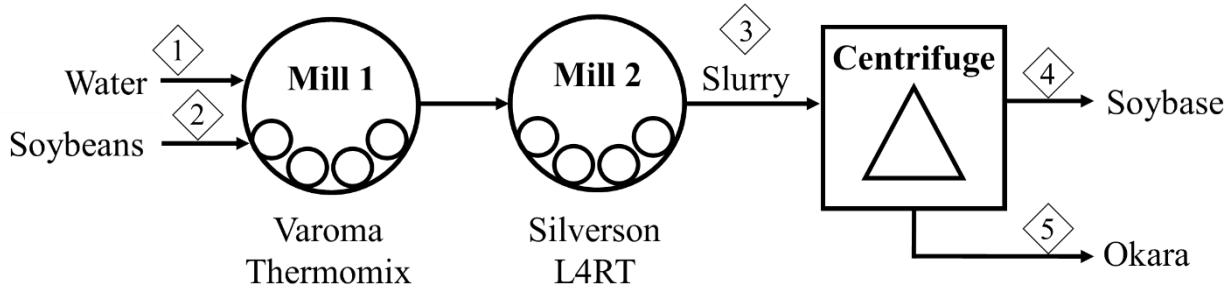


$$\text{Total mass in} = \text{Total mass out} + \text{Accumulation}$$

$$\therefore \text{ Overall: } 1 + 2 = 3 \neq 4 + 5$$

Figure 3.1. Process flow diagram for the lab-scale preparation of slurry, soybase and okara for visualisation. Milling was carried out at 80 °C and at ambient temperature to study the effects of thermal treatment.

To prepare soy milk soybeans are commonly extracted at temperatures between 80-100 °C to minimise lipid oxidation by enzymes and denature trypsin inhibitors. Non-heat treated protein extraction was also carried out at ambient temperature as a control. After a total of 30 min grinding, the soy slurry increased to 41.4 °C as no temperature control was performed, which is well below the denaturation temperatures for the main storage proteins, β-conglycinin and glycinin (68 °C and 86 °C, respectively; Peng *et al.*, 2016). The mass balances for protein, water and other component streams is shown for both the extraction at 80 °C (Table 3.1A) and at ambient temperature (Table 3.1B). For both extraction systems, the mass balance was incomplete and components were lost throughout the process. During the extraction, the slurry had to be transferred from one mill to another, then into centrifugation tubes. Although care was taken to remove all of the product during transfer, 10-15% of the total mass was lost during processing. This information was utilised to calculate extraction yields based on the distribution of components over the various material streams.

Table 3.1A. Mass balance of protein, water and other components during soybase and okara production at 80 °C. Stream numbers correspond to streams presented in Figure 3.1.

| | **In** | | | | | **Out (80 °C grinding)** | | | | | | |
|---|---|---|---|---|---|---|---|---|---|---|---|---|
| **Stream** | 1 | | 2 | | Total (1 + 2) | 4 | | 5 | | Total (4 + 5) | Total loss | |
| **Component** | Mass | % wt. | Mass | % wt. | Mass | Mass | % wt. | Mass | % wt. | Mass | Mass | % |
| **Solid** | **0** | **0** | **127** | **91** | **127** | **45** | **8** | **72** | **20** | **117** | **10** | **8** |
| **Protein** | - | - | 50 | 36 | 50 | 18 | 3 | 26 | 7 | 44 | 6 | 11 |
| **Other (fibres, oil, etc.)** | - | - | 77 | 55 | 77 | 27 | 5 | 46 | 13 | 73 | 4 | 6 |
| **Water** | **860** | **100** | **13** | **9** | **873** | **499** | **92** | **282** | **80** | **781** | **92** | **11** |
| **Total** | 860 | | 140 | | 1000 | 544 | | 354 | | 898 | 102 | 10 |

Table 3.1B. Mass balance of protein, water and other components during soybean processing involving ambient temperature grinding. Please refer to Figure 3.1 for assignment of stream numbers.

| | **In** | | | | | **Out (ambient temperature grinding)** | | | | | | |
|---|---|---|---|---|---|---|---|---|---|---|---|---|
| **Stream** | 1 | | 2 | | Total (1 + 2) | 4 | | 5 | | Total (4 + 5) | Total loss | |
| **Component** | Mass | % wt. | Mass | % wt. | Mass | Mass | % wt. | Mass | % wt. | Mass | Mass | % |
| **Solid** | **0** | **0** | **127** | **91** | **127** | **63** | **10** | **44** | **19** | **107** | **20** | **16** |
| **Protein** | - | - | 50 | 36 | 50 | 23 | 4 | 25 | 11 | 48 | 2 | 4 |
| **Other (fibres, oil, etc.)** | - | - | 77 | 55 | 77 | 41 | 6 | 18 | 8 | 59 | 18 | 24 |
| **Water** | **860** | **100** | **13** | **9** | **873** | **568** | **90** | **188** | **81** | **756** | **117** | **13** |
| **Total** | 860 | | 140 | | 1000 | 631 | | 232 | | 863 | 137 | 14 |

### 3.2.3 Determination of protein & moisture contents

Okara, soybase and soy slurry samples were analysed for protein concentration using the Dumas method (Vario MAX CNS, Elementar Analysensysteme GmbH, Germany) and L(+)-glutamic acid (VWR International BVBA, Belgium) as a standard (Jung *et al.*, 2003). From the nitrogen content the protein concentration was calculated with a protein conversion factor of 6.25×N. The extraction yields were determined using equation 3.1, where $mass_{p,s}$ is the mass of protein in the soybase and $mass_{p,o}$ is the mass of protein found in okara.

$$\text{Protein extraction yield } (\%) = \frac{\text{mass}_{\text{p,s}}}{(\text{mass}_{\text{p,s}}+\text{mass}_{\text{p,o}})} \times 100\% \qquad (3.1)$$

Protein concentrations are determined on a wet basis (w.b.). Moisture content was also determined for all samples using a microwave moisture analysis system (SMART System5, CEM GmbH, Germany).

All of the analytical measurements were carried out in triplicate for each sample.

### 3.2.4 Particle size analysis

Particle sizes of samples were measured using laser diffraction techniques, using Mastersizer 2000 Hydro S (Malvern Instruments Ltd, UK). Refractive indices of 1.33 and 1.45 were used for the dispersant and particles respectively.

### 3.2.5 Confocal laser scanning microscopy (CLSM)

Soy microstructures were visualised by confocal microscopy using Leica TCS-SP5 coupled with DMI6000 inverted optical microscope (Leica Microsystems Inc., Germany). Fluorochromes were selected based on their affinity to associate with various components within the samples; acridine orange, nile blue and rhodamine B were shortlisted. The dyes excitation and emission wavelength,

including the user set colours for emitted light, are shown in Table 3.2. For all samples, one drop of dye stock solution was added to 1-1.5 mL of sample and mixed well before slide preparation, which is less tedious and time consuming than previously reported techniques. The microscope is equipped with three lasers for excitation: an Argon laser ($\lambda_{excitation}$ 488 nm), a Diode-Pumped-Solid-State laser ($\lambda_{excitation}$ 561 nm) and a Helium-Neon laser ($\lambda_{excitation}$ 633 nm). For the visualisation of samples using nile blue, emission caused by the excitation laser is avoided by using sequential scanning. A 40× oil immersion objective (1.25 NA) was utilised for visualisation of all materials.

Table 3.2. Excitation & emission settings for dye stock solutions used for confocal laser scanning microscopy.

| Dye | Excitation wavelength (nm) | Emission wavelengths (nm) | Corresponding colour in micrographs |
|---|---|---|---|
| **1% w/v Acridine orange** | 488 | 497-556 | Green |
| | 561 | 569-646 | Red |
| | | 655-724 | Blue |
| **1% w/v Nile blue** | 488 | 520-626 | Green |
| | 633 | 662-749 | Red |
| **0.5% w/v Rhodamine B** | 488 | 492-555 | Green |
| | | 566-631 | Red |
| | | 645-751 | Blue |

More information on the theory of confocal microscopy can be found in Appendix 8.2.1.

## 3.3 RESULTS & DISCUSSION

Acridine orange was used to visualise a soy slurry sample using confocal microscopy; Figure 3.2 shows a representative micrograph. Intact cotyledon cells are present within soy slurry containing intact intracellular material: areas emitting purple in colour, a combination of blue and red are the oleosins around oil bodies and areas emitting green are protein bodies. Similar structures found within soybean flour were observed by transmission electron microscopy (TEM) (Campbell and Glatz, 2009). In the extraction medium (outside the intact cells), agglomerated material depicted in green was observed within the size range approximately 5-20 µm. The wavelength at which the material in the aqueous medium emits fluorescence (497-556 nm, green), and their size both suggest that the material consist of aggregated protein bodies. To confirm that the agglomerated material in the continuous phase were not starch granules; iodine solution was used in conjunction with light microscopy. No significant purple-black staining of the observed extracellular features occurred when examined using light microscopy, confirming the material was not starch (data not shown). However, it is important not to neglect that starch grains are present within the soybean, and subsequently starch is present in the soy slurry (He *et al.*, 2007). A number of extracellular materials can be visualised in the aqueous medium and within intact cotyledon cells using acridine orange.

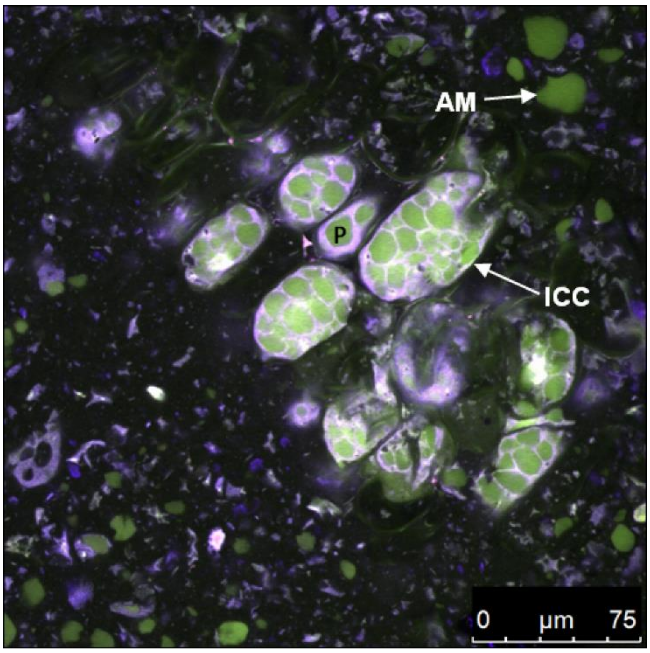


Figure 3.2. Representative confocal laser scanning micrograph of soy slurry sample obtained after grinding at 80 °C with acridine orange. Examples of intact cotyledon cells (ICC), protein bodies within cotyledon cells (P, green) and agglomerated material (AM, green) are annotated on the image. Fibrous material appears as a combination of blue and red emission, i.e. purple.

To verify the composition of agglomerated material observed in the soy slurry using acridine orange (Figure 3.2), a dye specifically used to label proteins was explored; rhodamine B. Agglomerated material was visualised in soy slurry when rhodamine B was employed for protein localisation, shown in Figure 3.3. Protein within intact cotyledon cells was also revealed using rhodamine B; rhodamine B associated with aggregated material in the aqueous medium was shown to emit fluorescence at the same wavelength as dye associated with protein bodies located within the cells. The use of rhodamine B further confirms the agglomeration of protein in- and outside the cotyledon cells when the soy slurry was thermally processed.

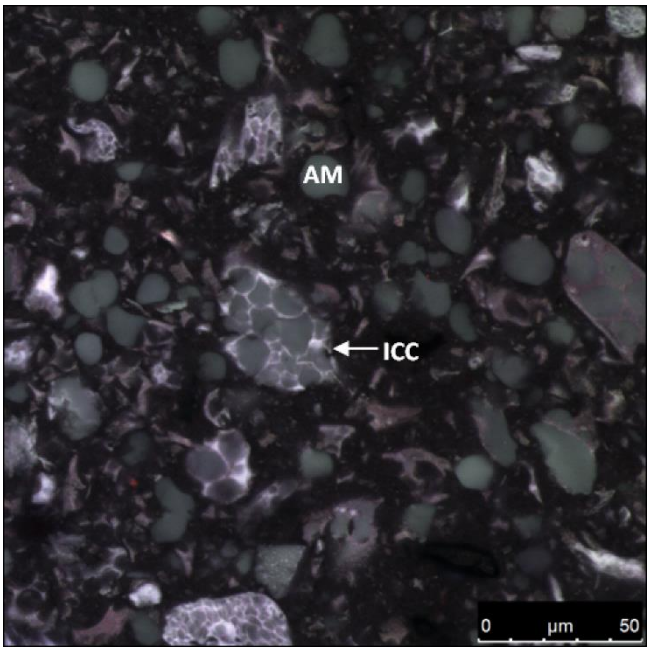


Figure 3.3. Confocal micrograph of soy slurry with preparation including thermal treatment (80 °C), stained using rhodamine B. Examples of agglomerated material (AM) and intact cotyledon cells (ICC) are labelled in the figure. Proteinaceous material is highlighted using this fluorochrome.

Nile blue is primarily used as a lipid stain; lipids are also considered an important substituent of soybeans when performing an extraction (Rosenthal *et al.*, 1998), which are not visualised using acridine orange or rhodamine B due to their poor solubility in oil. In Figure 3.4, lipids are depicted green and other apolar material red in the soy slurry prepared at room temperature. Clusters of cell wall material were present in the soy slurry, which appears to contain only aqueous media; protein and oil have been extracted. During grinding of the soybeans, the cell wall is disrupted which exposes the intracellular components from within the cell to the aqueous medium for diffusion of the internal components into the extraction medium (Campbell *et al.*, 2009). The agglomerated material in the size range 5-20 µm presented in Figures 3.2 and 3.3 are absent using nile blue in the soy slurry when extraction was performed at ambient temperature.

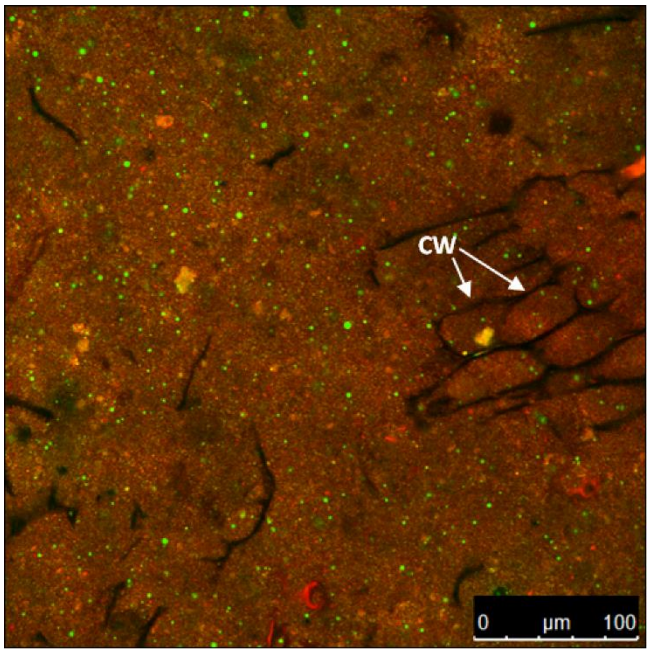


Figure 3.4. Confocal micrograph of soy slurry prepared at ambient temperature, stained with fluorochrome nile blue. Oil is represented in the colour green and other apolar material, including protein, in red. Examples of cotyledon cell wall material (CW, black lines) are annotated on the image.

Agglomerated material (most likely protein bodies) as shown in Figures 3.2 and 3.3 are also visible in Figure 3.5 (depicted in red), which is obtained by CSLM of a soy slurry prepared at 80 °C and visualised with nile blue. The agglomerated material is surrounded by green dots, which are most likely liberated oil bodies. It has been suggested before that heating whilst grinding aqueous soy slurry causes proteinaceous material to aggregate due to denaturation (Nishinari *et al.*, 2014). Thermal denaturation of the main storage proteins β-conglycinin and glycinin occurs in the ranges 68 °C and 86 °C, respectively, which accounts for aggregation when soybeans were ground at 80 °C (Peng *et al.*, 2016). Aggregation of supernatant protein of a size less than 40 nm occurs upon heating of soymilk to increase the concentration of protein particles in the size range 40-110 nm (Ono *et al.*, 1991). The present study suggests that the protein bodies already aggregate prior to protein solubilisation in the aqueous phase at 80 °C, as their size did not change.

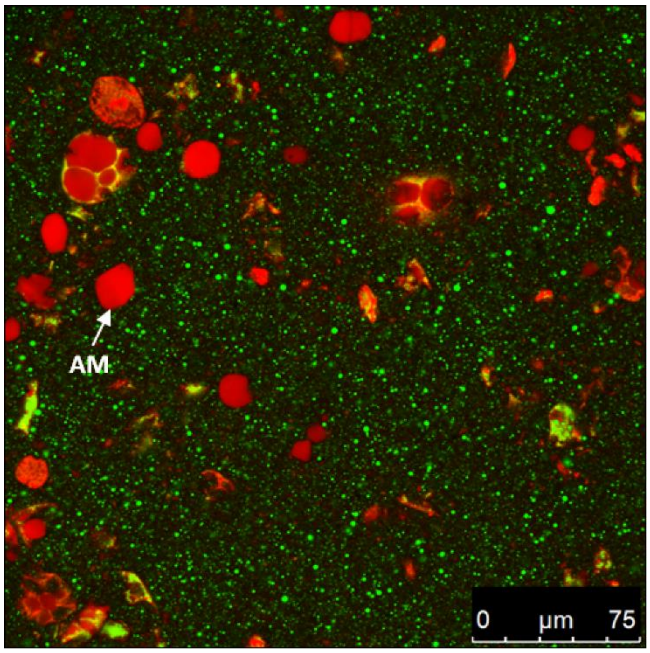


Figure 3.5. A representative confocal micrograph of soy slurry with preparation including thermal treatment (80 °C) visualised with nile blue. Oil is presented in green and agglomerated material within the heat treated sample (also labelled AM), is depicted in red.

Approximately 26% more protein is extracted into the soybase when no thermal treatment is applied compared to extraction at 80 °C in this present study (Table 3.3), which has also been observed in the literature (Campbell *et al.*, 2011; Johnson & Snyder, 1978; Rosenthal *et al.*, 1998). The difference in protein extraction yields is not due to differences in particle sizes ($D_{4,3}$ and $D_{3,2}$) as the efficiency of grinding is not extensively affected by thermal treatment (Table 3.4). One may assume that only cells which are broken release their (protein) content. Campbell *et al.* (2011) suggested that for complete extraction to occur, the particle size needs to be in the size range of individual cotyledon cells, which assumes all cells are broken. It was assumed that only soybean cells on the outside of milled flour are disrupted resulting in a lower extraction yield with larger particle sizes of the milled flour. This was not the case when observing soy slurry in the present study; intact cotyledon cells were normally found singularly (see Figures 3.2-3.5 and 3.7). With

combined flaking and pin milling of soybeans approximately 95% of cotyledon cells were disrupted when 57% of the total flour volume was made up of particles smaller than 55 µm, as confirmed using microscopy (Campbell and Glatz, 2009).

Table 3.3. Summary of protein extraction yield, protein availability and predicted yields by [a]Campbell and Glatz (2009) and [b]Rosenthal *et al.* (1998).

| Processing conditions | Protein extraction yield (%) | Total protein availability (%) | Predicted protein extraction yield[a] (%) | Predicted protein extraction yield[b] (%) |
|---|---|---|---|---|
| **Ambient temperature grinding** | 67.3 ± 1.9 | 89.7 ± 1.9 | 70.3 ± 2.2 | 74.3 ± 0.1 |
| **80 °C grinding** | 41.5 ± 0.2 | 64.9 ± 0.2 | 70.9 ± 2.2 | 63.8 ± 0.6 |

Table 3.4. Soy slurry processing conditions and resulting extraction yield and concentration of protein within the by-product, okara.

| Processing conditions | Particle size | | Soybase | | Okara | |
|---|---|---|---|---|---|---|
| | $D_{4,3}$ (µm) | $D_{3,2}$ (µm) | Protein content (w.b.) (%) | Water content (%) | Protein content (w.b.) (%) | Water content (%) |
| **Ambient temperature grinding** | 330.8 ± 16.6 | 17.5 ± 1.0 | 3.6 ± 0.3 | 90.0 ± 0.1 | 4.7 ± 0.04 | 81.2 ± 0.1 |
| **80 °C grinding** | 267.8 ± 24.3 | 20.9 ± 1.9 | 3.4 ± 0.02 | 91.7 ± 0.6 | 7.3 ± 0.3 | 79.7 ± 0.6 |

Aggregated protein bodies were observed in the soy slurry processed at 80 °C (Figure 3.4). After separation by centrifugation, the soybase did not contain the visualised aggregated protein bodies. Figure 3.6 shows the presence of only small (<5 µm) colloidal material homogenously dispersed throughout the aqueous environment, with fragmented fibrous material also visible. The absence

of the agglomerated material in the soybase after separation of insoluble material could be used to explain the reduced protein extraction upon thermal treatment. A higher protein extraction yield was obtained upon processing at ambient temperature than after processing at 80 °C (67% versus 42% respectively, see Table 3.3). However, aqueous extraction from soybeans at an elevated temperature is essential for the production of a flavoursome and safe final product due to the prevention of the enzyme lipoxygenase and trypsin inhibitors actions (Nik *et al.*, 2009).

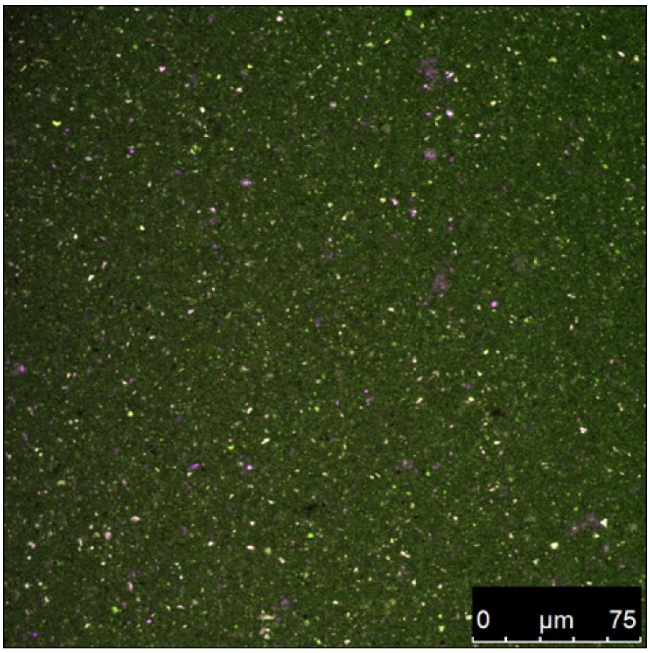


Figure 3.6. Representative confocal micrograph of soybase obtained at 80 °C visualised using fluorochrome acridine orange.

Figure 3.7 depicts the microstructure of okara produced using thermal processing and stained with the fluorochrome acridine orange. Cell wall material and intact cells are observed that were present in the soy slurry prior to separation. Agglomerated material can be observed in the micrograph which have the same size and colour as seen in Figure 3.3 in the continuous phase. Next to the removal of the protein aggregates during separation of the fibrous by-product okara, the loss in

protein extraction yield can also be caused by the high moisture content of okara, approximately 80%; the cell walls of disrupted cells possess a robust incompressible network (see Table 3.4).

Within this article, the micrographs have been described as representative; however, the images only reveal a small insight into a microscale slice of the samples. Only one drop from a pipette was utilised to obtain each image. Several images were obtained from different samples of the processing materials and can be found in Appendix 8.2.2.

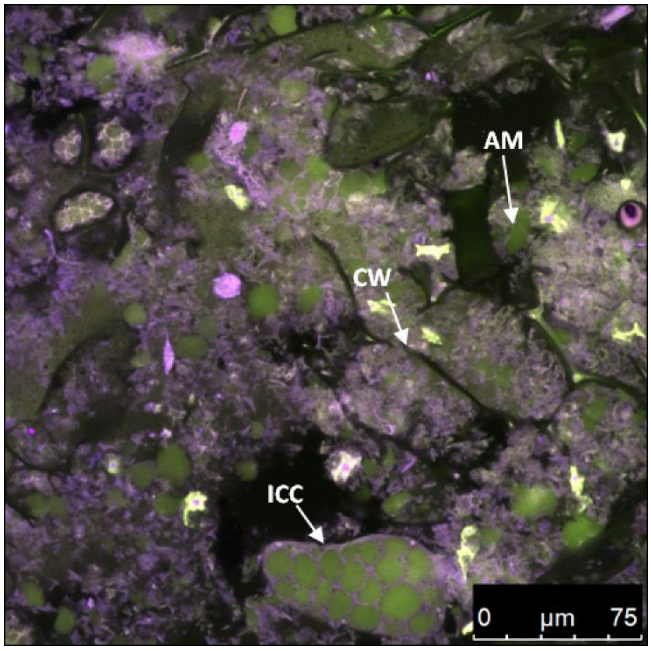


Figure 3.7. CLSM micrograph of fibrous by-product of soybase production at 80 °C, okara, visualised using acridine orange. Intact cotyledon cells (ICC), cell walls of disrupted cells (CW) and agglomerated material (AM in green, most likely protein bodies) are annotated on the image.

Campbell and Glatz (2009) based their model on particle size based on volume, whilst a model by Rosenthal *et al.* (1998) was based on mass balance, where it was assumed that the protein concentration at equilibrium can be related to that in the 'solid' phase by a partition coefficient. Despite the differences in models and our finding that we could not confirm the assumption of

Campbell and Glatz (2009) that only the outside soybeans cells are disrupted (see above), the calculated yields of the proteins using these two models and our values were similar to these found experimentally at ambient temperature (see Table 3.3). When examining the predicted yields for processing at 80 °C (between the denaturation temperatures of the main storage proteins), the yield was much larger than actually found, as unavailability due to protein aggregation was not considered within either model.

Okara produced using thermal treatment contains 2.6% more protein than when no thermal treatment was employed. The proteins located within okara after thermal treatment are found to possess good nutritive value, therefore could be extracted for human consumption (Stanojevic *et al.*, 2012). The aqueous phase within the okara is also believed to have the same composition as the soybase; if more of it is removed from okara, the protein extraction yield will be increased.

SEM was a technique investigated for this study; however limited information was obtained from this technique. Similar SEM images as already published of frozen soybeans (Bair and Snyder, 1980) were obtained during this study (Figure 2.3 presented in **chapter 2** shows the microstructure of a pre-soaked soybean). Intact protein bodies were observed which coincides with findings from confocal microscopy. SEM with energy dispersive spectroscopy (EDX) was also used to confirm the composition of aggregated material found in the continuous phase. Nitrogen was difficult to detect using this technique due to its low atomic number, especially with the concentrations found within the soy slurry; however it was detectable for some images of okara (data not shown). Although our SEM images in combination with EDX confirmed the composition of the aggregated material, it provided less informative insights relevant for the extraction process than CLSM.

Moreover, SEM is a more tedious and time consuming technique than CSLM and the structures might also be affected by the freezing prior to SEM analysis.

Localisation of protein within the by-product is important for looking at methods for protein recovery; the avoidance of protein insolubility is one method to target increased protein extraction. Enzymatic treatment to reduce rigidity of the disrupted cell wall matrix has shown promising results for improved oil and protein extraction yields, and could be one approach to target extraction from the by-product okara (Kasai *et al.*, 2004; Rosenthal *et al.*, 2001).

## 3.4 CONCLUSIONS

In this novel study we have shown the microstructures of soy slurry, soybase and the fibrous waste material okara, including localisation of oil and protein using CLSM in combination with carefully selected fluorochromes. Agglomerated protein bodies caused by thermal treatment were found in- and outside intact cotyledon cells in the soy slurry, and after separation in the okara only. Protein aggregation can be used to explain why a lower protein extraction yield was obtained upon processing at 80 °C than after processing at ambient temperature (42% versus 67% respectively). Treatments to disrupt the complex okara microstructure and/or achieve lower water content will be investigated in further studies with the aim of increasing the protein extraction yield.

## 3.5 REFERENCES

Adams, R.B., Demmig-Adams, B. (2013). Impact of contrasting food sources on health versus environment. *Nutrition and Food Science, 43*, 228-235.

Aiking, H. (2011). Future protein supply. *Trends Food Sci Tech, 22*, 112-120.

Bair, C.W., Snyder, H.E. (1980). Electron microscopy of soybean lipid bodies. *J Am Oil Chem Soc,* 57, 279-282.

Bruinsma, J. (2009). The resource outlook to 2050: By how much do land, water and crop yields need to increase by 2050? In *FAO Expert Meeting on How to Feed the World in 2050*, Rome, Italy.

Cakmak, I. (2002). Plant nutrition research: Priorities to meet human needs for food in sustainable ways. *Plant Soil, 247,* 3-24.

Campbell, K.A., Glatz, C.E. (2009). Mechanisms of aqueous extraction of soybean oil. *J Agric Food Chem, 57*, 10904-10912.

Campbell, K.A., Glatz, C.E., Johnson, L.A., Jung, S., de Moura, J.M.N., Kapchie, V., Murphy, P. (2011). Advances in aqueous extraction processing of soybeans. *J Am Oil Chem Soc, 88*, 449-465.

Giri, S.K., Mangaraj, S. (2012). Processing Influences on Composition and Quality Attributes of Soymilk and its Powder. *Food Eng Rev, 4*, 149-164.

He, F., Huang, F., Wilson, K.A., Tan-Wilson, A. (2007). Protein storage vacuole acidification as a control of storage protein mobilization in soybeans. *J Exp Bot*, *58*, 1059-1070.

Horisberger, M., Clerc, M.F., Pahud, J.J. (1986). Ultrastructural localization of glycinin and β-conglycinin in *Glycine max* (soybean) cv. Maple Arrow by the immunogold method. *Histochemistry*, *85*, 291-294.

Jankowiak, L., Trifunovic, O., Boom, R.M., Van Der Groot, A.J. (2014). The potential of crude okara for isoflavone production. *J Food Eng, 124*, 166-172.

Johnson, K.W., Synder, H.E. (2014). Soymilk: A comparison of processing methods on yields and composition. *J Food Sci, 43*, 349-353.

Jung, S., Rickert, D.A., Deak, N.A., Aldin, E.D., Recknor, J., Johnson, L.A., Murphy, P.A. (2003). Comparison of Kjeldahl and Dumas methods for determining protein contents of soybean products. *J Am Oil Chem Soc, 80*, 1169-1173.

Kasai, N., Ikehara, H. (2005). Stepwise extraction of proteins and carbohydrates from soybean seed. *J Agric Food Chem, 53*, 4245-4252.

Kasai, N., Murata, A., Inui, H., Sakamoto, T., Kahn, R.I. (2004). Enzymatic high digestion of soybean milk residue (okara). *J Agric Food Chem, 52*, 5709-5716.

Leiserowitz, A.A., Kates, R.W., Parris, T.M. (2006). Sustainability Values, Attitudes, and Behaviors: A Review of Multinational and Global Trends. *Annu Rev Environ Resour, 31,* 413-444.

Lili, W., Yeming, C., Zaigui, L. (2013). The effects of freezing on soybean microstructure and qualities of soymilk. *J Food Eng, 116,* 1-6.

Nik, A.M., Tosh, S.M., Woodrow, L., Poysa, V., Corredig, M. (2009). Effect of soy protein subunit composition and processing conditions on stability and particle size distribution of soymilk. *LWT-Food Sci Technol, 42*, 1245-1252.

Masuda, T., Goldsmith, P.D. (2009). World soybean production: area harvested, yield, and long-term projections. *Int Food Agribus Man, 12*, 143-162.

Nishinari, K., Fang, Y., Guo, S., Phillips, G.O. (2014). Soy proteins: A review on composition, aggregation and emulsification. *Food Hydrocolloid, 39*, 301-318.

O'Toole, D.K. (1999). Characteristics and use of okara, the soybean residue from soy milk production a review. *J Agric Food Chem, 47,* 363-371.

Ono, T., Choi, M.R., Ikeda, A., Odagiri, S. (1991). Changes in the Composition and Size Distribution of Soymilk Protein Particles by Heating (Food & Nutrition). *Agric Biol Chem, 55*, 2291-2297.

Pimentel, D., Pimentel, M. (2003). Sustainability of meat-based and plant-based diets and the environment. *Am J Clin Nutr, 78*, 660S-663S.

Rosenthal, A., Pyle, D.L., Niranjan, K. (1998). Simultaneous aqueous extraction of oil and protein from soybean: Mechanisms for process design. *Food Bioprod Process, 76*, 224-230.

Rosenthal, A., Pyle, D.L., Niranjan, K., Gilmour, S., Trinca, L. (2001). Combined effect of operational variables and enzyme activity on aqueous enzymatic extraction of oil and protein from soybean. *Enzyme Microb Technol, 28,* 499-509.

Stanojevic, S.P., Barac, M.B., Pesic, M.B., Vucelic-Radovic, B.V. (2012). Composition of Proteins in Okara as a Byproduct in Hydrothermal Processing of Soy Milk. *J Agric Food Chem, 60,* 9221-9228.

Tombs, M.P. (1967). Protein bodies of the soybean. *Plant physiol, 42,* 797-813.

Vishwanathan, K.H., Singh, V., Subramanian, R. (2011). Influence of particle size on protein extractability from soybean and okara. *J Food Eng, 102,* 240-246.

Wijngaard, H.H., Zuidam, N.J. (2014). *Soybean extraction process*. International Publication WO14154472.

# CHAPTER 4

# INTENSIFIED SOY PROTEIN EXTRACTION AT LAB-SCALE BY ULTRASOUND

This chapter is based on a published manuscript:

Preece, K. E., Hooshyar, N., Krijgsman, A., Fryer, P. J., Zuidam, N. J. (2017). Intensified soy protein extraction by ultrasound. *Chem Eng Process*, *113*, 94-101.

## ABSTRACT

During soymilk production, aqueous extraction conditions are utilised resulting in suboptimal protein extraction yields. This research focuses on the intensification of extraction yields from soybeans using ultrasound and understanding the reasoning behind the results. Milled soybean slurry and okara samples were treated with ultrasound using a lab-scale probe system (20 kHz, 400 watts) for 0, 0.5, 1, 5 and 15 min. Ultrasound increased the protein, oil and solids extraction yield from soy slurry by ca. 10% after 1 min treatment, especially due to reduced aggregation and in a less extent to enhanced separation efficiency. Particles in the size range of 2-35 μm, corresponding to insoluble protein bodies in the continuous phase, were reduced in frequency but surprisingly not by a stepwise decline in size upon ultrasound treatment, as shown by both laser diffraction and confocal laser scanning microscopy. No effects of ultrasound were observed on intact cells present in okara solution and soy slurries. Scanning electron microscopy could not reveal a hypothesised internal organisation of protein bodies within cells, although phytic acid stores were localised which have not been reported before. In conclusion, ultrasound has been identified as a technology with promise in soybean extraction systems where protein solubility requires improvement.

## 4.1 INTRODUCTION

Plant-based protein products are currently gaining much interest as a more sustainable alternative to animal-based protein products. One such product gaining popularity across the world is soymilk, due to its complete set of essential amino acids, cholesterol-lowering attributes and lactose free nature (Carroll, 1991). Soymilk production consists of aqueous extraction from soybeans using alkaline conditions at elevated temperatures, followed by removal of insoluble material to produce the resulting soybase. This soybase is then used as a precursor to produce soymilk by adding other ingredients such as sugar, gums, flavours, minerals and vitamins. The extraction of various components from soybeans is suboptimal; after extraction, a significant amount of protein resides in the insoluble fraction, termed okara. Thermal treatment during processing is often employed to reduce the activity of lipoxygenase; which, if left in its native state, results in off-flavour production (Murphy, 2008). Vishwanathan *et al.* (2011) show that alkaline conditions (optimal pH 8+) gave enhanced protein solubility when compared to acidic conditions due to the proteins isoelectric points. Assistance during protein extraction from soybeans is supported by industry for reasons including: less expenditure on raw materials, less waste and lower costs associated with its subsequent treatment.

An alternative energy source that has been commonly studied for laboratory scale extraction assistance in the food industry is ultrasound (Chemat *et al.*, 2011; Dolatowski & Stasiak, 2011; Knorr *et al.*, 2004; Leonelli & Mason, 2010; Pingret *et al.*, 2011; Shirsath *et al.*, 2012; Soria & Villamiel, 2010; Tiwari & Mason, 2012; Vilkhu *et al.*, 2008). The mechanism involved in enhancing extraction yields is attributed to the cavitation phenomenon. Upon the application of ultrasound, alternating mechanical waves cause microbubbles located in the liquid medium to form

and grow up to a sufficiently negative threshold pressure, where bubble collapse occurs (Shirsath *et al.*, 2012). As a consequence of bubble implosion, local physical effects may result in very high temperatures (5000 K) and pressures (2000 atm) (Leonelli & Mason, 2010). Local regions of turbulence occur as a result of cavitation aiding mass transfer in solid-liquid extraction (Dolatowski & Stasiak, 2011). Many lab-scale studies claim that ultrasound can also enhance extraction yields of intracellular materials from vegetal tissue due to cell disruption (Chemat *et al.*, 2011; Khanal *et al.*, 2007; Leonelli & Mason, 2010; Shirsath *et al.*, 2011; Vinatoru, 2001; Vinatoru *et al.*, 1997). This intensification of extraction yield caused by cell disruption is attributed to liquid jets of solvent resulting from asymmetric microbubble collapse (Wang & Weller, 2006).

More recently, this technology has begun to show promise for implementation at industrial scale (Esclapez *et al.*, 2010; Gallego-Juarez, 2010). Pilot scale studies have shown the positive effects of ultrasound on a number of food extraction systems. One such study by Pingret, *et al.* (2012) show the comparable results for ultrasound-assisted aqueous extraction of polyphenols from apple pomace at pilot-scale to those improvements observed at lab-scale. Boonkird *et al.* (2008) showed the positive effects of ultrasound treatment on the extraction of capsaicinoids from chilli peppers at pilot scale. Within the food industry, there has been implementation of ultrasonic processing on an industrial scale for assistance during extraction from vegetal materials (Chemat *et al.*, 2011). Ultrasound-assisted extraction has been regarded as a green extraction process, for reasons including reductions in processing times, energy consumption and enhanced rates of extraction (Chemat *et al.*, 2016). These factors are of interest when considering protein extraction during soymilk production: protein that is currently used for low quality functions, such as animal feed, is made available for human consumption.

A key factor to be explored when considering the effects of ultrasound is the microstructure of the processing materials. It is important to understand the matrix from which the extraction occurs and the diffusion pathway by which protein can escape the solid, but so far little information is available in the literature about processed soybean microstructures. The soybean is composed of approximately 90% cotyledon cells, with the length range of 70-80 μm and a diameter of 15-20 μm once hydrated (Imram *et al.*, 2003; Rosenthal *et al.*, 1998). These cells contain protein bodies (5-20 μm) and a cytoplasmic network containing oil bodies (0.2-0.5 μm) stabilised by proteins termed oleosins (Rosenthal *et al.*, 1998). The physical constraints for non-optimal protein extraction yields upon preparation of soybase in an aqueous environment have been studied in previous work (Preece *et al.*, 2015; **chapter 3**). Barriers for extraction included intact cotyledon cells, aggregated protein bodies within the extraction medium caused by thermal treatment and a considerable amount of okara containing 80% moisture in which soluble proteins reside (Preece *et al.*, 2015; **chapter 3**).

Earlier studies of soy-based systems investigating ultrasonically-assisted extraction have been shown to improve extraction yields or to enhance the functionality of components (Fukase *et al.*, 1994; Hu *et al.* 2013; Jambrak *et al.*, 2009; Karki *et al.*, 2010; Li *et al.*, 2004; Moulton & Wang, 1982; Tang *et al.*, 2009). Fukase *et al.* (1994) investigated the effects of ultrasound on soybeans that underwent defatting using ether prior to protein extraction. The ultrasound-assisted extraction from defatted soybean flakes yielded 50% more protein versus the control sample (no US) after 10 min treatment at ultrasonic pressure of 106 kPa in an aqueous system (Fukase *et al.*, 1994). Another system showed the extraction of oil from soybeans using hexane was enhanced by 20% with the application of ultrasound for 30 min (20 kHz) compared to a control sample (Li *et al.*, 2004). However, there are very limited studies investigating the effects of ultrasound on aqueous

extraction from soybean as the starting material, without pre-treatment. One study by Fahmi *et al.* (2011) investigated the effects of ultrasound treatment (35 kHz, up to 60 min) on soy slurry protein extraction from pre-soaked soybeans. The protein extraction was intensified: the protein content of soymilk increased by 6.3% (Fahmi *et al.*, 2011).

This study investigates the effects of ultrasound-assisted extraction, after initial grinding of soybeans at elevated temperatures. We hypothesise that ultrasound assistance will improve the extraction yields of protein, oil and solids due to increased cell disruption, as discussed above. Ultrasonic treatment of both the soy slurry and okara solution is investigated and extraction yields, solubilisation and separation efficiencies will be discussed. In addition, confocal laser scanning microscopy (CLSM) and scanning electron microscopy (SEM) has been used to study the microstructure of the soybeans, to understand the target of ultrasound in our soybean extraction system.

## 4.2 MATERIALS AND METHODS

### 4.2.1 Slurry preparation

Preece *et al.* (2015; **chapter 3**) describe a method for aqueous extraction to produce soy slurry and okara for subsequent treatments. This methodology has been adapted from a patent (Wijngaard & Zuidam, WO14154472, 2014). Figures 4.1 (A) and (B) show the process schematically. Firstly, ('Milling 1' in Figure 4.1(A) and (B)) commercially available soybeans were ground in demineralised water at a ratio of 1:6 (w/w) and at 80 °C using a commercial blender (Varoma Thermomix, Vorwerk, Germany) for 10 min (stepwise levels 2-8). Then the ground soybeans were treated ('Milling 2') with a high shear mixer (Silverson L4RT, Silverson Machines International, UK) for 20 min (stepwise 3000-6500 rpm) to produce a slurry with a volume-weighted mean diameter ($D_{4,3}$) of less than 300 μm.

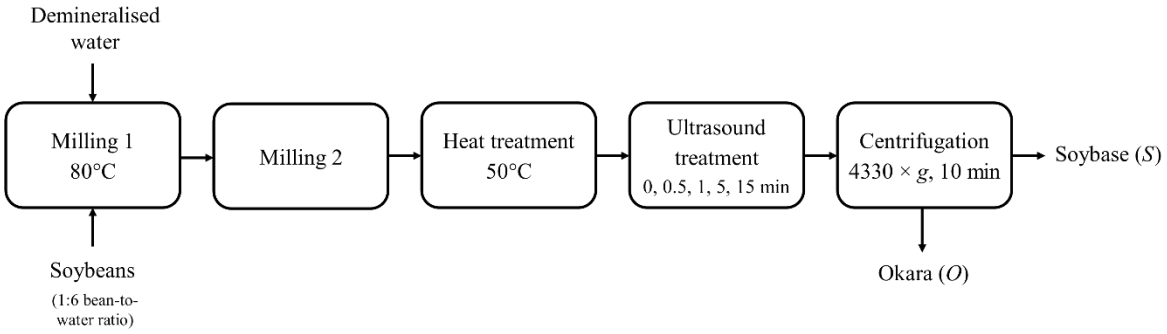


Figure 4.1A. Schematic diagram of preparation and treatments applied to slurry during processing.

### 4.2.2 Okara solution preparation

The slurry was centrifuged (4330 × *g*, 10 min) to produce soybase *S* (supernatant) and okara *O* (pellet). The solid content of okara was measured using methods described in Section 4.2.3. A solution of 2.85% solids was then made by diluting the okara with demineralised water.

### 4.2.3 Ultrasonic treatment

After sample preparation, 100 g of sample (slurry or okara solution) was weighed and added to a water bath at 50 ± 1 °C whilst stirring at 200 rpm using a magnetic stirrer bar (25 mm in length, 10 mm in diameter cylindrical bar with central ring). Once the sample achieved the desired temperature, the sample was either subjected to sonication or held at 50 °C in the water bath (control). Various times of exposure to ultrasound were investigated to understand the effects of sonication on extraction.

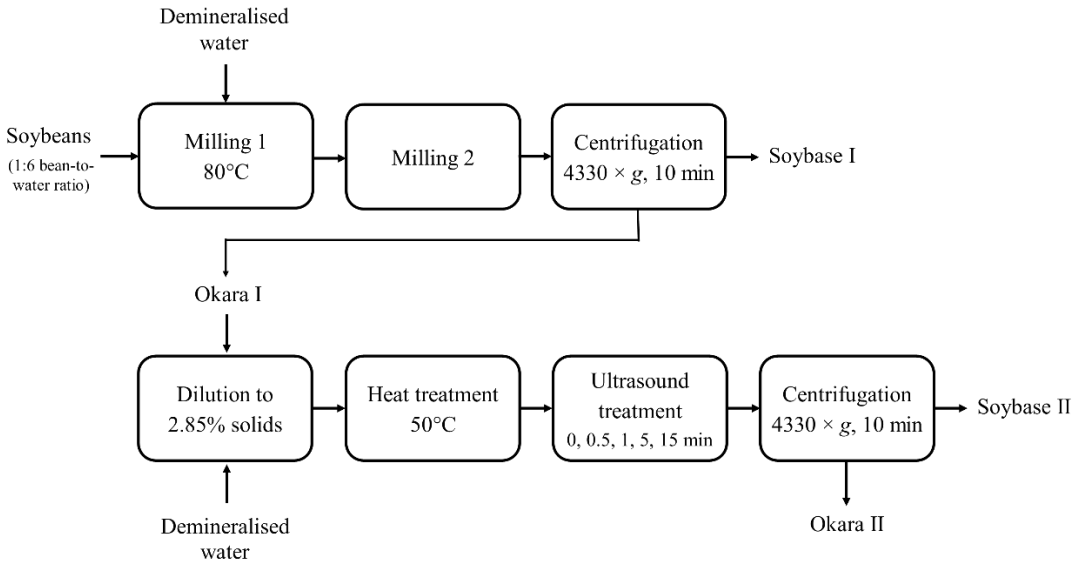


Figure 4.1B. Schematic diagram of okara preparation and subsequent treatments.

Sonicated samples were treated with an ultrasonic probe (Branson Sonifier 450, Branson Ultrasonics Corporation, Danbury, CT), (20 kHz, output level 7 which translates to a power output of 65 W, 13 mm probe tip) for various time periods; 0.5 min, 1 min, 5 min & 15 min. In the data presented, no temperature control was employed during ultrasonic treatment, however the temperature was recorded prior and post treatment (Table 4.1). The lab-scale probe can be seen in

Figure 4.2, including the box for sound dampening. From the recorded temperature increase, it was possible to calculate the actual ultrasonic energies and power inputs introduced using calorimetry: $Q = mC_P\Delta T$, where $Q$ is the energy input as heat (J), $m$ is the mass of sample (kg), $C_P$ is the specific heat capacity (assumed to be that of water, (4181 J $kg^{-1}$ $K^{-1}$)) and $\Delta T$ is the temperature change (Table 4.1). The specific heat capacity of the soybean has been quoted previously as 1444 J $kg^{-1}$ $K^{-1}$ by Deshpande & Bal (1993), therefore the values for energy and power inputs quoted in Table 4.1 should be used for relative comparison. The power input was calculated by dividing the energy input by the treatment time (in s), assuming that all energy was transferred to heat energy in the system. Those powers quoted are less than those detailed by the probe manufacturer as 65 W, which might indicate that especially at high temperatures some of the heat energy was transferred from the system into the environment. A reduction in power is quoted for increasing the ultrasonic treatment time from 5 to 15 min, this is a result of poor insulation of the beaker and heat being lost to the surroundings.


Figure 4.2. Photograph of the lab-scale probe system used for ultrasonic treatment of okara solution and slurry samples. A sound protection box was utilised for all ultrasonic treatments and a clamp stand was used to position the probe tip in the middle of the sample.

Table 4.1. Temperature increase reported during ultrasound (US) treatment of soy slurry and corresponding energy and power input calculated using calorimetry.

| US treatment time (min) | Start T (°C) | End T (°C) | ΔT (°C) | Energy input (J) | Power input (W) |
|---|---|---|---|---|---|
| **0** | 49 | - | - | - | - |
| **0.5** | 49.7 | 49.9 | 0.2 | 84 | 3 |
| **1** | 50.2 | 54.8 | 4.6 | 1923 | 32 |
| **5** | 50 | 80.5 | 30.5 | 12752 | 43 |
| **15** | 50.2 | 90.4 | 40.2 | 16808 | 19 |
| **15 (No US)** | 49.5 | 49.8 | 0.3 | - | - |

After reaching the desired process time, the samples were immediately centrifuged (4330 × $g$, 10 min) to prevent further extraction occurring. Pellets and supernatants were weighed and analysed to determine extraction yields.

### 4.2.4 Protein & solids content determination

To determine protein extraction yields, the protein content on a wet basis (w.b.) was defined in the pellets and supernatants using the Dumas method (Vario MAX CNS, Elementar Analysensysteme GmbH, Germany). L(+)-glutamic acid (VWR International BVBA, Belgium) was used as a standard sample and UHT milk (3.5% fat) (muva kempten, Germany) as a reference material. For soy samples, a protein conversion factor of 6.25 × N was utilised to determine protein content from the measured nitrogen content. From the protein concentrations and masses of streams, the protein extraction yield into the soybase was calculated using equation 4.1.

$$\text{Protein extraction yield} = Y\ (\%) = \left[\frac{S \cdot x_{\mathrm{p,s}}}{(S \cdot x_{\mathrm{p,s}} + O \cdot x_{\mathrm{p,o}})}\right] \times 100\% \qquad (4.1)$$

Here $S$ (soybase) and $O$ (okara) represent the total weight of samples and $x_{\mathrm{p}}$ is the mass fraction of protein. To analyse the effects of ultrasound on okara solution, it was necessary to consider the total protein extraction yield calculated using equation 4.2. In this equation the nomenclature is that shown in Figure 4.1(B); $Y_{\mathrm{I}}$ refers to the primary extraction yield and centrifugation for the production of soybase and okara; $Y_{\mathrm{II}}$ corresponds to the okara solution treatment described.

$$\text{Total protein extraction yield}\ (\%) = Y_{\mathrm{I}} + (100\% - Y_{\mathrm{I}}) \times Y_{\mathrm{II}} \qquad (4.2)$$

In addition to the extraction yields, the separation efficiency (equation 4.3) was derived to show the efficiency of deliquoring of okara during centrifugation. The availability of protein was also calculated using equation 4.4, defined as the percentage of protein that can be solubilised or

dispersed in the extraction medium, here water. Unavailable protein can be large aggregates in the continuous phase, which end up in okara, or entrapped within intact cells (Preece *et al.*, 2015; **chapter 3**). In these calculations, it was assumed that the moisture content found in okara retained the same protein concentration as the soybase ($x_{p,s}$).

$$\text{Separation efficiency } (\%) = \left[\frac{S \cdot x_{w,s}}{(S \cdot x_{w,s} + O \cdot x_{w,o})}\right] \times 100\% \quad (4.3)$$

$$\text{Availability of protein } (\%) = \left[\frac{S + \frac{O \cdot x_{w,o}}{x_{w,s}}}{S + \frac{O \cdot x_{p,o}}{x_{p,s}}}\right] \times 100\% \quad (4.4)$$

where:

$x_{w,s}$ Mass fraction of water in soybase

$x_{w,o}$ Mass fraction of water in okara

$x_{p,s}$ Mass fraction of protein in soybase

$x_{p,o}$ Mass fraction of protein in okara

Note that the extraction yield (equation 4.1) is equal to separation efficiency (equation 4.3) multiplied by the availability of protein (equation 4.4).

Fat and solid contents were measured using a microwave moisture analysis system equipped with NMR for direct detection of fat content (SMART System5, CEM GmbH, Germany). Oil and solid extraction yields were also determined using equation 4.1, replacing the masses of protein, with the respective masses. All measurements were carried out in triplicate for each sample.

### 4.2.5 SDS-PAGE

In order to assess the quality of the protein after ultrasonic treatment, SDS-PAGE was employed. With this technique it was possible to deduce if polypeptide bonds were broken during ultrasonic treatment, however, it is not possible to determine amount of denaturation due to complete sample denaturation during sample preparation. 2X Laemmli Sample Buffer was added at a ratio of 1:1 with the sample once β-mercaptoethanol was added. After vortexing, the samples were heated to 95 °C for 5 min and mixed at 1000 rpm in a heating block for microcentrifuge tubes. 10X TGS Running Buffer was diluted to the correct concentration with deionised water and added to the electrophoresis tank. A 14-well pre-cast gel was used for this study (AnykD Criterion TGX Stain-Free Protein Gel). Initially the wells were rinsed with running buffer before loading the samples. 20 μL of Precision Plus Protein All Blue Prestained standard was added to lanes 1 & 14. Bands for the standard range in size from 10 kDa to 250 kDa. 30 μL of sample was loaded into wells 2-13. Initially, the voltage was fixed at 80 V for 5 min. Once the samples had entered the gel, the voltage was increased to 200 V and left to run for approximately 30 min. A ChemiDoc XRS+ imaging system was utilised to assign the molecular weights of the standards.

### 4.2.6 Particle size analysis

The particle sizes of soy slurries after extraction were determined using laser diffraction (Mastersizer 2000 Hydro S, Malvern Instruments Ltd, UK). To determine particle size distributions, refractive indices of 1.33 and 1.45 were used for the water and the particles, respectively. Particle sizes were measured in triplicate for each sample.

### 4.2.7 Confocal laser scanning microscopy (CLSM)

A Leica TCS-SP5 microscope in conjunction with DMI6000 inverted microscope (Leica Microsystems Inc., Germany) was used with the dye nile blue A (Janssen Chimica, Belgium) to visualise the effects of ultrasound treatment on soy slurries. One drop of dye stock solution (1% w/v nile blue) was added to 1-1.5 mL of sample and mixed well before adding the sample to the slide. For visualisation using nile blue, sequential scanning was employed to prevent the excitation laser occurring in the emission signals. Table 4.2 shows the scans utilised and the corresponding colours assigned to the emission channels.

Table 4.2. CLSM excitation and emission settings specified for nile blue.

| Fluorochrome | Excitation wavelength (nm) | Emission wavelengths (nm) | Representing colour in micrographs |
|---|---|---|---|
| **1% w/v nile blue** | 488 | 520-626 | Green |
| | 633 | 662-749 | Red |

### 4.2.8 Cryo-scanning electron microscopy (cryo-SEM)

A soybean was cut into 2 pieces using a razorblade. One piece was placed in an aluminium sample cup and plunged into liquid nitrogen. The sample was then cryo-planed using a cryo-ultramicrotome (Ultracut UCT EM FCS, Leica Microsystems Inc., Germany), to obtain a freshly prepared cross-section. The sample was freeze-etched for 2 min at -90°C to reveal the microstructure and then sputter coated with platinum (120 s) in order to obtain a better image contrast. Samples were imaged using a Zeiss Auriga field emission SEM (Carl Zeiss Microscopy GmbH, Germany) at -125°C and an accelerating voltage of 3 kV. The microscope was equipped with an energy dispersive X-ray spectroscopy (EDX) unit; therefore, it was possible to chemically characterise regions visualised using the microscope.

## 4.3 RESULTS & DISCUSSION

### 4.3.1 Extraction yields

#### *4.3.1.1 Soy slurry treatment*

To understand the mechanisms of ultrasound on the soy slurry matrix, it was necessary to determine the extraction yields for the components of interest. Extraction yields were calculated from measurements of oil, protein and solid contents of samples after treatment. Figure 4.3 shows the effect of ultrasound treatment time versus extraction yield for the treatment of soy slurry. Ultrasound was shown to improve the extraction of oil, proteins and solids vs. the control sample. After 1 min treatment time, protein and oil extraction yields had improved by approximately 10% versus the zero time point. It was shown that there was no benefits to perform ultrasound-assisted extraction for more than 5 min as the maximum yields had been achieved. A control sample was also analysed at 15 min to show the thermal treatment with stirring was not responsible for the increases in extraction yields observed. An improvement in extraction yields was also observed for control samples; however, not as much as those observed for respective ultrasound treatments.

Temperature control was not employed for the data shown within this study. Without temperature control, 15 min ultrasonic treatment caused the temperature of the solution to increase by 40.2 ± 0.8 °C. In a separate study, the effect of temperature was determined by controlling the temperature of the sample using a jacketed vessel cooled using counter-current flow of water at 20 ± 1 °C. The protein extraction yields for US-treated samples (0.5-5 min, without temperature control) yielded insignificant differences when compared to US-treated samples with temperature control (data not shown). Considering the effects of ultrasound with temperature control for the 15 min US-treated

sample, the protein extraction yield was approximately 5% lower (absolute value) when the temperature of the sample was held at 50 °C.

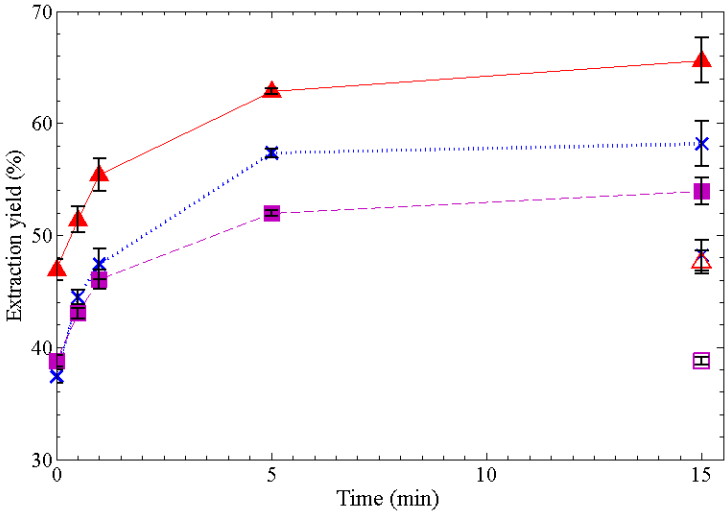


Figure 4.3. Improvement of extraction yields of slurry, oil (▲), protein (x) and solids (■) at various sonication times. Non-filled shapes correspond to control samples with corresponding component labels. Each data point is an average of three separate experiments and the error bar represents its standard error.

#### *4.3.1.2 Okara solution treatment*

It has been previously reported that ultrasound has a significant effect on the extraction yield of protein from okara during soybase production (Wijngaard & Zuidam, 2014). Total extraction yield refers to the addition of initial extraction yield during soybase production (soybase I and okara I production in Figure 4.1B) plus the extra materials which solubilised after subsequent okara treatments. Figure 4.4 shows that an increase in protein extraction yield upon ultrasound treatment was indeed achievable in comparison to the control samples, recorded for each time point in this instance. Total oil and solid extraction yields were also intensified during ultrasound treatment. In contrast, the total extraction yields from the control samples (no ultrasound) remained unchanged during all time periods. In this study, no temperature control was employed during the ultrasonic treatment of okara solution. It was previously shown that the 80 °C thermal treatment included with

the milling of the soybeans in water (detailed in Section 4.2.1) for okara preparation affected the protein extraction yield (Preece *et al.*, 2015, **chapter 3**). Based on the limited effect of temperature control shown for the slurry data, the effect of subsequent thermal treatments after sample preparation was considered negligible. All samples were heated to 50 °C prior to ultrasonic treatment, including the control which was not treated with ultrasound.

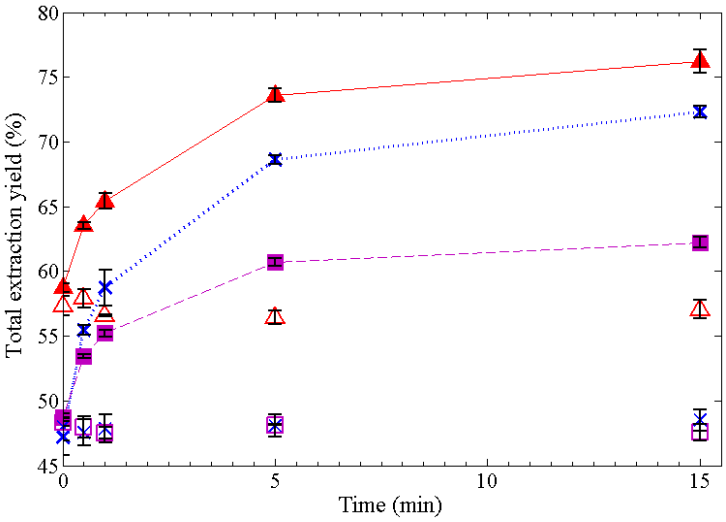


Figure 4.4. Effect of ultrasound treatment when applied to okara solution. Oil (▲), protein (X) and solids (■) extraction yields are presented. Non-filled shapes are corresponding control samples. Data points are averages of three separate experiments. Error bars represent standard error of the mean from 3 separate experiments.

### 4.3.2 Protein availability and separation efficiencies

During treatments of soy slurry using ultrasound, it was possible to identify whether the availability of protein was attributed to the increase in protein extraction yield and/or in the separation efficiency (deliquoring of okara). For the control sample, it was observed that the availability and separation efficiency of protein were approximately 60% and 65%, respectively. As can be seen from Figure 4.5, the availability of protein had the greatest impact on the protein extraction yield during ultrasound treatment. Separation efficiency was also positively influenced (to a lesser

extent) by increasing ultrasonic treatment time; less water was present within the waste stream (okara), reducing the amount of soluble proteins entrapped within the matrix.

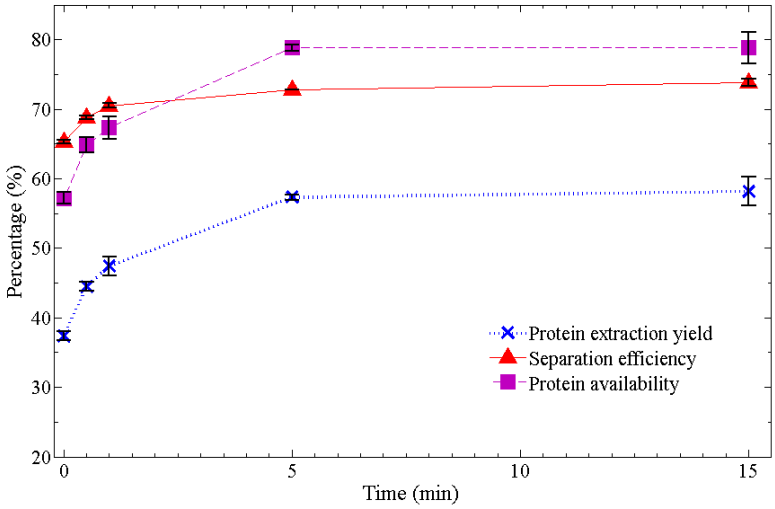


Figure 4.5. Protein extraction yield, protein availability and separation efficiency as a function of ultrasonic treatment time on soy slurry. Error bars represent standard error from 3 separate experiments.

### 4.3.3 SDS-PAGE analysis

To ensure that breakage of peptide bonds did not occur during ultrasound treatment, SDS-PAGE was performed. Figure 4.6 shows the effects of ultrasound treatment of soy slurry on the resultant soybase for treatments up to 1 min. There is protein present in the empty lanes of the gel (Lanes 2, 4, 6, 8, 10 12 & 13), therefore overrun during addition of the samples to the gel. It can be seen that increasing the ultrasonic treatment time resulted in a stepwise increase in the concentration of protein for each band in the resultant soybase from 20 seconds up to 1 min. It was possible to observe an overall increase in total protein for each lane with increasing ultrasonic treatment time, and there was no reduction in size of proteins at the larger molecular weights (15-75 kDa). This is a positive result as the presence of peptides in a food product can lead to…

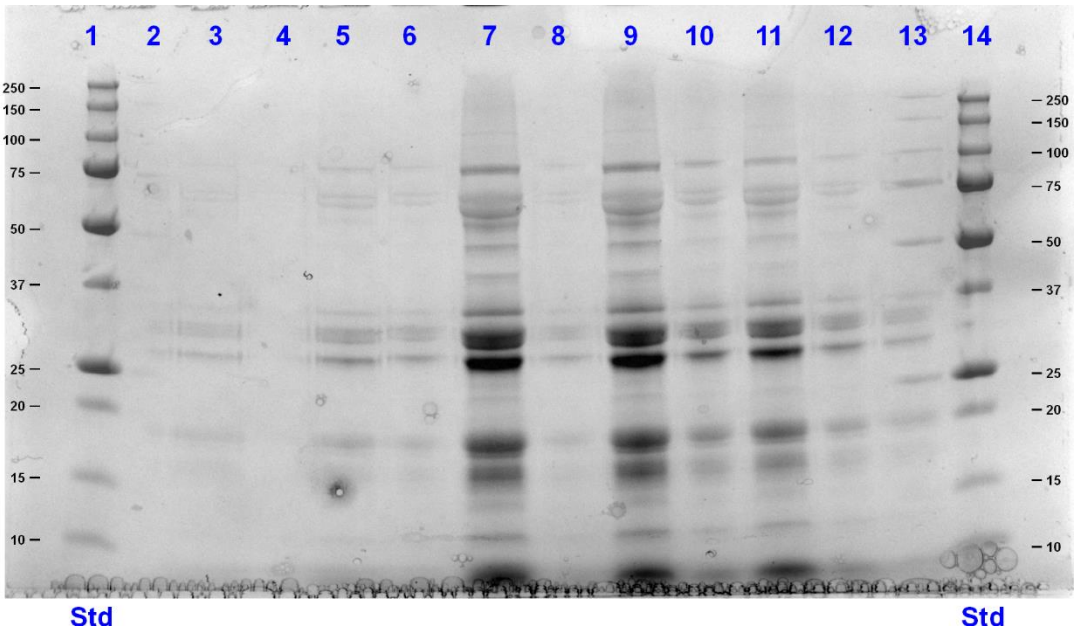


Figure 4.6. SDS-PAGE gel analysis to investigate ultrasonic treatment on the quality of protein in the soybase. Lanes 1 & 14 contain known molecular weight standards. Lane 3: Control sample (no US); lane 5: 20 s US treated sample; lane 7: 40 s US treated sample; lane 9: 1 min US treated sample; lane 11: 10X diluted soy slurry control.

### 4.3.4 Particle size distribution

During ultrasound treatment, it has been well-documented that a reduction in particle size is observed for many systems (Bates & Patist, 2008; Khanal *et al.*, 2007; Shirsath *et al.*, 2012; Vilkhu *et al.*, 2008). During the present study, particle size distributions of the treated samples were recorded and are shown in Figure 4.7A. The control slurry sample (0 min) showed a bimodal distribution of particles in the size range 2.5-2000 μm. The peak in the range of 2.5-35 μm is caused by the insoluble protein bodies located in the continuous phase of the sample, which have been visualised previously under the same processing conditions (Preece *et al.*, 2015; **chapter 3**). The larger size particles include fibres, intact cells and seed coat materials. Upon treatment with ultrasound, the peak in the 2.5-35 μm range (Figure 4.7A) containing insoluble protein bodies was visibly reduced after 0.5 min and a stepwise reduction was observed with increasing treatment time.

Interestingly, no stepwise peak shift to smaller sizes was observed. Using the Malvern Mastersizer software, it was possible to perform a number transformation on the particle size data, resulting in a plot of number fraction versus particle size (Figure 4.7B). The greatest number of particles in the control sample (0 min) were within the size range of 2.5-30 µm. The number-based particle size distribution confirms that ultrasound caused the particles to disintegrate; even after 0.5 min ultrasound treatment, the number of particles shifted to a smaller particle size (in the range 0.3-1.1 µm). Particles within this size range can be found within the soybase after centrifugation. The particles in the size range 0.3-1.1 µm can be attributed to oil droplets stabilised by protein (emulsion).

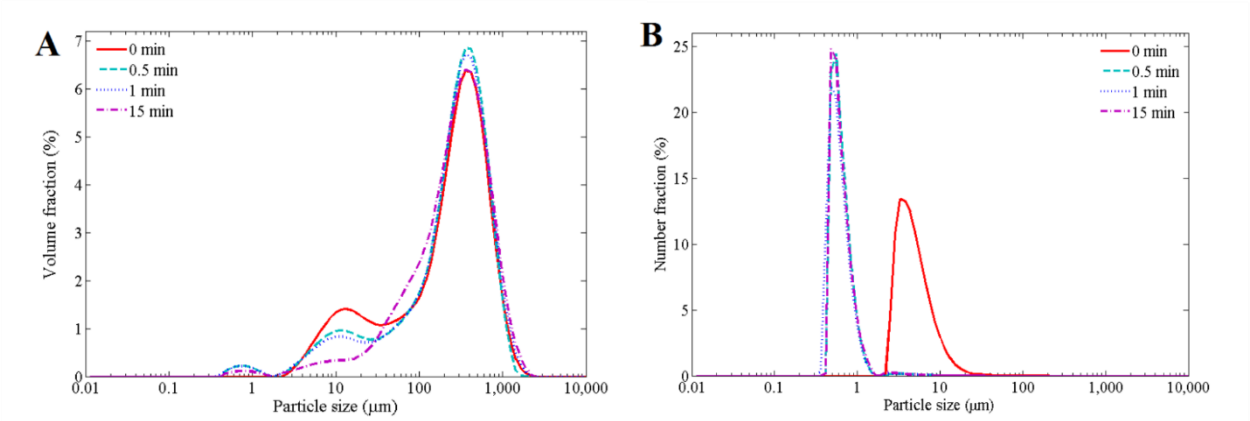


Figure 4.7. Particle size distributions of soy slurry after ultrasound treatment for 0 min (control), 0.5 min, 1 and 15 min based on volume fraction (A) and number fraction (B).

The instrumentation used to determine the particle size was based on laser diffraction technology. During the determination of the size, the particles are estimated to be spherical, which was not the case for this system, as confirmed by laser scanning confocal microscopy (detailed in Section 4.3.4). Particle size measurements are thus to be used for comparisons to one another, and not as absolute values.

### 4.3.5 CLSM

Confocal laser scanning microscopy was employed to observe the visual effects of the ultrasound treatment. To highlight the apolar features in the soy samples of interest, nile blue was employed. Nile blue can be excited by two excitation wavelengths; emission at shorter wavelengths (520-626 nm) was highlighted green in this study, visualising oil. Longer wavelengths (662-749 nm) of emission are depicted in red and correspond to protein and fibrous materials. Figure 4.8 shows typical images that were observed by CLSM. Within the control micrograph (i.e. the unprocessed material) intact cells were seen, each containing complete protein bodies, shown as red within the cells (Figure 4.8A). Protein was also present in the continuous phase of the sample with the same size range observed within the intact cells (again coloured red in this instance). Submicron oil droplets were also observed in the continuous phase (highlighted in green). With increasing ultrasonic treatment time, the presence of the protein bodies free in solution reduced in concentration. Interestingly, no reduction in particle size of the protein bodies was observed, which correlates with the particle size distribution data (Figure 4.7). Intact cells were observed throughout all samples, even after 15 min of treatment (Figure 4.8E). If the cells are intact, the materials present within are unavailable for extraction. Protein bodies within the intact cells were not affected by the ultrasound treatment; CLSM visualises intact cells containing protein bodies including after 15 min US treatment (Figure 4.8E). Upon the application of ultrasound at a frequency of 20 kHz, it is proposed that transient cavitation will be the main cause of effects in a liquid system (Soria & Villamiel, 2010). Liquid jet formation occurs as a result of asymmetric bubble collapse during transient cavitation and this phenomena is independent of the frequency of applied ultrasound (Shirsath *et al.*, 2012). In the soybean slurry system, the cell wall disruption force was apparently much higher than that supplied with liquid jet impingement on the cell wall surface, as no change

in the number of intact cells was observed via CLSM. The force required to overcome the energy holding together the insoluble protein must be lower than supplied with liquid jet impingement.

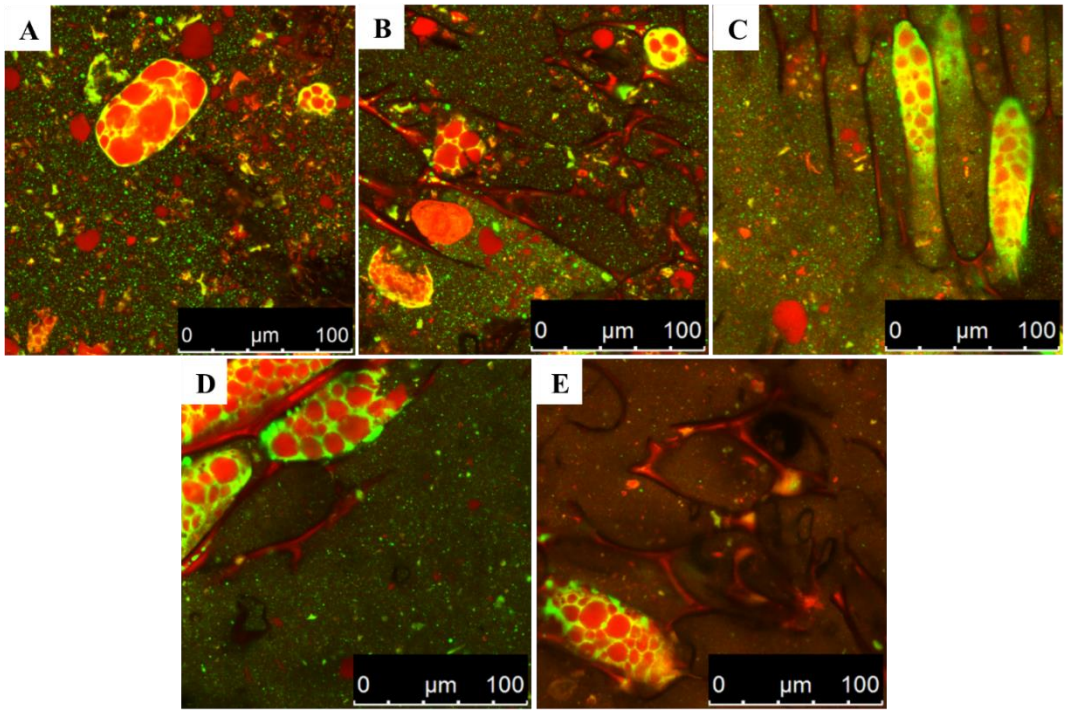


Figure 4.8. CLSM images of soy slurry after various ultrasound treatments visualised with nile blue A: (A) Control (0 min); (B) 0.5 min; (C) 1 min; (D) 5 min; (E) 15 min. Oil is presented in the green channel and other apolar material such as agglomerated protein, protein entrapped within intact cells and fibres are highlighted in red.

### 4.3.6 Cryo SEM-EDX

Surprisingly, no stepwise reduction in particle size of the protein bodies was found upon ultrasound treatment during soybase production (see Figures 4.7 and 4.8). We hypothesise that internal compartments within the protein bodies of the soybean are responsible for this 'all or nothing' effect, and that ultrasound is either able to disrupt this internal organisation holding these internal compartments completely, or not at all. This is believed to be a result of a shattering breaking mechanism resulting from ultrasound treatment. In a study by Krishnan *et al.* (1992) compartmentalisation of protein bodies within rice seeds (*Oryza sativa* L.) was indeed shown.

Storage proteins made in the endoplasmic reticulum within plant cells may accumulate in the form of smaller protein bodies primarily into so-called protein storage vacuoles by autophagy (Herman & Larkins, 1999). The limiting membrane of the sequestered protein bodies is then digested by vacuolar enzymes, resulting in aggregated, larger protein bodies (those visible in Figure 4.8).

SEM-EDX was utilised to investigate the structure and composition of the protein bodies within dry soybeans (Figure 4.9). The figure shows protein bodies surrounded by oil bodies, which were lighter in appearance. The protein bodies ranged in size (2.4-13.5 μm), which fall in the lower part of the size range quoted in the literature of 2-20 μm, derived from imaging hydrated samples by transmission electron microscopy (Rosenthal *et al.*, 1998). Bright white spots are artefacts arising from cryo-planing during sample preparation and sample transfer (labelled on Figure 4.9). It was possible to visualise spherical features within the protein bodies, these show as a lighter grey signal and annotated in Figure 4.9. EDX analysis (insets to Figure 4.9) showed these were carbon-deficient, oxygen-rich spherical structures within the protein bodies; EDX also clearly shows the difference in oxygen and carbon composition between the protein and oil bodies. Nitrogen was difficult to observe using EDX analysis due to its low abundance throughout the soybean; therefore, little difference in spatial arrangement was not apparent in the signal (Figure 4.9). These spherical structures (annotated on Figure 4.9 as PA) are most likely phytic acid, which act as a store of phosphorus and other cations during germination of the soybean (Boatright & Kim, 2000; Urbano *et al.* 2000). Magnesium was also present within these external structures (data not shown), which is explained by the chelating ability of the phytic acid. The hypothesised compartmentalisation of soybean protein bodies was not observed in Figure 4.9.

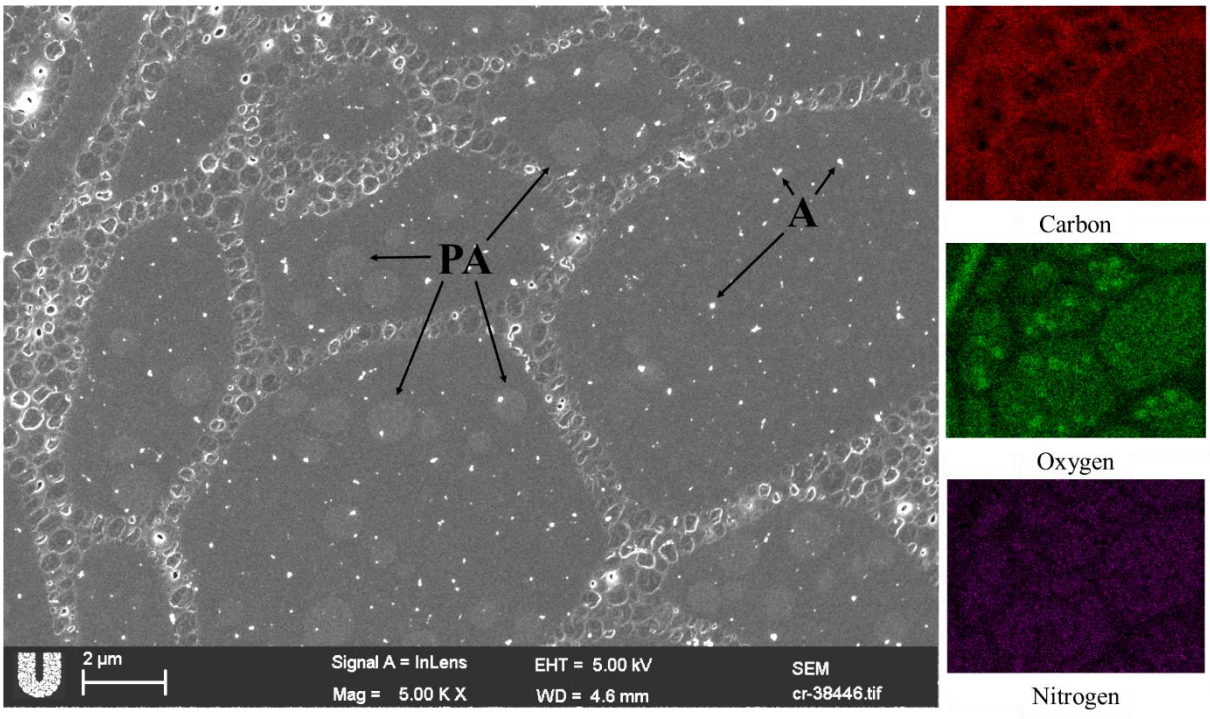


Figure 4.9. SEM image of dry soybean with examples of phytic acid (PA) and artefacts (A) annotated. Scale bar represents 2 µm. Red, green and purple colour channels correspond to carbon, oxygen and nitrogen signals, respectively, during EDX analysis.

## 4.4 CONCLUSIONS

Soymilk production consists of aqueous extraction from soybeans, followed by removal of insoluble materials. The conventional extraction of various components from soybeans is suboptimal. The effect of ultrasound on separation and extraction has been studied. Ultrasound intensifies the extraction of valuable components from soybeans, leading to improved yields of protein, oil and solids of ca. 10% after 1 min treatment. It is important to understand the effects of ultrasound on the aqueous extraction system for its industrial application during soymilk production, which has not been extensively covered within recent literature. The microstructural analysis undertaken in this study indicates reduced aggregation as the main cause of the improved yields upon ultrasound treatment, and not cell disruption as is frequently stated in the literature. The amounts of particles in the size range of 2.5-35 μm, most likely protein bodies, were found to reduce for all ultrasound treatments investigated in an 'all or nothing' effect as no intermediately sized features were observed.

## 4.5 REFERENCES

Boatright, W. L., Kim, K. S. (2000). Effect of electron microscopy fixation pH on the ultrastructure of soybean protein bodies. *J Agric Food Chem, 48,* 302-304.

Boonkird, S., Phisalaphong, C., Phisalaphong, M. (2008). Ultrasound-assisted extraction of capsaicinoids from Capsicum frutescens on a lab- and pilot-plant scale. *Ultrason Sonochem, 15,* 1075-1079.

Carroll, K. K. (1991). Review of clinical studies on cholesterol-lowering response to soy protein. *J Am Diet Assoc, 91,* 820-827.

Chemat, F., Khan, M. K. (2011). Applications of ultrasound in food technology: Processing, preservation and extraction. *Ultrason Sonochem, 18*(4), 813-835.

Chemat, F., Vian, M. A., Cravotto, G. (2012). Green extraction of natural products: Concept and principles. *Int J Mol Sci, 13,* 8615-8627.

Deshpande, S. D., Bal, S. (1999). Specific heat of soybean. *Journal of Food Process Engineering, 22*(6), 469-477.

Dolatowski, Z. J. Stasiak, D. M. (2011). Ultrasonically Assisted Diffusion Processes. In F. Lebovka, N. Vorobiev, E. Chemat (Eds.). *Enhancing Extraction Processes in the Food Industry,* New York: CRC Press. 123-144.

Esclapez, M. D., García-Pérez, J. V., Mulet, A., Cárcel, J. A. (2011). Ultrasound-assisted extraction of natural products. *Food Eng Rev, 3,* 108-120.

Fahmi, R., Khodaiyan, F., Pourahmad, R., Emam-Djomeh, Z. (2011). Effect of ultrasound assisted extraction upon the protein content and rheological properties of the resultant soymilk. *Adv J Food Sci Technol, 3,* 245-249.

Fukase, H., Ohdaira, E., Masuzawa, N., Ide, M. (1994). Effect of ultrasound in soybean protein extraction. *Jpn J Appl Phys, 33,* 3088.

Gallego-Juarez, J. A. (2010). High-power ultrasonic processing: recent developments and prospective advances. *Physics Procedia, 3,* 35-47.

Herman, E. M., Larkins, B. A. (1999). Protein storage bodies and vacuoles. *Plant Cell, 11,* 601-613.

Hu, H., Wu, J. H., Li-Chan, E. C. Y., Zhu, L., Zhang, F., Xu, X., Fan, G., Wang, L., Huang, X., Pan, S. (2013). Effects of ultrasound on structural and physical properties of soy protein isolate (SPI) dispersions. *Food Hydrocolloids, 30,* 647-655.

Imram, N., Gomez, I., Soh, V. (2003). Soya Handbook. *Tetra Pak, Singapore*.

Jambrak, A. R., Lelas, V., Mason, T. J., Kresic, G., Badanjak, M. (2009). Physical properties of ultrasound treated soy proteins. *J Food Eng, 93,* 386-393.

Karki, B., Lamsal, B. P., Jung, S., van Leeuwen, J., Pometto, A. L., Grewell, D., Khanal, S. K. (2010). Enhancing protein and sugar release from defatted soy flakes using ultrasound technology. *J Food Eng, 96,* 270-278.

Khanal, S. K., Montalbo, M., van Leeuwen, J., Srinivasan, G., Grewell, D. (2007). Ultrasound enhanced glucose release from corn in ethanol plants. *Biotechnol Bioeng, 98,* 978-985.

Knorr, D., Zenker, M., Heinz, V., Lee, D. U. (2004). Applications and potential of ultrasonics in food processing. *Trends Food Sci Tech, 15,* 261-266.

Krishnan, H. B., White, J. A., Pueppke, S. G. (1992). Characterization and localization of rice (Oryza sativa L.) seed globulins. *Plant Sci, 81,* 1-11.

Leonelli, C., Mason, T. J. (2010). Microwave and ultrasonic processing: Now a realistic option for industry. *Chem Eng Process, 49,* 885-900.

Li, H., Pordesimo, L., Weiss, J. (2004). High intensity ultrasound-assisted extraction of oil from soybeans. *Food Res Int, 37,* 731-738.

Moulton, K. J., Wang, L. C. (1982). A Pilot-Plant Study of Continuous Ultrasonic Extraction of Soybean Protein. *J Food Sci, 47,* 1127.

Murphy, P. A. (2008). Soybean proteins. In L.A.Johnson, P. J. White, & R. Galloway (Eds.), *Soybeans - Chemistry, Production, Processing and Utilization* (pp. 229-267). Urbana: AOCS Press.

Patist, A., Bates, D. (2008). Ultrasonic innovations in the food industry: From the laboratory to commercial production. *Innov Food Sci Emerg Technol, 9,* 147-154.

Pingret, D., Fabiano-Tixier, A. S., Petitcolas, E., Canselier, J. P., Chemat, F. (2011). First Investigation on Ultrasound-Assisted Preparation of Food Products: Sensory and Physicochemical Characteristics. *J Food Sci, 76,* C287-C292.

Pingret, D., Fabiano-Tixier, A. S., Le Bourvellec, C., Renard, C. M., Chemat, F. (2012). Lab and pilot-scale ultrasound-assisted water extraction of polyphenols from apple pomace. *J Food Eng, 111,* 73-81.

Preece, K. E., Drost, E., Hooshyar, N., Krijgsman, A., Cox, P. W., Zuidam, N. J. (2015). Confocal imaging to reveal the microstructure of soybean processing materials. *J Food Eng, 147,* 8-13.

Rosenthal, A., Pyle, D. L., Niranjan, K. (1998). Simultaneous aqueous extraction of oil and protein from soybean: Mechanisms for process design. *Trans IChemE, Part C, 76,* 224-230.

Shirsath, S. R., Sonawane, S. H., Gogate, P. R. (2012). Intensification of extraction of natural products using ultrasonic irradiations: A review of current status. *Chem Eng Process, 53,* 10-23.

Soria, A. C., Villamiel, M. (2010). Effect of ultrasound on the technological properties and bioactivity of food: a review. *Trends Food Sci Tech, 21,* 323-331.

Tang, C. H., Wang, X. Y., Yang, X. Q., Li, L. (2009). Formation of soluble aggregates from insoluble commercial soy protein isolate by means of ultrasonic treatment and their gelling properties. *J Food Eng, 92,* 432-437.

Tiwari, B. K., Mason, T. J. (2012). Chapter 6 - Ultrasound Processing of Fluid Foods. In P.J.Cullen, K. T. Brijesh, V. Vasilis, & V. Vasilis (Eds.), *Novel Thermal and Non-Thermal Technologies for Fluid Foods* (pp. 135-165). San Diego: Academic Press.

Urbano, G., Lopez-Jurado, M., Aranda, P., Vidal-Valverde, C., Tenorio, E., Porres, J. (2000). The role of phytic acid in legumes: antinutrient or beneficial function? *J Physiol Biochem, 56,* 283-294.

Vilkhu, K., Mawson, R., Simons, L., Bates, D. (2008). Applications and opportunities for ultrasound assisted extraction in the food industry - A review. *Innov Food Sci Emerg Technol, 9,* 161-169.

Vinatoru, M. (2001). An overview of the ultrasonically assisted extraction of bioactive principles from herbs. *Ultrason Sonochem, 8,* 303-313.

Vinatoru, M., Toma, M., Radu, O., Filip, P. I., Lazurca, D., Mason, T. J. (1997). The use of ultrasound for the extraction of bioactive principles from plant materials. *Ultrason Sonochem, 4,* 135-139.

Vishwanathan, K. H., Singh, V., Subramanian, R. (2011). Influence of particle size on protein extractability from soybean and okara. *J Food Eng, 102,* 240-246.

Wang, L., Weller, C. L. (2006). Recent advances in extraction of nutraceuticals from plants. *Trends Food Sci Tech, 17,* 300-312.

Wijngaard, H.H., Zuidam, N.J. (2014). *Soybean extraction process*. International Publication WO14154472.

# CHAPTER 5

# COMPARING LAB AND PILOT-SCALE ULTRASOUND-ASSISTED EXTRACTION OF PROTEIN FROM SOYBEAN PROCESSING MATERIALS

This chapter is based on a published manuscript:

Preece, K. E., Hooshyar, N., Krijgsman, A. J., Fryer, P. J., Zuidam, N. J. (2017). Pilot-scale ultrasound-assisted extraction of protein from soybean processing materials shows it is not recommended for industrial usage. *J Food Eng, 206*, 1-12.

## ABSTRACT

Unit operations to enhance protein extraction within the food industry are vital to improve current processes, especially for cost reductions and sustainability. Here we show a study of ultrasound-assisted extraction (UAE) from soy slurry and okara produced at pilot-scale and further processed using a lab or pilot-scale probe system. Confocal laser scanning microscopy (CLSM) and particle size measurements were used to study the physical effects of UAE on these soy processing materials. Ultrasound at pilot-scale was unfeasible for soy slurry, in contrast to lab-scale. UAE from okara solution significantly increased protein yield by 4.2% at pilot-scale ($p < 0.05$). Okara solution flow rate and okara concentration also significantly improved the protein extraction yield. During lab-scale sonication of okara solution, a greater energy intensity resulted in a higher yield of up to 19% after 15 min treatment. The effects of pilot-scale sonication on okara solution were examined using CLSM; intact cells were still present and contained intact protein bodies within them. Reduced effects of UAE were noted in comparison to previous results obtained for okara prepared at lab-scale, this is attributed to the lack of aggregated protein bodies outside the cells within the pre-treated okara solution. Considering total extraction yields at pilot-scale during soybase production, ultrasound is not considered viable for industrial processing.

## 5.1 INTRODUCTION

Soybeans are a source of 'complete' protein, providing the body with all of the essential amino acids that humans are unable to synthesise. Soybeans range in composition and their use is dependent on their desired function; for soymilk preparation, soybeans are chosen with a high protein content, compared to those utilised for oil extraction. In terms of resources: less energy, water and land is required to provide the world with sufficient protein from plant-based sources compared to animal-based (Aiking, 2011). For these benefits to be realised, the processing of raw materials to provide the final products needs to be efficient. During current soymilk processing plants, a significant portion of the available protein enters the waste stream currently utilised as animal feed (O'Toole, 1999). A more sustainable extraction of components is required using a green technology to make soymilk manufacture more profitable on social, economic and environmental levels.

The soybean microstructure is complex. Within the storage cells of the soybean, protein is organised in 5-20 μm protein bodies, surrounded by a cytoplasmic network containing oil bodies in the size range of 0.2-0.5 μm stabilised by proteinaceous oleosins (Rosenthal *et al.*, 1998). In order to solubilise components inside the cells, the solvent needs to be in direct contact with those components. This is most easily facilitated by cell disruption. During soymilk production, soybeans are milled under hot (>80 °C), alkaline (pH 8+) conditions to solubilise protein, as well as inactivate the enzyme lipoxygenase and trypsin inhibitors (Vishwanathan *et al.*, 2011). Insoluble materials are removed from the slurry using centrifugation; this gives two streams: soybase, the precursor for soymilk, and a waste stream, termed okara. The okara has been shown, using confocal laser scanning microscopy (CLSM) (Preece *et al.*, 2015; **chapter 3**), to contain both intact cells and

insoluble protein in the continuous phase. It would obviously be valuable to increase the process yield by breaking up a higher proportion of the cells.

Ultrasound has been widely studied in the food industry for aiding the extraction of vegetal components of interest (Chandrapala *et al.*, 2013; Chemat *et al.*, 2011; Esclapez *et al.*, 2011; Patist & Bates, 2008; Shirsath *et al.*, 2012; Vilkhu *et al.*, 2008). Ultrasound is regarded as a green technology for reasons including reductions in extraction times, solvent use and energy consumption, as well as improving product quality (Sicaire *et al.*, 2016). The success of ultrasound is attributed to the cavitation phenomenon. Microbubbles are located within the liquid medium, and upon the application of ultrasound, sound waves cause pressure fluctuations which results in oscillation of the microbubbles. Upon a sufficiently negative pressure threshold, these bubbles can violently collapse, resulting in local regions of high temperature of 5000 K and pressures in the region of 1000 atm (Patist & Bates, 2008). These conditions aid with the solubilisation of materials into the liquid medium, enhancing the extraction. Upon asymmetric bubble collapse, liquid jets are formed which can disrupt cells upon contact with cell walls (Li *et al.*, 2004; Shirsath *et al.*, 2012), causing the release of intracellular compounds.

Soy-based studies are present examining the effects of ultrasound on the extraction of various compounds. For protein and sugar extraction, one such study by Karki *et al.* (2010) showed the application of ultrasound (20 kHz, $\leq$ 2 min treatment) improved the extraction yields from hexane-defatted soy flakes at lab-scale. Protein functionality improvement from soy protein isolate (SPI) and concentrates (SPC) has also been reported with positive results in protein solubility and particle size reduction (Lee *et al.*, 2016). Some studies on ultrasound-assisted extraction (UAE) from soy-based systems as the starting material exist, yet direct extraction from the soybean has largely been

neglected. Preece *et al.* (2017; **chapter 4**) showed that ultrasound (20 kHz, ≤ 15 min) improved protein extraction yield directly from soybeans in a lab-scale system, through slurry treatment and okara treatment on samples prepared at lab-scale. This research supported the patent of Wijngaard & Zuidam. (WO14154472, 2014). During the preparation of soy-based beverages, direct extraction of proteins, oils and other alkali-soluble components by wet milling from soybeans is commonly used during factory-scale manufacture (Vishwanathan *et al.*, 2011). UAE of soy protein has been studied previously (Moulton & Wang, 1982) under continuous conditions on pilot-scale, using defatted soy flakes as the starting material. However, this study was carried out more than 30 years ago, and key experimental data, such as particle size measurement and visualisation of the microstructure, were neglected. Direct extraction from soybeans are rarely studied at a lab-scale, and no pilot-scale studies were found in the literature.

Pilot-scale use of ultrasound has been documented for a limited number of food systems, other than soy protein extraction. Pingret *et al.* (2012) showed an improvement of 30% extraction of polyphenols was achievable using ultrasound-assistance (20 kHz, 40°C, 40 min) versus conventional extraction from apple pomace in a 30 L tank. Another study focused on waste stream valorisation; phenolic compounds were extracted from maritime sawdust waste using UAE (25 kHz, 40 min) with an increased phenolic yield of 30% compared to conventional maceration on a pilot-scale (Meullemiestre *et al.*, 2015). A lower recovery of capsaicinoids from chilli peppers on a pilot-scale (20 L tank) was obtained using UAE compared to hot maceration at industrial scale, although reductions in temperature and time were achieved (Boonkird *et al.*, 2008).

Pilot-scale studies of UAE directly from soybeans has not been previously reported in the literature. Here we show the effects of ultrasound on the protein extraction yield during soybase production

(pilot-scale) using lab and pilot-scale probe systems. We hypothesise that an improvement in extraction yield, as found before at lab-scale (Preece *et al.*, 2017; **chapter 4**), will be observed at pilot-scale as well due to the improved solubility of protein. A central composite design (CCD) was employed to examine the effects of okara concentration, okara flow rate and temperature of ultrasound treatment on the protein extraction yield at pilot-scale versus a conventional method for extraction. The optimum conditions are identified for the specific conditions tested and analysis of variance (ANOVA) will be employed to determine the significance of factors. Particle size and an examination of the microstructure of the materials is performed to aid in identification of the mechanisms of ultrasound.

## 5.2 MATERIALS AND METHODS

### 5.2.1 Sample production

Soy slurry and okara were prepared from commercially available soybeans using pilot plant facilities (Unilever Research & Development, Vlaardingen). An image of the equipment can be found in Appendix 8.3. A process flow diagram and stream information can be seen in Figure 5.1 and Table 5.1. Under these processing conditions, it was possible to prepare soy slurry and okara to test the effects of ultrasound. Soybeans (stream 1, Figure 5.1) went through two wet milling stages to produce a soy slurry under alkaline conditions. The processing input consisted of 28 kg $h^{-1}$ of soybeans treated with 175 kg $h^{-1}$ of softened water and 0.2 kg $h^{-1}$ of sodium bicarbonate. To prepare soybase and okara for subsequent treatment, the slurry was fed into a decanter centrifuge operating at a *g*-force-time of $1.5 \times 10^5$ *g*-s. Table 5.2 shows the average compositions of okara (Figure 5.1, stream 8) and soy slurry (Figure 5.1, stream 4) produced using the pilot plant processing equipment *without ultrasonic treatment*.

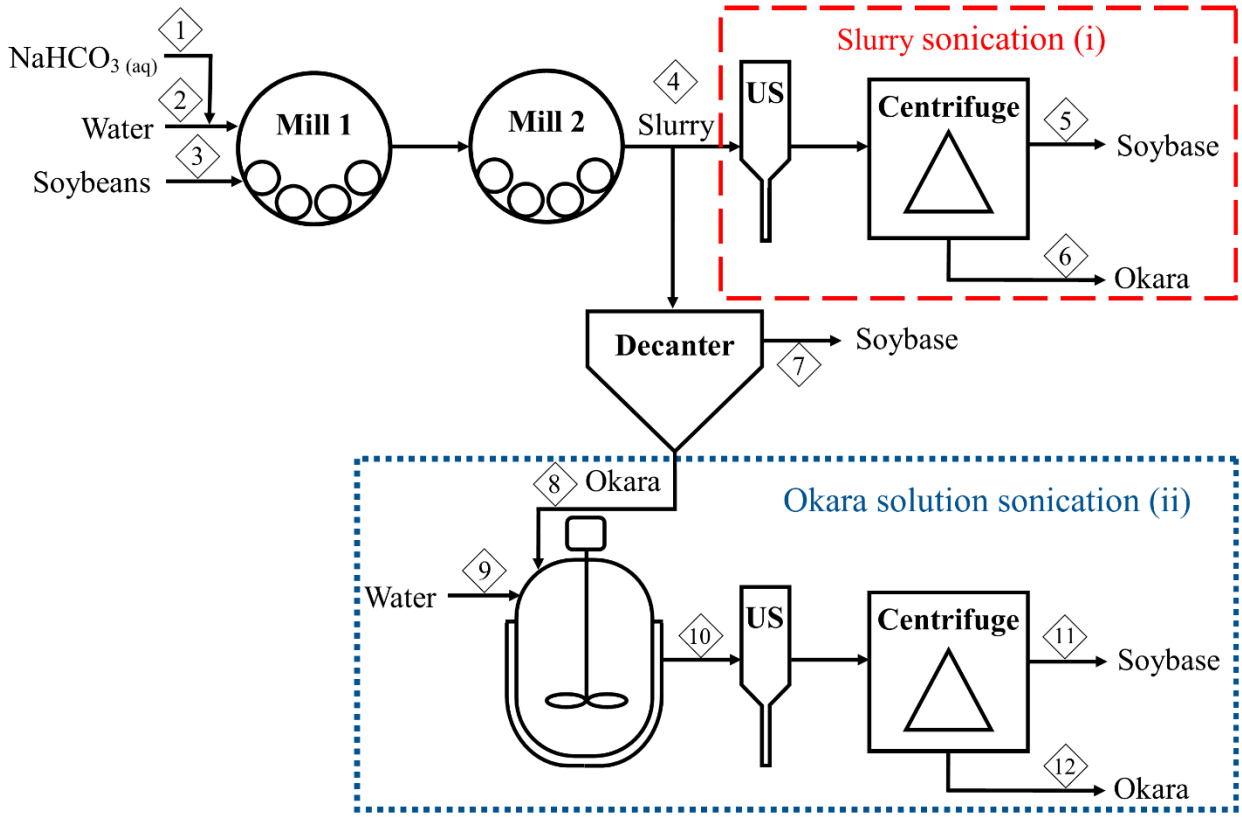


Figure 5.1. Process flow diagram of pilot plant slurry preparation and ultrasound treatments of slurry and okara solution samples. The red box (— —) shows the flowsheet for slurry sonication, only investigated at lab-scale. The blue box (···) shows the process for okara solution sonication, carried out at lab & pilot-scale.

Table 5.1. Mass flow rates of components and temperatures of streams described in Figure 5.1.

| | **Stream** | | | | | |
|---|---|---|---|---|---|---|
| | 1 | 2 | 3 | 4 | 7 | 8 |
| **T (°C)** | 25 | 85 | 25 | 85 | - | - |
| $\dot{m}_{protein}$ **(kg h$^{-1}$)** | 0 | 0 | 10.3 | 10.4 | 7 | 3.2 |
| $\dot{m}_{oil}$ **(kg h$^{-1}$)** | 0 | 0 | 5.5 | 5.6 | 3.3 | 1.8 |
| $\dot{m}_{moisture}$ **(kg h$^{-1}$)** | 8.9 | 163.6 | 2.4 | 174 | 126.2 | 48.2 |
| $\dot{m}_{other}$ **(kg h$^{-1}$)** | 0.2 | 0 | 10 | 10 | 4.3 | 6 |
| $\dot{m}_{total}$ **(kg h$^{-1}$)** | 9.1 | 163.6 | 28.2 | 200 | 140.8 | 59.2 |

Figure 5.1 also shows the process flow diagram for:

(i) & (ii) *Lab-scale ultrasonic treatment* of the okara and slurry from pilot-scale production (see Section 5.2.2). Here, materials were transferred from the pilot plant and treated with a bench-scale 400 W probe previously used to study lab-scale extraction (Preece *et al.*, 2017; **chapter 4**).

(ii) *Pilot-scale ultrasonic treatment* of okara, where the okara was treated using a pilot-scale 2000 W probe (see Section 5.2.3).

Table 5.2. Average okara and slurry composition produced without ultrasonic treatment. The error shown is the deviation in production over 5 different productions. Stream (no.) corresponds to the stream number labelled in Figure 5.1.

| | **Stream (no.)** | |
|---|---|---|
| Component | **Slurry (4)** | **Okara (8)** |
| **Protein** | 5.2 ± 0.1% | 5.4 ± 0.2% |
| **Oil** | 2.8 ± 0.1% | 3.1 ± 0.3% |
| **Moisture** | 87.2 ± 0.2% | 81.4 ± 0.5% |
| **Other** | 4.8 ± 0.2% | 10.1 ± 0.6% |

### 5.2.2 Laboratory-scale sonication

A bench-scale batch ultrasound probe system (Branson Sonifier 450, Branson Ultrasonics Corporation, Danbury, CT), (20 kHz, 65 W (output according to manual), 13 mm probe tip) was utilised to examine the effects of ultrasound on slurry and okara solution samples produced in the pilot plant. Ultrasound treatment times from 0 min (control) up to 15 min were investigated to vary the energy input to the system. After the sample was treated for the desired time, the sample was immediately centrifuged at $4330 \times g$ for 10 min. Using the data shown in Section 5.2.8, it was possible to calculate the energy input based on the recorded temperature increase. The energy input was calculated using the equations reported by Bates & Patist (2010), which gives a unit independent of the scale of treatment for continuous and batch operation:

$$Energy\ input, W_{\text{input}} = \frac{P}{Q} = \frac{P \times t}{3.6 \times 10^6 \times V} \quad (5.1)$$

where power ($P$ in kW) was calculated assuming all energy input was transferred to heat energy and no heat was lost to the surroundings and $Q$ is the volumetric flow rate (L $h^{-1}$) for continuous application. Power ($P$), time ($t$ in s) and volume ($V$ in L) were necessary to calculate energy based on batch operation.

#### *5.2.2.1 Soy slurry treatment*

Soy slurry (100 g) from pilot-scale production (Figure 5.1, stream 4; i.e. prior to separation in the decanter, for composition, see Table 5.2) was heated to 80 °C using a hot plate and stirred using a magnetic stirrer bar set to a speed of 200 rpm (25 mm in length, 10 mm in diameter cylindrical bar). Once the desired temperature was reached after approximately 15 min, the sample was transferred to a jacketed vessel and the ultrasound treatment was commenced with temperature control.

#### *5.2.2.2 Okara solution treatment*

Okara produced in the pilot plant facilities (Figure 5.1, stream 8; for composition, see Table 5.2) was diluted approximately 7 times to an okara concentration of 13.7% (w/w, solid content about 2.5 ± 0.1%) using demineralised water. A sample size of 100 g of okara solution was heated to 50 °C using the same method described in Section 5.2.2.1. Temperature control was also employed during okara solution sonication by counter-current flow of cool water in a jacketed vessel.

### 5.2.3 Pilot-scale sonication

To examine the effects of ultrasound on a larger scale, samples were prepared and treated using continuous ultrasonic pilot-scale equipment. When choosing parameters for investigation, the energy input (kWh $L^{-1}$) was calculated using equation 5.1 for the lab scale sonication system (using input information from the supplier) and scaled to a larger scale probe ((UIP2000hd, Hielscher Ultrasonics GmbH, Germany) (20 kHz, 2000 W, 100% amplitude) fitted with booster B2-1.4 and sonotrode CS2d40L3) (Bates & Patist, 2010). A photograph of the probe system can be seen in Figure 5.2. The flow rate through the ultrasonic cell could be varied using a pump operating within the range 20-300 kg $h^{-1}$. However, the number of passes required through the flow cell (0.8 L) to achieve similar energy inputs for slurry treatment at the operating flow rate of 200 kg $h^{-1}$ was more than 9. Soy slurry sonication (slurry sonication (i), Figure 5.1) was deemed unfeasible for this pilot-scale study as there was access to only one large scale probe system. Only okara solution was considered at pilot-scale for this reason (okara solution sonication (ii), Figure 5.1). A single pass through the flow cell could be achieved using the equipment available; however, multiple passes of the material through the ultrasonic field would require an outlet valve which was not available.

Once produced, okara was diluted to the desired concentration using water in a tank stirred at 600 rpm suitable for heating (100 L capacity). Okara solution was pumped using a positive displacement pump through a jacketed ultrasonic flow cell; the jacketed vessel was employed to reduce heating of the okara solution samples during ultrasonic treatment. A counter-current flow of cold tap water was employed; an approximate flow rate of water of 10 kg $h^{-1}$ was recorded. For each trial, a sonicated okara solution sample was collected and also a control sample which passed through the same set-up, with the ultrasound switched off. Samples were then centrifuged in a

bench top centrifuge (4330 × *g*, 10 min) and analysed for their compositions in order to calculate extraction yields.


Figure 5.2. Photographs of the pilot-scale probe in the sound protection box (A) and the contents of the box with annotation (B).

### 5.2.4 Oil, protein and solids determination and extraction yield calculations (%)

To examine the effects of ultrasound, extraction yields for oil, protein and solids were calculated from the relevant concentrations in the process streams.

To determine protein extraction yields, the protein content on a wet basis (w.b.) was defined in the pellets and supernatants using the Dumas method (Vario MAX CNS, Elementar Analysensysteme GmbH, Germany). L(+)-glutamic acid (VWR International BVBA, Belgium) was used as a standard sample and UHT milk (3.5% fat) (muva kempten, Germany) as a reference material. For soy samples, a protein conversion factor of 6.25 × N was utilised to determine protein content from the measured nitrogen content. From the protein concentrations and masses of streams, the protein extraction yield into the soybase could be calculated using equation 5.2:

$$\text{Protein extraction yield} = Y\ (\%) = \left[\frac{S \cdot x_{\mathrm{p,s}}}{(S \cdot x_{\mathrm{p,s}} + O \cdot x_{\mathrm{p,o}})}\right] \times 100\% \qquad (5.2)$$

Here *S* (soybase) and *O* (okara) represent the total weight of samples, and $x_{\mathrm{p,s\ and}}\ x_{\mathrm{p,o}}$ are the mass fractions of protein in *S* and *O*, respectively.

To analyse the effects of ultrasound on okara solution on the whole process, it was necessary to consider the total protein extraction yield calculated using equation 5.3; i.e. the recovery from both soybase and okara. Yield $Y_{\mathrm{I}}$ refers to the primary extraction producing soybase and okara (streams 7 & 8, Figure 5.1); yield $Y_{\mathrm{II}}$ corresponds to the extraction from okara solution (streams 11 & 12, Figure 5.1).

$$\text{Total protein extraction yield}\ (\%) = Y_{\mathrm{I}} + (100\% - Y_{\mathrm{I}}) \times Y_{\mathrm{II}} \qquad (5.3)$$

Oil and solid contents were measured using a microwave moisture analysis system equipped with NMR for direct detection of fat content (SMART System5, CEM GmbH, Germany). Oil and solid extraction yields were also determined using equation 5.2, replacing the masses of protein, with the respective masses. For the analytical measurements of oil, protein and solids, every sample was measured in duplicate and an average was calculated. A pooled standard deviation ($SD_{pooled}$) was calculated for each method of analysis based on the measurement of 159 samples in duplicate: values of 0.01%, 0.04% & 0.06% were calculated for oil, protein and solids respectively.

### 5.2.5 Experimental design

Experiments for the pilot-scale were defined using response surface methodology (RSM) to test the importance of three input variables: okara concentration ($X_1$), okara solution flow rate through the ultrasonic flow cell ($X_2$) and temperature ($X_3$) on the output response: protein extraction yield. A central composite design was made using the software JMP (v11 from SAS, Cary, NC), including measurement of the centre point twice, totalling 16 trials. The input variables and randomised trial order can be found in Table 5.3. All input variables were tested on 5 levels ($-\alpha$, -1, 0, +1, $+\alpha$) with an $\alpha$-value of 1.287. The upper and lower levels were set based on limitations of the pump (flow rate and okara concentration) and sensible temperature values. An analysis of variance (ANOVA) was performed once results were gathered to determine the significance of the three parameters tested.

Table 5.3. Experimental domain of central composite design for pilot plant study.

| $X_j$ | Uncoded | Lower level | Upper level |
|---|---|---|---|
| Okara concentration (%) | $X_1$ | 14 | 50 |
| Flow rate (kg $h^{-1}$) | $X_2$ | 20 | 100 |
| Temperature (°C) | $X_3$ | 50 | 85 |

| | **Input variables** | | | **Experimental protein extraction yield (%)** | |
|---|---|---|---|---|---|
| Trial | $X_1$ | $X_2$ | $X_3$ | Control | Ultrasound |
| 1 | 32 | 60 | 68 | 42 | 51 |
| 2 | 46 | 91 | 81 | 40 | 42 |
| 3 | 46 | 29 | 81 | 40 | 46 |
| 4 | 18 | 29 | 81 | 58 | 64 |
| 5 | 32 | 20 | 68 | 40 | 44 |
| 6 | 14 | 60 | 68 | 59 | 56 |
| 7 | 50 | 60 | 68 | 42 | 44 |
| 8 | 32 | 60 | 50 | 43 | 45 |
| 9 | 32 | 100 | 68 | 38 | 51 |
| 10 | 18 | 91 | 54 | 51 | 54 |
| 11 | 18 | 29 | 54 | 51 | 58 |
| 12 | 32 | 60 | 85 | 42 | 46 |
| 13 | 18 | 91 | 81 | 41 | 47 |
| 14 | 46 | 29 | 54 | 41 | 45 |
| 15 | 32 | 60 | 68 | 41 | 43 |
| 16 | 46 | 91 | 54 | 39 | 38 |

### 5.2.6 Particle size measurement

The particle sizes of soy slurries after extraction were determined using laser diffraction (Mastersizer 2000 Hydro S, Malvern Instruments Ltd, UK). To determine particle size distributions (PSDs), refractive indices of 1.33 and 1.45 were used for the water and the particles, respectively. Particle sizes were measured in triplicate for each sample.

### 5.2.7 Confocal laser scanning microscopy (CLSM)

A Leica TCS-SP5 microscope in conjunction with a DMI6000 inverted microscope (Leica Microsystems Inc., Germany) was used with the dye acridine orange (Polysciences Inc., Warrington, PA) for visualisation using of the effects of ultrasound treatment. One drop of dye stock solution (1% w/v acridine orange) was added to 1-1.5 mL of sample and mixed well before adding the sample to the glass slide. Table 5.4 shows the lasers utilised for excitation and the corresponding colours assigned to the emission channels.

Table 5.4. CLSM excitation and emission settings specified for acridine orange.

| Fluorochrome | Excitation wavelength (nm) | Emission wavelengths (nm) | Representing colour in micrographs |
|---|---|---|---|
| **1% w/v Acridine orange** | 488 | 497-556 | Green |
| | 561 | 569-646 | Red |
| | | 655-724 | Blue |

### 5.2.8 Gas chromatography – mass spectrometry (GC-MS)

To assess oil oxidation, headspace analysis was performed on the okara solution samples prepared in the 16 pilot plant trials. A comparison was made between the ultrasound treated sample and the control sample to detect oil oxidation associated with ultrasonic processing. Okara solution samples were frozen after production, defrosted and 4 g of sample was added to a 20 mL vial and stored overnight at 4 °C before analysis of hexanal in the headspace. The gas chromatography system was an Agilent 7890B (Agilent Technologies, California, USA) and a Rxi-5ms column (Restek, Pennsylvania, USA) coupled with a TruTOF mass spectrometer (LECO, Michigan, USA) Measurements were carried out in triplicate.

### 5.2.9 Comparison of lab-scale and pilot-scale probes

When studying the effects of ultrasound, it is important that the power input is calculated, rather than quoting values from the manufacturer. Several factors affect the actual power supplied to the system by ultrasound, such as the age of the probe tip (Vinatoru, 2015). For both probe systems, a calorimetry study was carried out in which the temperature increase was measured during ultrasound treatment of demineralised water. For the lab-scale probe, a sample of 0.1 kg was studied, compared to the pilot-scale probe used to treat a 0.8 kg water sample. The mass of water studied at pilot-scale was chosen due to the volume of the pilot-scale flow cell. Assuming all of the energy supplied to the system by ultrasound ($Q$) was transferred to heat, it can be calculated as:

$$Q = mC_P\Delta T \tag{5.4}$$

where ($m$, kg) is the mass of the sample, $C_P$ is the specific heat capacity (4181 J kg$^{-1}$ K$^{-1}$) (Sicaire *et al.*, 2016) and $\Delta T$ is the temperature increase.

To assess the scalability of ultrasound, it was possible to calculate parameters independent of scale. Energy intensity ($EI$, W cm$^{-2}$) and acoustic energy density ($AED$, W cm$^{-3}$) were calculated using equations from Tiwari & Mason (2012), shown in Equations 5.5 & 5.6.

$$Energy\ intensity, EI = \frac{4P}{\pi D^2} \tag{5.5}$$

where $P$ is the power (W) and $D$ is the diameter (cm) of the probe tip.

$$Acoustic\ energy\ density, AED\ = \frac{P}{V} \tag{5.6}$$

where $P$ is the power (W) and $V$ (cm$^3$) is the volume of sample treated.

## 5.3 RESULTS & DISCUSSION

### 5.3.1 Laboratory-scale sonication

Figure 5.1 shows the process flow diagram for the production of soy samples. To determine the potential for ultrasound-assisted extraction (UAE), it was performed (i) on the slurry from the primary production (stream 4, Figure 5.1) and (ii) diluted okara solution (with a solid content of 2.5 ± 0.1% w/w) prepared on pilot plant scale (stream 10, Figure 5.1) using a lab-scale probe system. The effects of ultrasound on the oil, protein and solid extraction yields from soy slurry can be seen in Figure 5.3. An improvement was observed for each component upon ultrasound treatment, and after 15 min of ultrasound treatment (absolute values compared to the 0 min control sample) was:

- Protein extraction increased by 4%
- Oil extraction enhanced by 12%
- The yield of solids increased by 6%

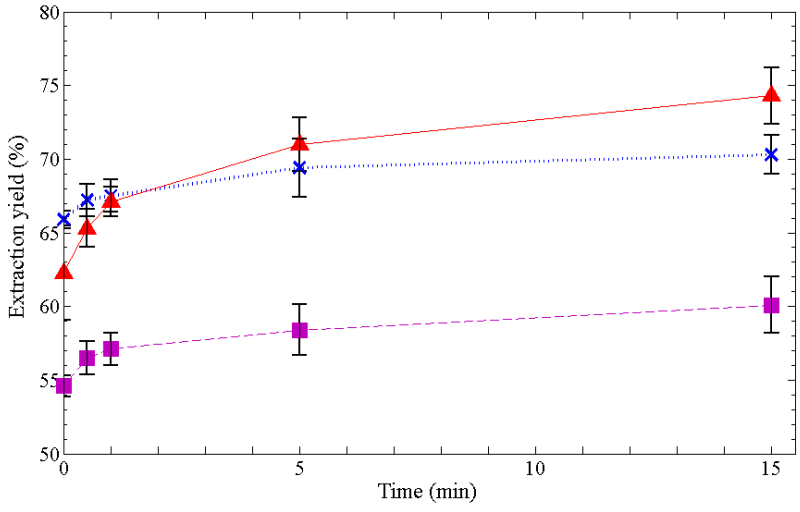


Figure 5.3. The effect of lab-scale batch ultrasonic treatment time on the extraction yields of oil (▲), protein (X) and solids (■) from soy slurry (resulting in streams 5 & 6, Figure 5.1). Error bars show standard error of 3 mean values.

The temperature was held at 80 °C throughout the experiment for slurry treatment. As a control a slurry sample was heated to 80 °C and held at this temperature for 15 min whilst stirring (no ultrasound treatment). No difference in extraction yield of protein, oil or solids was observed, as apparently equilibrium had been reached at the zero time point (data not shown).

Ultrasound was also used to treat a solution containing the okara waste stream from soymilk production (stream 10, Figure 5.1). An improvement in extraction yields was observed for all of the components examined during ultrasonic treatment to the okara solution, seen in Figure 5.4. An improvement of 19% in extraction of the protein available in the okara using ultrasound after 15 min treatment was observed, compared to the 0 min sample (Figure 5.4). Oil extraction was increased by 23% after 15 min US treatment compared to the control sample. Extraction of solids found within okara was enhanced by 9% with 15 min ultrasonic treatment compared to 0 min control. When considering the total protein extraction yield, $Y_{II}$ calculated using equation 5.3, an increase of up to 5% was observed during okara solution US treatment (84% versus 89%: control (no US) and 15 min treatment respectively). To understand the mechanism behind this improvement, the separation efficiencies and availability of protein were calculated using equations presented by Preece *et al.* (2017; **chapter 4**). It was found that during okara solution sonication, blue box ii, Figure 5.1, the separation efficiency remained constant at a value of 80% throughout the control and all treated samples. However, when studying the availability of protein, a stepwise improvement was seen: an increase of up to 24% was observed during okara solution US treatment (58% versus 82%: control (no US) and 15 min treatment respectively). Thus, ultrasound caused an improvement in protein extraction yield by improving the protein availability, not by the

deliquoring of okara, as has been previously stated for ultrasound treatment of another soybean extract system (Preece *et al.*, 2017; **chapter 4**).

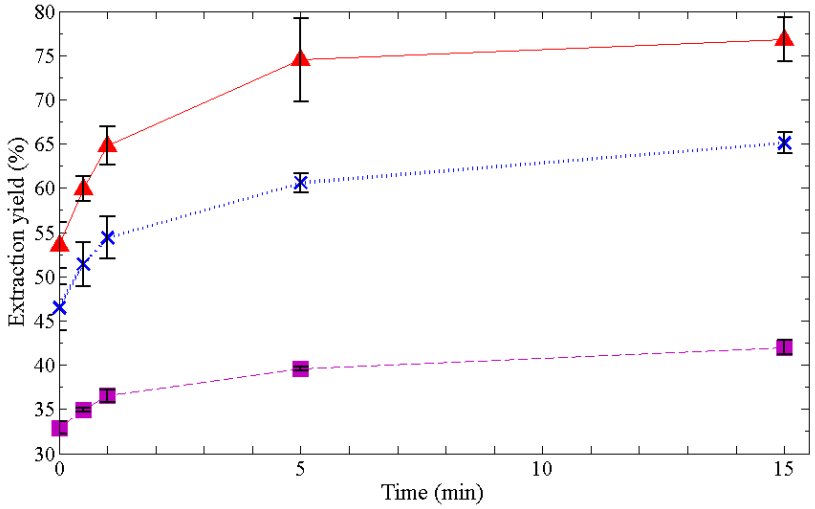


Figure 5.4. Extraction yields of oil (▲), protein (X) and solids (■) from okara solution versus ultrasonic treatment times using lab-scale probe system (resulting in streams 11 & 12, Figure 5.1). Error bars represent standard error of 3 mean values.

### 5.3.2 Pilot-scale sonication

#### *5.3.2.1 Experimental design studies*

Now that positive effects of ultrasound had been observed at bench scale, it was important to explore the scale-up opportunity of the technology at pilot-scale. As ultrasound treatment of slurry was not feasible at pilot-scale (see Section 5.2.3), only okara was studied here. There are a large number of factors that affect the outcome of ultrasonic treatment (Soria & Villamiel, 2010), therefore design of experiments was employed to test a large investigational area. Three important variables were examined using a central composite design (CCD) in this instance: okara concentration ($X_1$), okara flow rate (ultrasonic duration, $X_2$) and temperature of treatment ($X_3$). Table 5.3 shows the response variable (experimental protein extraction yield) and how this

responds to different processing conditions related to ultrasonic treatment. An analysis of variance (ANOVA) was carried out to determine the significance of the studied variables as well as the ultrasonic treatment itself. All terms were examined for linear, quadratic and interaction effects. Results of the ANOVA from the model can be seen in Table 5.5. Factors were considered to be significant at a confidence level of 95% ($p$-value < 0.05). Temperature was excluded from the model, as its effects were not found to be significant ($p$-value = 0.8858) in the range investigated (50-80 °C). The insignificance of this factor is due to the previous heat treatment during okara production (85 °C milling of soybeans). Even though the solubilisation time is low during the milling stages and prior to separation, the residual heat after production is high, therefore denaturation of protein is possible. There are no further effects of heating the okara solution to 85 °C compared to 50 °C. It was found that the linear effects of input variables examined were significant, as well as the effects of ultrasound treatment and the quadratic effect of okara concentration ($X_1^2$) (Table 5.5). Interactions between input variables were not found to be significant, therefore no synergistic effects were observed (p-value > 0.05).

Table 5.5. ANOVA for quadratic model of relationship between independent input variables ($X_1$, $X_2$, $X_3$ and ultrasonic treatment) and output (Protein extraction yield (%). Significant sources (p-value <0.05) are highlighted as bold.

| Source | Sum of Squares | DF | Mean square | F Value | Prob > F |
|---|---|---|---|---|---|
| Model | 1187.15 | 6 | 197.86 | 15.76 | **<.0001*** |
| $X_1$ | 734.66 | 1 | 734.66 | 58.52 | **<.0001*** |
| $X_2$ | 89.65 | 1 | 89.65 | 7.14 | **0.0131*** |
| Ultrasonic treatment | 142.23 | 1 | 142.23 | 11.33 | **0.0025*** |
| $X_1^2$ | 140.35 | 1 | 140.35 | 11.18 | **0.0026*** |
| $X_1$*$X_2$ | 41.02 | 1 | 41.02 | 3.27 | 0.0827 |
| $X_2$*$X_3$ | 39.24 | 1 | 39.24 | 3.13 | 0.0893 |
| Lack of fit | 278.34 | 23 | 12.10 | 0.68 | 0.7488 |
| Pure error | 35.53 | 2 | 17.76 | | |
| Total error | 313.86 | 25 | | | |
| C.Total | 1501.02 | 31 | | | |
| $R^2$ | 0.791 | | | | |
| $R^2_{adj}$ | 0.741 | | | | |

With the data obtained from the CCD, it was possible to deduce a relationship between the variables and the protein extraction yield. This relationship can be seen in equation 5.7 containing only the significant factors:

$$Y_{II} = 43.7 - 7.3X_1 - 2.56X_2 + 2.1(US) + 5.9X_1^2 \quad (5.7)$$

where $Y_{II}$ represents protein extraction yield from okara, $X_1$ is the okara concentration, $X_2$ is the okara solution flow rate through the ultrasonic flow cell and *US* corresponds to ultrasonic treatment (*US* = +1 for ultrasound, *US* = -1 for control experiment). The model has a reasonable fit to the variability of the data ($R^2$ = 0.791) obtained from these pilot plant trials. The adjusted $R^2$ value is corrected for the number of input parameters investigated in the model; the value presented ($R^2_{adj}$ = 0.741) shows a good correlation between observed and predicted data. Equation 5.7 shows that ultrasonic treatment improves the protein yield ($Y_{II}$) by 4.2% (difference between 2.1 × +1 for

ultrasound and 2.1 × -1 for control), independent of okara solution flow rate and okara concentration.

#### *5.3.2.2 Response surface plots of ultrasound-assisted extraction (UAE) at pilot-scale*

According to the model, the greatest effects on the protein extraction yield at pilot scale came from the okara concentration and the okara flow rate, and not from the ultrasound treatment. The effects of the variables on control samples without ultrasound are visualised in Figure 5.5. From this plot, it is possible to examine the effects of okara concentration and flow rate on the output variable of interest for the control sample without ultrasonic treatment. The okara concentration affects the solid-liquid ratio which is an important parameter when studying solid-liquid extraction. At the lowest okara concentration, the separation efficiency and thus the yield is higher as there is relatively more water in the soybase than in the okara waste stream. At the highest okara concentration of 50%, there was less solvent available per unit of protein to be extracted and the increased solids, therefore a lower protein extraction yield was observed. The reduction in protein extraction yield can be linked to the effect of solid-to-liquid ratio on the separation efficiency, discussed in Section 2.4.

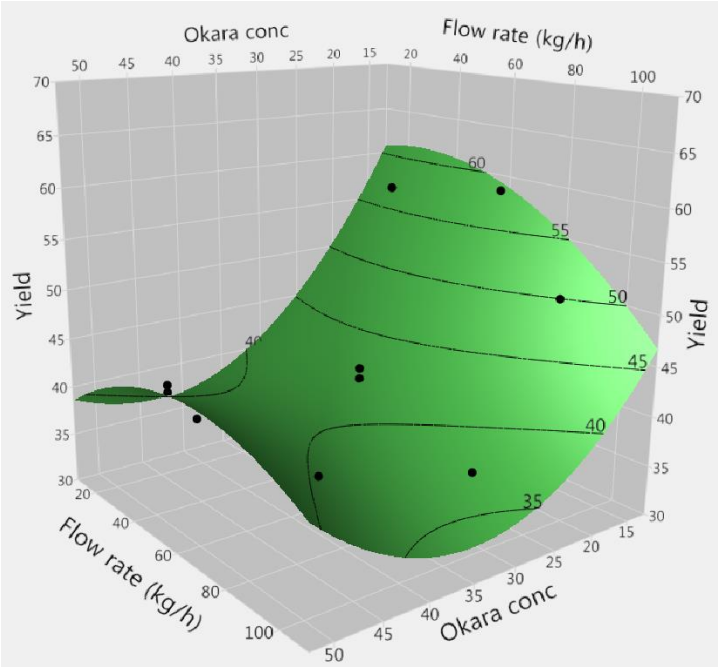


Figure 5.5. Response surface plot for protein extraction yield (equation 5.2) as a function of okara concentration and okara flow rate through the ultrasonic flow cell at 68 °C for control sample at pilot-scale (without ultrasound). Black dots are experimental points.

When considering the okara flow rate, it is vital to consider the residence time within the system as well as fluid mechanics, even for the control sample which travels the same path as the treated sample, but without the ultrasonic field. At the lowest tested okara solution flow rate, the protein extraction yield was not optimal, although the residence time was 6 min (Table 5.6). Another important factor to consider is the flow pattern of the sample and to do this, the Reynolds number (*Re*) was calculated for each flow rate studied using dynamic viscosity data from the literature (Table 5.6) (Poling *et al.*, 2008) using equation 5.8:

$$Re = \frac{QD_{\mathrm{H}}}{\nu A} \tag{5.8}$$

where $Q$ represents the volumetric flow rate ($m^3\ s^{-1}$), ν is the kinematic viscosity ($m^2\ s^{-1}$), $D_H$ is the hydraulic diameter of the pipe (m) and $A$ is the cross sectional surface area of the pipe ($m^2$).

As the flow rate increases, the residence time and the contact time between the extraction medium (alkali water) and components, such as protein, will decrease. When considering the flow regime of the solution through the piping, it has been calculated that the flow was laminar at 60 kg $h^{-1}$ and below, with the motion of fluid always following fluid streamlines (Table 5.6). For okara solution flow rates of 91 and 100 kg $h^{-1}$, the flow is in a transition region and this corresponds to less regular flow caused by irregular transverse eddies. From the studied conditions, a maximal extraction yield was observed at a mid-range of okara solution flow rate; this was probably caused by a balance between fluid dynamics and solubilisation times. The greatest yield was 59% without ultrasonic treatment (at 14% okara concentration, 60 kg $h^{-1}$ okara solution flow rate, temperature of 68 °C) and 64% when ultrasound was added (at 18% okara concentration, okara solution flow rate of 29 kg $h^{-1}$, and temperature of 81°C, Figure 5.6). The maximum effects observed experimentally are different for okara solution washing versus okara solution sonication. During ultrasonic treatment, the Reynolds number was not calculated. A heterogeneous environment is created upon the application of ultrasound, caused by localised cavitation where bubble formation, growth and collapse resulting in regions of irregular velocity: turbulence. Local turbulence is assumed during all of the ultrasonic treatments.

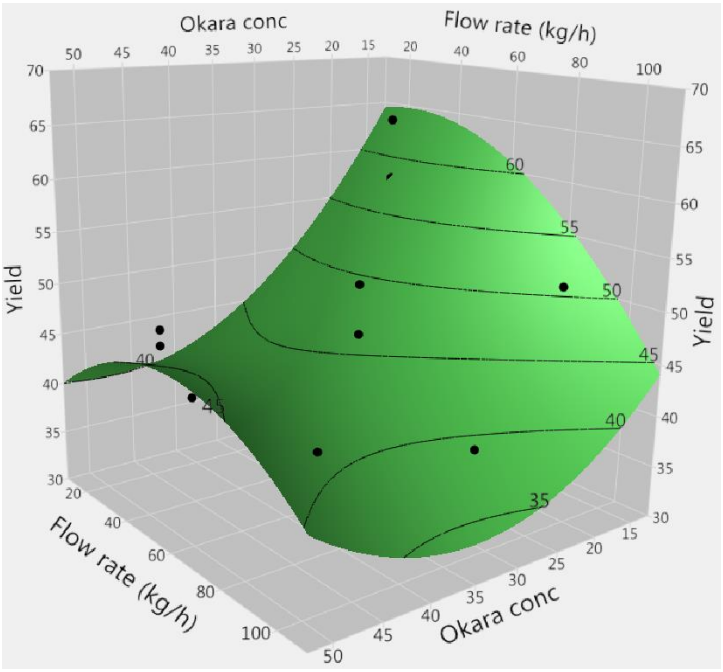


Figure 5.6. Response surface plot for protein extraction yield (equation 5.2) as a function of okara concentration and okara flow rate through the flow cell at 68 °C for ultrasonically treated okara at pilot-scale. Black dots are experimental points.

Table 5.6. Okara solution mass flow rates and corresponding flow parameters through the piping and flow cell, without ultrasonic treatment. The Reynolds number was calculated for the okara solution which behaved as a Newtonian fluid (data not shown).

| **Mass flow rate (kg $h^{-1}$)** | **20** | **29** | **60** | **91** | **100** |
|---|---|---|---|---|---|
| **Residence time (min)** | 6 | 4 | 2 | 1 | 1 |
| **Reynolds number (*Re*)** | 732 | 1062 | 2197 | 3332 | 3662 |
| | Laminar flow | | | Transition region | |

*5.3.2.3 PSD*

One important characteristic of the sample that changes as a result of ultrasonic treatment is the PSD. It is well documented that ultrasonic processing results in a reduction in particle size. These effects on resulting supernatant (stream 11, Figure 5.1) can be seen in Figure 5.7. In the control sample, the soybase obtained after centrifugation of okara solution without ultrasound treatment

had a broad particle size distribution with particles up to 10 µm present. Ultrasonic treatment of all okara solution flow rates investigated resulted in a reduction of the particle size of the corresponding soybase. A stepwise reduction in the particle size can be observed. The slowest flow rate of 20 kg $h^{-1}$, corresponding to the longest residence time in the ultrasonic field, yielded particles up to 1 µm in size. Reducing the particle size of the resulting soybase may improve the storage stability of the final soy beverage products.

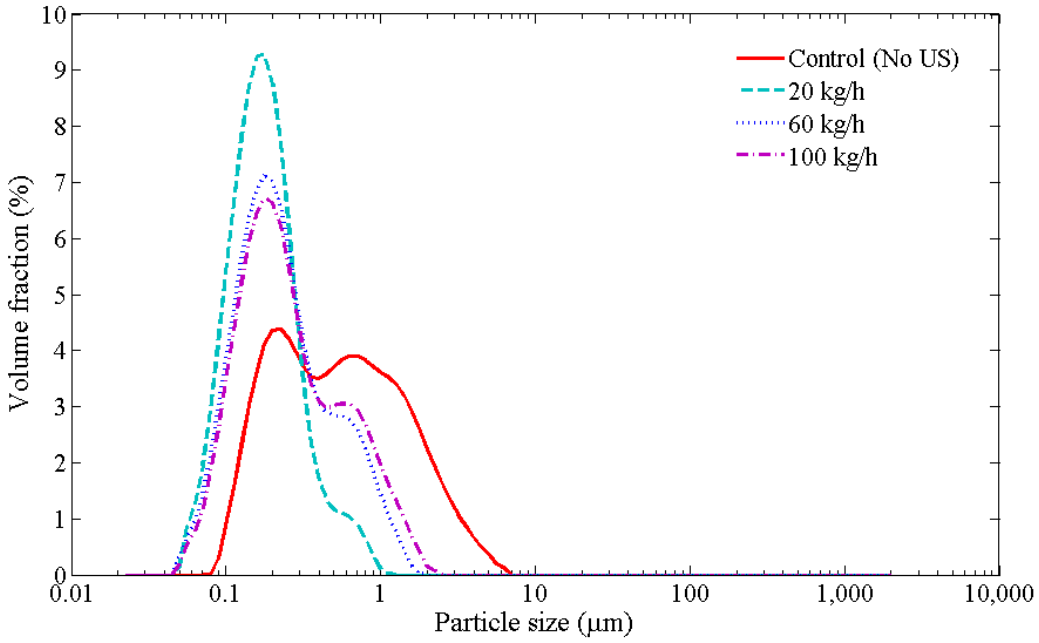


Figure 5.7. Effects of okara solution flow rate on the particle size distribution of resulting soybase after centrifugation (stream 11, Figure 5.1). Okara solution – no US shows the PSD of the supernatant after separation without ultrasound.

#### *5.3.2.4 CLSM*

To understand the effects of ultrasound, the microstructure of processing materials were investigated using CLSM. Figure 5.8 shows representative micrographs of okara solution prior to ultrasonic treatment at various magnifications visualised using acridine orange. It is possible to visualise fibrous materials, protein and other biopolymers within these samples (Preece *et al.*, 2015; **chapter 3**). In Figure 5.8A, many features are highlighted in purple (a combination of blue and red emission); these correspond to empty cell wall structures or fibrous material. Green features under these visualisation conditions highlight the more hydrophobic regions and here represent intact soybean cell walls (Figure 5.8B and 5.8C). Within these cells it is possible to visualise intact protein bodies (appearing green, Figure 5.8C) and the cytoplasmic network containing oil bodies stabilised by oleosins are highlighted in purple. These findings are similar to those found by Preece *et al.* (2015; **chapter 3**) when visualising soy slurry and okara. It was not possible to locate insoluble protein bodies in the size range 5-20 μm in okara solution samples outside cells prior to treatment with ultrasound. These insoluble protein bodies found outside of the cellular matrix were observed in soy slurry and okara that were prepared in the lab (Preece *et al.*, 2015; **chapter 3**). Apparently, aggregation of protein bodies during pilot plant production does not take place or they reduce in size immediately, most likely due to shorter residence times and more efficient milling.

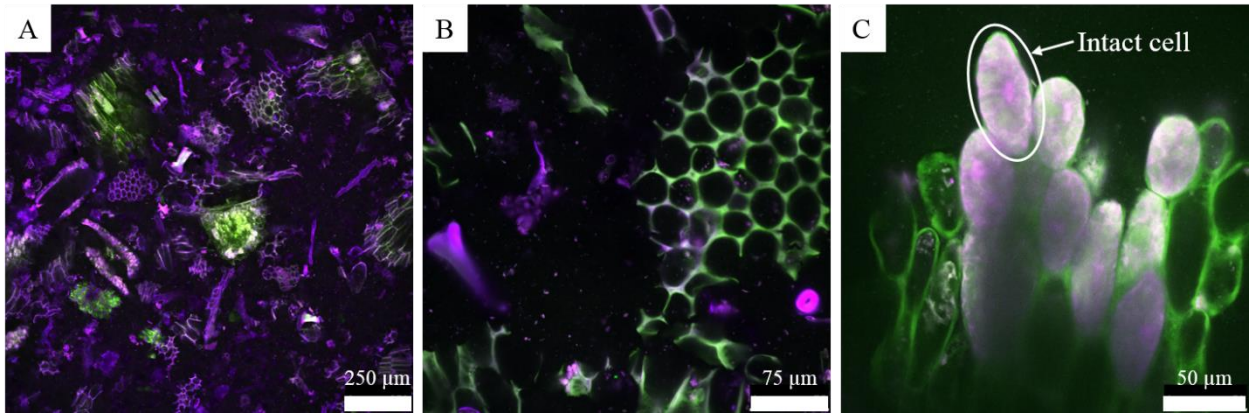


Figure 5.8. Representative confocal laser scanning micrographs of okara solution prior to ultrasonic treatment. Features are visualised using acridine orange at various magnification levels.

The okara solution processing materials were also investigated with CLSM following ultrasonic treatment (Figure 5.9). After treatment of 13.7% okara solution with a flow rate of 20 kg $h^{-1}$ at 50 °C, the microstructure of the ultrasound treated samples were unchanged. It was possible to see that under the tested conditions, ultrasound did not cause intact cells to disrupt, as was also found previously at lab-scale (Preece *et al.*, 2017; **chapter 4**).

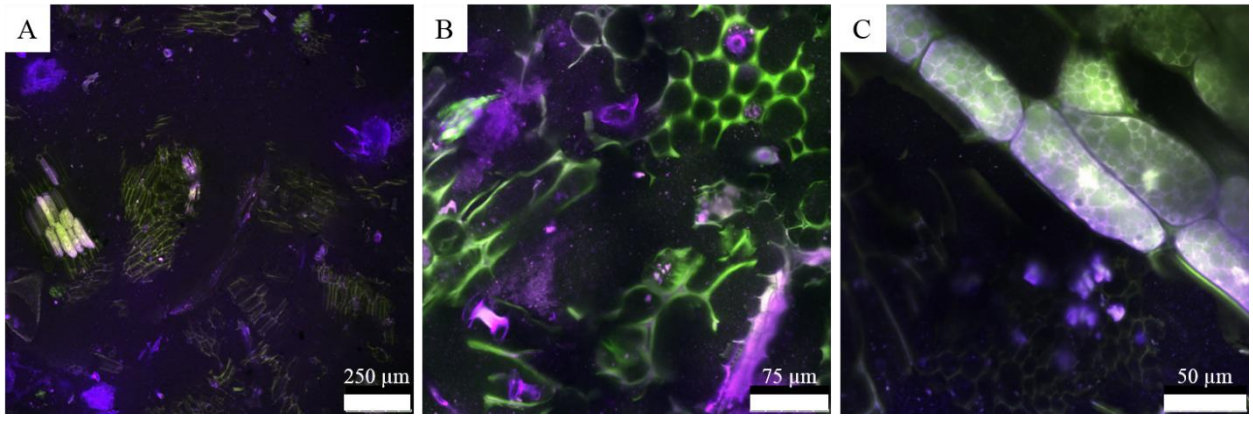


Figure 5.9. Representative confocal laser scanning micrographs of okara solution after ultrasonic treatment (13.7% okara solution at a 20 kg $h^{-1}$ flow rate at 50 °C) observed using acridine orange at various magnification levels.

There are several factors that could be responsible for the presence of intact cells after ultrasonic treatment. The concentration of intact cells within the okara solution is low and therefore the spatial mismatch in liquid jets, a result of cavitation, and intact cells makes disruption less inclined. The action of cavitation will be relatively localised close to the tip of the ultrasonic probe. The force required to disrupt the cell wall of a soybean cell can also be greater than that supplied by liquid jet impingements. In contrast to lab-scale extraction (Preece *et al.*, 2017; **chapter 4**), there was also no visible sign of aggregated protein outside intact cells during pilot-scale extraction before UAE. The microstructural analysis undertaken in our previous lab-scale study indicates reduced protein aggregation as the main cause of the improved yields upon ultrasound treatment (from 47 to about 72% after 15 min), and not cell disruption as is frequently stated in the literature (Preece *et al.*, 2017; **chapter 4**). As we do not find aggregated protein bodies in the current pilot-scale study, it is proposed that the mechanism for the reduced increase in protein extraction yield of the current study (4.2%) can be attributed to the effects of cavitation on the fibres. Some proteins are available for solubilisation located in the extracellular material, but are bound to fibres of the cell walls of disrupted cells and subsequently enter the okara waste stream.

### 5.3.3 Lab-scale and pilot-scale probe comparison

To investigate the differences between lab-scale and pilot-scale sonication, a calorimetry study was undertaken. Details of the experimental method and equations can be found within Section 5.2.8. To compare the two systems utilised in this study energy intensity (EI), acoustic energy density (AED) and the energy input ($W_{input}$) were calculated (Table 5.7). When comparing the acoustic energy densities, the values for both probe systems investigated were comparable. These values give an indication of the power experienced per volume of sample. The energy intensities were vastly different between the systems studied. The lab-scale probe was approximately 300 times more intense compared to the pilot-scale probe. Energy intensity is the power supplied per surface area of the probe tip. The energy input ($W_{input}$) ranges studied also had some differences. Table 5.7 shows that the pilot-scale probe was unable to offer an energy input of more than 0.03 kWh $L^{-1}$, which was limited by the lower processing flow rate of the pump for okara solution.

Table 5.7. Energy intensity (EI), acoustic energy density (AED) and energy input range ($W_{input}$) for both lab (Branson Sonifier 450) and pilot-scale (Hielscher UIP2000hd) probe systems.

| | ***AED*** **(W $cm^{-3}$)** | ***EI*** **(W $cm^{-2}$)** | $W_{input}$ **range (kWh $L^{-1}$)** |
|---|---|---|---|
| **Branson Sonifier 450** (20 kHz, 400 W, 13 mm probe tip) | 0.5 | 3822 | 0.004 - 0.12 |
| **Hielscher UIP2000hd** (20 kHz, 2000 W, 1.5 inch probe tip**)** | 0.8 | 13 | 0.007 - 0.03 |

### 5.3.4 Viability of ultrasound treatment of okara solution during soymilk production

#### *5.3.4.1 Oxidation of oil during ultrasonic treatment*

It has been previously reported that excessive ultrasound treatment can cause oxidation of extracted oil in the soybase sample, leading to the generation of a rancid flavour of the final product (Pingret *et al.*, 2013). When considering the implementation of ultrasound at industrial scale, it is important to study the production of degradation products and to compare to the conventional production process. Here, headspace analysis was performed using gas chromatography-mass spectrometry (GC-MS), to detect the evolution of hexanal, one of the most abundant degradation products of oil found within the soybean (Table 5.8). There was no difference noted between the hexanal detected from control samples (no US) and those treated with ultrasound at all treatment times for samples treated at pilot-scale. Thus, UAE of these samples did not result in oil oxidation.

Table 5.8. Hexanal detection in okara solution samples produced and treated at pilot-scale to study the effects of ultrasound versus a control (no US).

| Trial | Sample type | Arbitrary units (AU) | | |
|---|---|---|---|---|
| | | 1 | 2 | 3 |
| **1** | Control | 1,272,966 | 313,539 | 989,888 |
| | US | 3,971,905 | 2,451,758 | 3,730,498 |
| **2** | Control | 1,007,831 | 247,583 | 24,771 |
| | US | 403,609 | 229,501 | 262,545 |
| **3** | Control | 860,418 | 239,675 | 29,288 |
| | US | 3,741,857 | 8,159,271 | 6,825,062 |
| **4** | Control | 55,570 | - | - |
| | US | 113,278 | 28,134 | 13,232 |
| **5** | Control | | - | - |
| | US | 197,052 | 105,901 | 6,134 |
| **6** | Control | | - | - |
| | US | 124,954 | 71,391 | 29,008 |
| **7** | Control | 31,197 | - | - |
| | US | 5,904,699 | 3,523,012 | 2,208,838 |
| **8** | Control | 24,058 | 14,253 | - |
| | US | 32,286 | 11,304 | 14,748 |
| **9** | Control | 18,099 | 9,504 | - |
| | US | 239,944 | 121,238 | 14,876 |
| **10** | Control | 16,248 | 12,313 | - |
| | US | 30,145 | - | - |
| **11** | Control | 20,568 | 12,259 | - |
| | US | 11,008 | - | - |
| **12** | Control | 651,344 | 290,014 | 75,949 |
| | US | 125,778 | 79,581 | 8,472 |
| **13** | Control | 87,738 | 38,929 | - |
| | US | 100,080 | 62,193 | - |
| **14** | Control | 130,522 | 79,455 | 1,507,957 |
| | US | 195,302 | 124,879 | 20,935 |
| **15** | Control | 229,917 | 71,533 | 25,586 |
| | US | 167,213 | 106,395 | 11,979 |
| **16** | Control | 9,733,135 | 6,068,069 | 5,451,401 |
| | US | 225,707 | 113,668 | 39,507 |

### *5.3.4.2 Productivity of ultrasonic treatment*

When considering okara solution UAE within industry, there are two viable options for utilisation of the newly created product stream. The side stream can be utilised for a low-protein product, or it can be recirculated back to the main slurry line, if the final protein concentration is not below the threshold value required for soymilk production. If the okara solution treated with the optimum extraction conditions (14% okara, 20 kg $h^{-1}$ okara solution flow rate, 50 °C) is fed into the slurry line (added to stream 4, Figure 5.1), then a final soybase protein concentration of 4.5% can be achieved. This is still considered an acceptable concentration of protein; however, over one hour more than 400 kg of okara solution will be produced, which requires 20 hours of side stream ultrasonic treatment. Recirculation of the okara is not considered feasible for this reason, as well as issues associated with recirculation and microbial spoilage (Vong & Liu, 2016).

It was not only important to consider the optimum extraction yield achievable, but also the optimal production process. Figure 5.10 shows the effects of okara solution flow rate on the protein extraction yield (PEY, %) and productivity. The efficiency of a process is indicated by productivity, defined as the ratio of output to output for a specific process (Rogers, 1998). In this case, productivity is calculated from the protein concentration (wt. %) of the resultant soybase (stream 11, Figure 5.1) as a function of the okara solution flow rate (kg $h^{-1}$). Varying the okara solution flow rate with fixed temperature and okara concentration (68 °C, 32%) yielded little difference in resulting protein extraction yield compared to the productivity. However, during the optimisation of UAE at pilot-scale (Section 5.3.2.2) the okara solution flow rate was shown to be a significant factor by ANOVA, with the lowest flow rate resulting in the highest protein extraction yield. The productivity was at its greatest when the okara solution flow rate was at its highest throughput

through the ultrasonic flow cell. Economically, it would be more beneficial to choose a faster flow rate and to sacrifice part of the protein extraction yield with a higher throughput of protein. To achieve the highest improvement in protein extraction yield from okara, a cell disruption technique would be better suited, for example, high pressure homogenisation, which is based on hydrodynamic cavitation (Gogate, 2011).

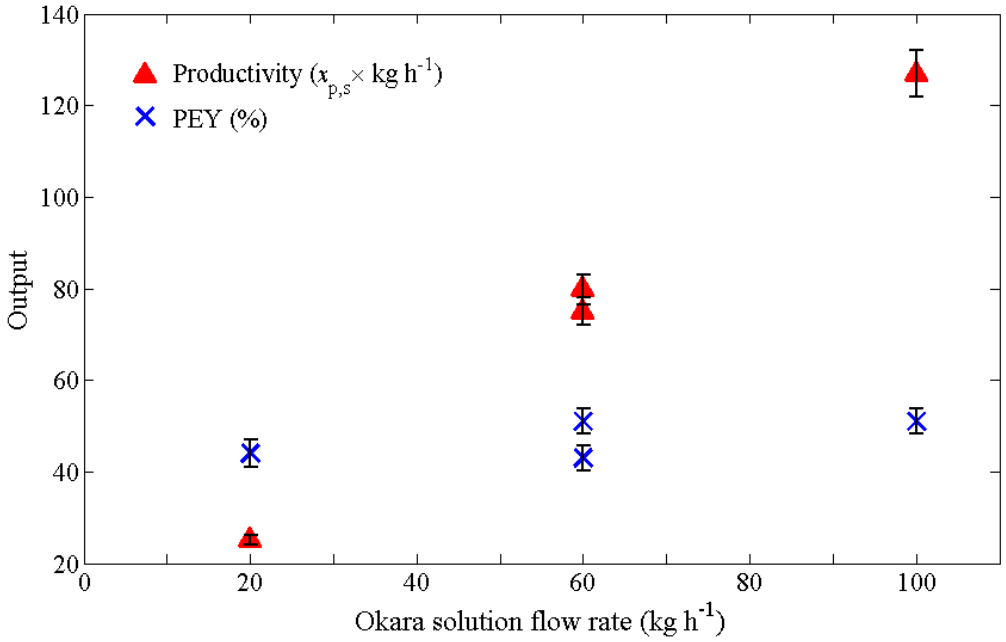


Figure 5.10. Productivity and protein extraction yield (PEY) versus okara solution flow rate. Okara concentration and temperature were fixed during ultrasonic treatment (32%, 68 °C). Error bars represent the standard deviation calculated from the $SD_{pooled}$ value for protein measurement. Two points are shown for the flow rate of 60 kg h$^{-1}$ as this was the central point from the experimental design, carried out in duplicate.

When considering soybase production, it was appropriate to calculate the total protein extraction yield (equation 5.3). Until now, only the protein extraction yield has been calculated for the single extraction step studied (equation 5.2, slurry or okara treatment). The largest improvement in total protein extraction yield compared to a control sample can be observed in trial 9 (Table 5.3), where

an improvement of 5% was measured (80% versus 85% for control sample and ultrasound treatment of okara solution at pilot-scale, respectively). However, the majority of UAE samples had an additional benefit of 1-2% on the total protein extraction yield compared to the control (washing of okara).

At the highest energy input for pilot-scale sonication, a value of 0.03 kWh $L^{-1}$ (30 kWh $m^{-3}$) was introduced into the okara solution system. When this value is compared to that of a stirred tank of 0.2-1.5 kWh $m^{-3}$ it is possible to see the energy input is up to 150 times higher for the ultrasonic pilot-scale probe system (Ditl et al., 1992). This should be considered when assessing the viability of the industrial application of ultrasound in any industry.

## 5.4 CONCLUSIONS

Ultrasound treatment was shown to significantly improve the protein extraction yield by 4.2% during the okara solution treatment on pilot plant scale. Okara solution flow rate and okara concentration also had significant effects on the protein extraction yield. However, considering the whole soybase production process, from soybeans to final processing materials studied, UAE was found to have comparable results to the washing of okara at pilot-scale, contrary to lab-scale sonication. During the lab-scale sonication treatment, a greater energy intensity was experienced by the samples compared to the pilot-scale system, resulting in a greater impact of ultrasound treatment. Okara solution visualised after pilot-scale sonication was found to still contain intact cells, complete with protein bodies inside. No aggregated protein bodies outside the cells were visualised within the starting materials for UAE, therefore a reduced effect was observed in contrast to previous results found for okara prepared at lab-scale. For the extraction of soy protein, one of the world's cheapest and most readily available protein sources, ultrasound is not considered to be the most beneficial unit operation for enhancing the extraction yield.

## 5.5 REFERENCES

Aiking, H. (2011). Future protein supply. *Trends Food Sci Tech, 22*, 112-120.

Bates, D., Patist, A. (2010). Industrial applications of high power ultrasonics in the food, beverage and wine industry. In: C.J. Doona, K. Kustin, F.E. Feeherry (Eds.), *Case Studies in Novel Food Processing Technologies* (pp. 119-138). Cambridge: Woodhead Publishing Series in Food Science, Technology and Nutrition.

Boonkird, S., Phisalaphong, Phisalaphong, C. M. (2008). Ultrasound-assisted extraction of capsaicinoids from Capsicum frutescens on a lab- and pilot-plant scale. *Ultrason Sonochem, 15*, 1075-1079.

Chandrapala, J., Oliver, C.M., Kentish, S., Ashokkumar, M. (2013). Use of Power Ultrasound to Improve Extraction and Modify Phase Transitions in Food Processing. *Food Rev Int, 29*, 67-91.

Chemat, F., Khan, M.K. (2011). Applications of ultrasound in food technology: Processing, preservation and extraction. *Ultrason Sonochem, 18*(4), 813-835.

Ditl, P., Rieger, F., Roušar, I. (1992). The design of agitated dissolution tanks. In: *Fluid Mechanics of Mixing* (pp. 131-138). Netherlands: Springer.

Esclapez, M.D., García-Pérez, J.V., Mulet, A., Cárcel, J.A. (2011). Ultrasound-Assisted Extraction of Natural Products. *Food Eng Rev, 3*, 108-120.

Gogate, P.R. (2011). Hydrodynamic Cavitation for Food and Water Processing. *Food Bioprocess Tech, 4*, 996-1011.

Karki, B., Lamsal, B.P., Jung, S., van Leeuwen, J., Pometto, A.L., Grewell, D., Khanal S.K. (2010). Enhancing protein and sugar release from defatted soy flakes using ultrasound technology. *J Food Eng*, *96*, 270-278.

Lee, H., Yildiz, G., dos Santos, L.C., Jiang, S., Andrade, J.E., Engeseth, N.J., Feng, H. (2016). Soy protein nano-aggregates with improved functional properties prepared by sequential pH treatment and ultrasonication. *Food Hydrocolloid, 55*, 200-209.

Li, H., Pordesimo, L., Weiss, J. (2004). High intensity ultrasound-assisted extraction of oil from soybeans. *Food Res Int, 37*, 731-738.

Meullemiestre, A., Petitcolas, E., Maache-Rezzoug, Z., Chemat, F., Rezzoug, S.A. (2015). Impact of ultrasound on solid-liquid extraction of phenolic compounds from maritime pine sawdust waste. Kinetics, optimization and large scale experiments. *Ultrason Sonochem*, *28*, 230-239.

Moulton, K.J., Wang, L.C. (1982). A Pilot-Plant Study of Continuous Ultrasonic Extraction of Soybean Protein. *J Food Sci, 47*, 1127-1129.

O'Toole, D.K. (1999). Characteristics and use of okara, the soybean residue from soy milk production a review. *J Agric Food Chem, 47*, 363-371.

Patist, A., Bates, D. (2008). Ultrasonic innovations in the food industry: From the laboratory to commercial production. *Innov Food Sci Emerg*, *9*, 147-154.

Pingret, D., Fabiano-Tixier, A.S., Bourvellec, C.L., Renard, C.M.G.C., Chemat, F. (2012). Lab and pilot-scale ultrasound-assisted water extraction of polyphenols from apple pomace. *J Food Eng, 111,* 73-81.

Pingret, D., Fabiano-Tixier, A. S., Chemat, F. (2013). Degradation during application of ultrasound in food processing: a review. *Food control*, *31*(2), 593-606.

Poling, B.E., Thomson, G.H., Friend, D.G., Rowley, R.L., Wilding, W.V. (2008). *Perry's Chemical Engineers' Handbook* (8th ed.) New York: The McGraw-Hill Companies, Inc. (Chapter 2).

Preece, K.E., Drost, E., Hooshyar, N., Krijgsman, A., Cox, P.W., Zuidam, N.J. (2015). Confocal imaging to reveal the microstructure of soybean processing materials. *J Food Eng, 147,* 8-13.

Preece, K. E., Hooshyar, N., Krijgsman, A., Fryer, P. J., Zuidam, N. J. (2017). Intensified soy protein extraction by ultrasound. *Chem Eng Process*, *113*, 94-101.

Rogers, M. (1998). *The definition and measurement of productivity*. Melbourne Institute of Applied Economic and Social Research.

Rosenthal, A., Pyle D.L., Niranjan, K. (1998). Simultaneous aqueous extraction of oil and protein from soybean: Mechanisms for process design. *Food Bioprod Process, 76,* 224-230.

Shirsath, S.R., Sonawane, S.H., Gogate, P.R. (2012). Intensification of extraction of natural products using ultrasonic irradiations: A review of current status. *Chem Eng Process, 53,* 10-23.

Sicaire, A.G., Vian, M.A., Fine, F., Carré, P., Tostain, S., Chemat,F. (2016). Ultrasound induced green solvent extraction of oil from oleaginous seeds. *Ultrason Sonochem, 31*, 319-329.

Soria, A.C., Villamiel, M. (2010). Effect of ultrasound on the technological properties and bioactivity of food: A review. *Trend Food Sci Tech, 21*, 323-331.

Tiwari, B.K., Mason, T.J. (2012). Ultrasound Processing of Fluid Foods. In: P.J. Cullen, K.T. Brijesh, V. Vasilis, V. Vasilis (Eds.), *Novel Thermal and Non-Thermal Technologies for Fluid Foods* (pp. 135-165). London: Academic Press.

Vilkhu, K., Mawson, R., Simons, L., Bates, D. (2008). Applications and opportunities for ultrasound assisted extraction in the food industry - A review. *Innov Food Sci Emerg, 9*, 161-169.

Vinatoru, M. (2015). Ultrasonically assisted extraction (UAE) of natural products some guidelines for good practice and reporting. *Ultrason Sonochem, 25*, 94-95.

Vishwanathan, K.H., Singh, V., Subramanian, R. (2011). Wet grinding characteristics of soybean for soymilk extraction. *J Food Eng, 106*, 28-34.

Vong, W.C. Liu, S.Q. (2016). Biovalorisation of okara (soybean residue) for food and nutrition. *Trend Food Sci Tech, 52*, 139-147.

Wijngaard, H.H., Zuidam, N.J. (2014). *Soybean extraction process*. International Publication WO14154472.

# CHAPTER 6

# INTENSIFICATION OF PROTEIN EXTRACTION FROM SOYBEAN PROCESSING MATERIALS USING HYDRODYNAMIC CAVITATION

This chapter was on a published manuscript:

Preece, K. E., Hooshyar, N., Krijgsman, A. J., Fryer, P. J., Zuidam, N. J. (2017). Intensification of protein extraction from soybean processing materials using hydrodynamic cavitation. *Innov Food Sci Emerg Technol., 41, 47-55.*

## ABSTRACT

High pressure homogenisation (HPH) has been investigated for its potential to aid the aqueous extraction of protein and other components from soybeans. HPH treatments (50-125 MPa) were applied to soy slurry and okara, the diluted waste stream from soybase production. Extraction yields of oil, protein and solids were calculated, and the feasibility of the technology was assessed. The most productive HPH treatment investigated improved extraction yields of protein by 16% with a single pass of soy slurry at 100 MPa. Results showed a particle size reduction upon HPH and disruption of intact cells, confirmed via confocal imaging. Multiple HPH passes of soy slurry caused an increase in dynamic viscosity and a small increase in particle size; resulting in decreased separation efficiency and consequently a reduced extraction yield. HPH offers extraction assistance, with more promising results reported in comparison to ultrasound-assisted extraction of soybean processing materials.

## 6.1 INTRODUCTION

Protein is an important nutrient to be considered when studying food production for human consumption, with major pressure to provide nourishment for an increasing population. The use of vegetable proteins like soy instead of animal derived protein sources is a rapidly increasing consumer trend. Extraction of protein and other soybean components from milled soybeans may happen under alkali aqueous conditions at high temperature to prepare soybase, the soybean extract further processed to soymilk or tofu. After the extraction, insoluble materials are removed from the extract typically by decanting, and the fibrous waste stream, termed okara, is utilised as animal feed (Preece *et al.*, 2016; **chapter 2**). This process requires attention as the current yield in factories is relatively low (50-60%); improved production methods may yield a greater mass of protein for human consumption.

The majority of the soybean structure (90%) is made up of cotyledon cells, ranging in length from 70 to 80 µm and 15-20 µm in width (Rosenthal *et al.*, 1998). Within the cotyledon cells, the majority of protein is organised in protein bodies that are typically 2-20 µm in diameter (Preece *et al.*, 2015; **chapter 3**). Oil is located within the cytoplasmic network in oil bodies stabilised by low molecular weight proteins termed oleosins (Rosenthal *et al.*, 1998). These oil bodies are smaller in size than protein bodies with sizes in the range 0.2-0.5 µm. The main barrier for the extraction of intracellular components of interest is the cell walls. Other limitations include insolubility of materials and entrapment in the continuous phase of the insoluble waste stream (Preece *et al.*, 2015; **chapter 3**).

Cavitation is a process responsible for the success of some extraction assistance process technologies (Gogate *et al.*, 2006). The phenomena of cavitation include air void formation within

a treated sample, growth of the voids and their potential violent collapse. Upon microbubble collapse, local regions of high pressure and temperatures result in the regions of 1000-5000 atm and 500-15000 K, which can aid the extraction process (Gogate *et al.*, 2009). Another result of cavitation is void collapse near a solid surface: leading to local regions of high shear resulting in solubilisation and also cell disruption.

Ultrasound, a processing technology based on acoustic cavitation, has been shown to enhance the extraction of protein and other components during the processing of soybean materials. Ultrasound improved the extraction of protein up to 19%, as was upon found 15 min treatment of okara solution with a lab probe system (Preece *et al.*, 2017a; **chapter 4**). The material was examined using confocal laser scanning microscopy (CLSM); improved protein solubilisation was found to be the main factor enhancing the yield, not cell disruption (Preece *et al.*, 2017a; **chapter 4**). Unfortunately, when ultrasound was applied at pilot plant scale it was not feasible to give the soy slurry a treatment equivalent to that possible at lab scale. Pilot scale ultrasound treatment of okara was shown to increase protein extraction yield by only 4.2% compared to control samples (Preece *et al.*, 2017b; **chapter 5**). Other parameters, including okara solution flow rate and okara concentration, also had a significant impact on the protein extraction yield. During the lab scale sonication treatment an approximately 300x greater energy intensity was experienced by the samples, compared to the pilot scale sonication. Considering the minimal total extraction yields for soybase production at pilot scale, ultrasound was not considered viable for industrial processing. It was found that the remaining protein within the okara was still within intact cells (Preece *et al.*, 2017b; **chapter 5**). Therefore, a processing technology that targets intact cells might be more beneficial.

Hydrodynamic cavitation is widely accepted as a technique for cell disruption of microbes and microalgae (Lee *et al.*, 2015; Save *et al.*, 1997). It can be achieved using a high pressure homogeniser (HPH) at pressures above 35 MPa (Donsì *et al.*, 2009). HPH has been employed in the food industry for large-scale microbial cell disruption, as well as for other purposes, such as emulsification (Gogate, 2011). Extraction with assistance from high pressure has been studied for several food systems with promising results, such as carotenoid extraction from tomato paste waste (Xi, 2006) and phenolic acids extraction from potato peel (Zhu *et al.*, 2016), as well as oil extraction from microalgae for use in biodiesel production (Dumay *et al.*, 2013; Lee *et al.*, 2012; Rastogi *et al.*, 2007; Xi, 2006).

High pressure treatment has also been applied to a number of soy-based systems. Typically pressures of greater than 300 MPa have been studied for the formation of soy protein gels (Apichartsrangkoon, 2003; Kajiyama *et al.*, 1995; Okamoto *et al.*, 1990). These studies did not include hydrodynamic cavitation; only the effects of high pressure achieved using a pressure cell were investigated. Some studies of the effects of HPH on soy protein, focused on the microbial stability of products and the production of fine emulsions rather than on extraction, have been published (Cruz *et al.*, 2007; Floury *et al.*, 2002; Poliseli-Scopel *et al.*, 2012).

For the implementation of HPH for extraction in industrial scale processes, a number of factors have to be considered, including energy consumption, instrument geometry and wear, and productivity (Dumay *et al.*, 2013). Many examples of the use of HPH within the food industry are available, yet current applications focus on the structuring of products, such as fine emulsion production. Creaming, which is an unwanted phenomenon seen in the dairy industry, is one such example for the possible industrial use of HPH (Tobin *et al.*, 2015). A scale up study by Donsì *et*

*al.* (2009) showed that the scale of HPH operation did not influence microbial cell disruption at a given pressure. This gives confidence for the scalability of HPH for use in extraction at an industrial scale, if positive results are achieved at lab scale for extraction.

Extraction of protein from soybeans has been reported previously in the literature as discussed above (Apichartsrangkoon, 2003; Cruz *et al.*, 2007; Floury *et al.*, 2002; Kajiyama *et al.*, 1995; Okamoto *et al.*, 1990; Poliseli-Scopel *et al.*, 2012); however, there are no studies describing the effects of HPH on soybean processing materials and extraction yields. Here we show an investigation of the extraction yields of oil, protein and solids with high pressure treatment compared to the industrial control sample, as well as the availability of protein and separation efficiency on soybean processing materials. Particle size measurements, flow behaviour and an investigation into the microstructure using confocal laser scanning microscopy (CLSM) are carried out to identify the mechanisms of HPH.

## 6.2 MATERIALS AND METHODS

### 6.2.1 Sample preparation

Slurry and okara were freshly prepared in the pilot plant facilities at Unilever R&D Vlaardingen. A process flow diagram can be seen in Figure 6.1. Commercially available soybeans (Stream 3, Figure 6.1) went through two wet milling stages to produce a soy slurry (Stream 4, Figure 6.1) under alkaline conditions (pH 8). The processing input consisted of 28 kg $h^{-1}$ of soybeans treated with 175 kg $h^{-1}$ of softened water and 0.2 kg $h^{-1}$ of sodium bicarbonate, which resulted in a water to soybean ratio of 7:1 (w/w) (water content of soybean not considered). To prepare soybase and okara for subsequent treatment (streams 7 and 8, respectively), the slurry was fed into a decanter centrifuge operating at a *g*-force-time of $1.5 \times 10^5$ *g*-s. Before homogenisation, the okara was diluted approximately 7 times (13.7 wt.%) with demineralised water on the day of homogenisation and stirred using a magnetic bar. For each homogenisation study, a fresh 1 L solution was made from okara stored below 5°C for no longer than 6 days. The composition of slurry (Stream 4, Figure 6.1) and okara (Stream 8, Figure 6.1) can be seen in Table 6.1.

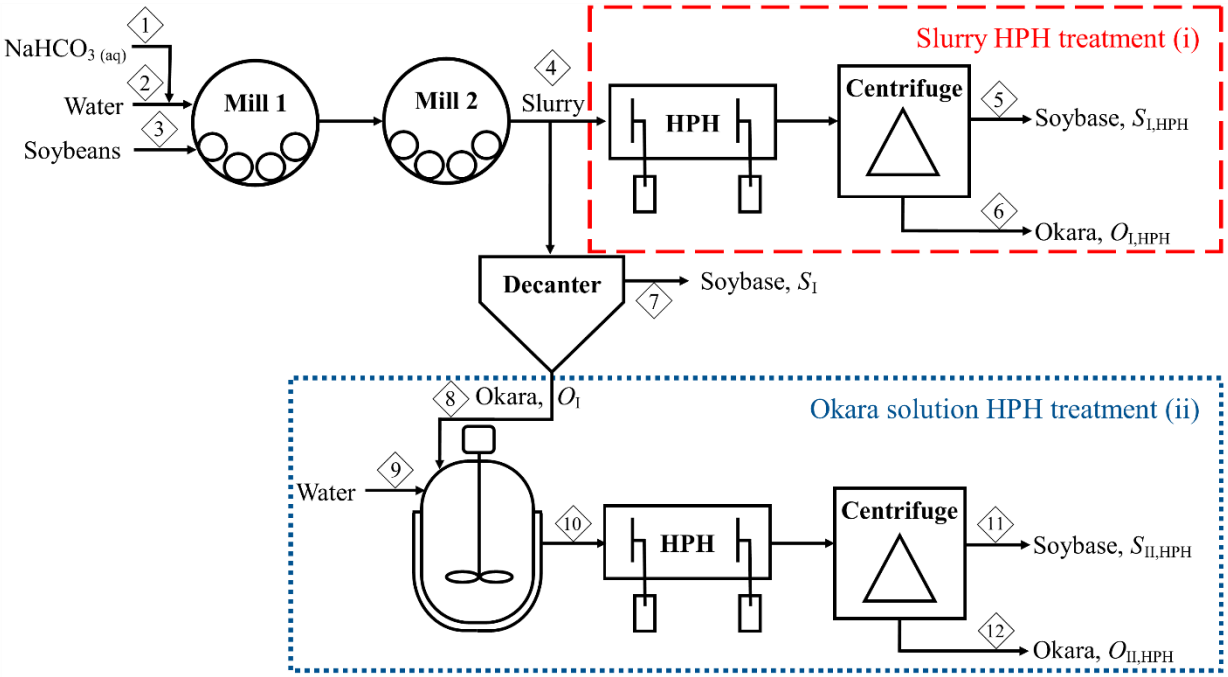


Figure 6.1. Process flow diagram of pilot plant preparation and HPH treatments of slurry and okara solution samples. The red box (— —) shows the process for slurry homogenisation and the blue box (···) shows okara solution treatment, both carried out using a lab scale HPH.

Table 6.1. Average composition of slurry and okara prepared using pilot plant facilities. Error represents standard deviation in production over 5 separate preparations using the Unilever Research & Development Vlaardingen facility.

| | **Stream (no.)** | |
|---|---|---|
| Component | **Slurry (4)** | **Okara (8)** |
| **Protein** | 5.2 ± 0.1 | 5.4 ± 0.2 |
| **Oil** | 2.8 ± 0.1 | 3.1 ± 0.3 |
| **Moisture** | 87.2 ± 0.2 | 81.4 ± 0.5 |
| **Other** | 4.8 ± 0.2 | 10.1 ± 0.6 |

### 6.2.2 High pressure homogenisation (HPH) treatment

Figure 6.1 shows the process flow diagram for experiments conducted on:

(i) Slurry prepared as above (Stream 4, Figure 6.1), and

(ii) Okara prepared using decanter centrifugation ($O_I$; stream 8, Figure 6.1),

to identify what effects of HPH can be identified on both materials.

All HPH treatments were conducted using a homogeniser, PandaPLUS 2000 (GEA Niro Soavi S.p.A, Parma, Italy), equipped with 2 stages as shown schematically in Figure 6.2. During the homogenisation treatments, the 2$^{nd}$ stage was always adjusted to 10 MPa using a manual hand wheel actuator on the equipment, and then the pressure was increased to the required total pressure by the 1$^{st}$ stage, using the 1$^{st}$ hand wheel. The approximate flow rate for demineralised water of 150 mL min$^{-1}$ (9 L h$^{-1}$) was recorded prior to each experiment using the homogeniser, with a lower limit set to 142.5 mL min$^{-1}$. The soy sample was introduced through the feed hopper of the homogeniser. A sample of approximately 100 mL was taken after each pass through the homogeniser for analysis. For the control samples (0 passes), the samples were heated to their relevant temperatures and stirred; however, they were not passed through the homogeniser.

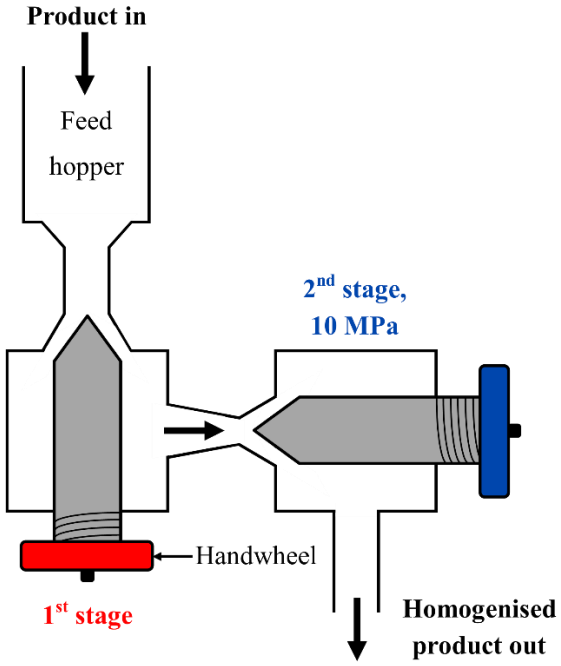


Figure 6.2. Schematic diagram of a 2-stage high pressure homogeniser.

#### *6.2.2.1 Slurry treatment*

For each trial using slurry (Stream 4, Figure 6.1), 1 L was heated to 80 °C and stirred using a magnetic stirrer bar. This temperature was chosen to replicate the conditions which would be found during processing in a factory after the milling process. Once the desired temperature was reached, a control sample was taken and the remaining slurry was introduced into the homogeniser, which was preheated using boiling water. For each treatment, the soy slurry was passed through the homogeniser and a sample was collected for analysis and further processing. The remaining slurry was added into the homogeniser for subsequent treatment, up to a maximum of 5 passes in total. After each sample was collected, all samples were further processed using a centrifuge operating at 4330 × $g$ for 10 min to determine extraction yields. The temperature was recorded before and after treatment.

#### 6.2.2.2 Okara solution treatment

Fresh okara solution, prepared as described in Section 6.2.1 ($O_I$, stream 8, Figure 6.1), was heated to 50 °C and stirred using a magnetic stirrer bar. This temperature was chosen due to the okara production temperature at pilot scale; when the milling was performed at 85°C and diluted to 13.7% using room temperature water, a solution temperature of 50 °C was achieved. Once heated, the solution was added to the homogeniser for treatment; a control sample was also collected (0 passes). After each pass through the homogeniser, a sample was taken for analysis and further processed using a centrifuge operating at 4330 × *g* for 10 min. The remaining solution was recirculated back through the homogeniser for up to 5 passes in total. The temperature was recorded before and after treatment.

### 6.2.3 Protein, oil and solid measurement methods and extraction yield calculation

To determine protein extraction yields, the protein content on a wet basis (w.b.) was defined in the pellets and supernatants using the Dumas method (Vario MAX CNS, Elementar Analysensysteme GmbH, Germany). L(+)-glutamic acid (VWR International BVBA, Belgium) was used as a standard sample and UHT milk (3.5% fat) (muva kempten, Germany) as a reference material. For soy samples, a protein conversion factor of 6.25 × N was utilised to determine protein content from the measured nitrogen content. From the protein concentrations and masses of streams, the protein extraction yield into the soybase could be calculated using equation 6.1.

$$\text{Protein extraction yield} = Y\ (\%) = \left[\frac{S \cdot x_{\mathrm{p,s}}}{(S \cdot x_{\mathrm{p,s}} + O \cdot x_{\mathrm{p,o}})}\right] \times 100\% \qquad (6.1)$$

Here *S* (soybase) and *O* (okara) represent the total weight of samples and $x_p$ is the mass fraction of protein for each respective stream. The *S* and *O* terms can be found labelled in Figure 6.1. To

analyse the effects of ultrasound on okara solution, it was necessary to consider the total protein extraction yield calculated using equation 6.2:

$$\text{Total protein extraction yield (\%)} = Y_I + (100\% - Y_I) \times Y_{II} \quad (6.2)$$

Yield I ($Y_I$) refers to the primary extraction and centrifugation for the production of soybase and okara (calculated from $S_I$ and $O_I$, Figure 6.1); yield II ($Y_{II}$) corresponds to the okara solution treatment described. In addition to the extraction yields, the separation efficiency (equation 6.3) was derived to show the efficiency of deliquoring of okara during centrifugation. The availability of protein was also calculated using equation 6.4; this is a measure combining losses due to protein insolubility as well as intact cells, i.e. all losses that occurred as a result of extraction, not incurred by separation. In these calculations, it was assumed that the moisture content found in okara retained the same protein concentration as the soybase ($x_{p,s}$).

$$\text{Separation efficiency (\%)} = \left[\frac{S \cdot x_{w,s}}{(S \cdot x_{w,s} + O \cdot x_{w,o})}\right] \times 100\% \quad (6.3)$$

$$\text{Availability of protein (\%)} = \left[\frac{S + \left(\frac{O \cdot x_{w,o}}{x_{w,s}}\right)}{S + \left(\frac{O \cdot x_{p,o}}{x_{p,s}}\right)}\right] \times 100\% \quad (6.4)$$

where:

$x_{w,s}$ Mass fraction of water in soybase

$x_{w,o}$ Mass fraction of water in okara

$x_{p,s}$ Mass fraction of protein in soybase

$x_{p,o}$ Mass fraction of protein in okara

Please note that the extraction yield (equation 6.1) is equal to separation efficiency (equation 6.3) multiplied by the availability of protein (equation 6.4).

Oil and solid contents were measured using a microwave moisture analysis system equipped with NMR for direct detection of fat content (SMART System5, CEM GmbH, Germany). Oil and solid extraction yields were also determined using equation 6.1, replacing the masses of protein, with the respective masses.

### 6.2.4 Particle size measurement

The particle sizes of soy slurries after extraction were determined using laser diffraction (Mastersizer 2000 Hydro S, Malvern Instruments Ltd, UK). To determine particle size distributions (PSDs), refractive indices of 1.33 and 1.45 were used for the water and the particles, respectively. Particle sizes were measured in triplicate for each sample. The D[4,3] and D[3,2] values represent the volume weighted and surface weighted mean particle size, respectively. The D90 value gives an indication of the particle size under which 90% of the total particles fall below.

### 6.2.5 Rheology

An AR G2 rheometer (TA instruments, New Castle, DE) equipped with a sand blasted steel parallel plate (40 mm diameter) was utilised to study the effects of homogenisation on samples. All experiments were carried out at 20°C with a gap width of 2500 µm. Flow curves were measured with increasing and decreasing shear rates in the range 0.1-200 $s^{-1}$ over a period of 2 min per sweep. The sweep of increasing shear rate was treated as a conditioning step and the shear viscosity measurements were recorded.

### 6.2.6 Confocal laser scanning microscopy (CLSM)

A Leica TCS-SP5 microscope in conjunction with DMI6000 inverted microscope (Leica Microsystems Inc., Germany) was used with the dye nile blue A (Janssen Chimica, Belgium) to visualise the effects of ultrasound treatment on soy slurries. One drop of dye stock solution (1% w/v nile blue) was added to 1-1.5 mL of sample and mixed well before adding the sample to the slide. For visualisation using nile blue, sequential scanning was employed to prevent the excitation laser occurring in the emission signals. Table 6.2 shows the scans utilised and the corresponding colours assigned to the emission channels.

Table 6.2. Excitation and emission conditions when acquiring CLSM images using the dye nile blue.

| Sequential scan | Excitation wavelength (nm) | Emission wavelengths (nm) | Illustrated colour in micrograph |
|---|---|---|---|
| **1** | 488 | 520-626 | Green |
| **2** | 633 | 662-749 | Red |

## 6.3 RESULTS & DISCUSSION

### 6.3.1 Extraction yields

Soybeans were milled and the resulting slurry was separated using a decanter centrifuge to obtain the soybase and the okara fraction ($S_I$ and $O_I$, Figure 6.1), as described in Section 6.2.1. To increase the protein extraction yield, HPH was applied to either the slurry or the okara solution. Okara solution treatment included a primary extraction of protein during okara preparation ($O_I$, Figure 6.1), followed by subsequent dilution, HPH treatment and separation of insoluble materials, such as fibres, insoluble proteins and intact cells, if present. Figure 6.3 shows the total protein extraction yield calculated as a function of HPH pressure after a single pass through the system. On first observation (Figure 6.3), the total protein extraction yield increased with increasing HPH pressure for both samples after a single pass. A pressure of 100 MPa (1000 bar) was chosen for all further experiments to ensure the optimal extraction yield of protein for both slurry and okara solution treatments was achieved. In the following sections, the resultant effects of the homogenisation treatment on the particle size, microstructure and rheology will be studied in order to explain the results from Figure 6.3.

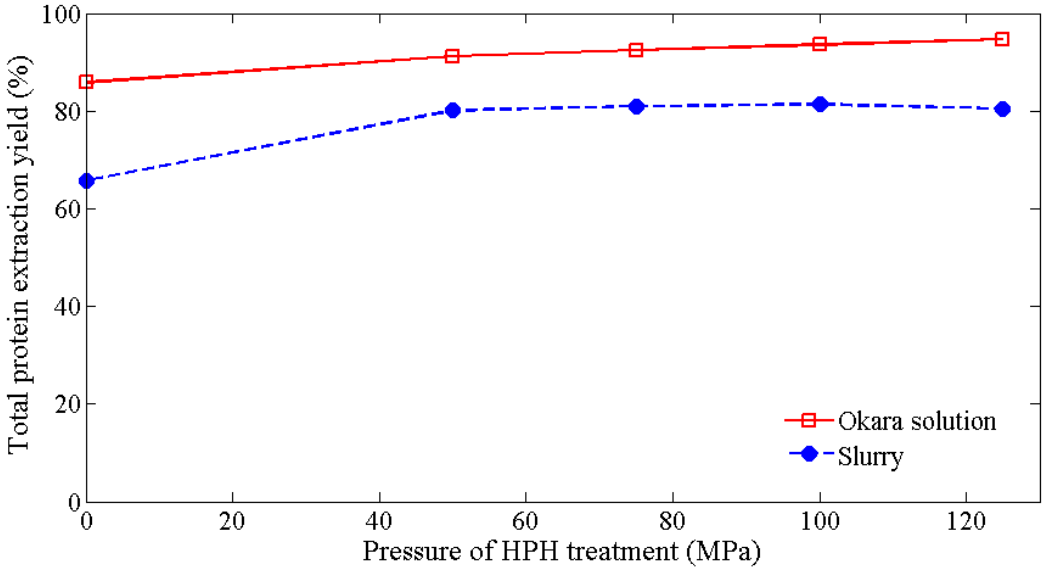


Figure 6.3. Effects of total homogenisation pressure (achieved over 2 stages, see Figure 6.2) for a single pass on the total protein extraction yield on okara solution at 50 °C and slurry samples at 80 °C. The control samples at 0 MPa were heated to the same temperatures and stirred, but not passed through the homogeniser.

#### *6.3.1.1 Soy slurry*

To locate the most optimal treatment conditions, an experiment was carried out to deduce the optimum number of passes through the homogeniser geometry at 100 MPa. For soy slurry, the homogeniser treatment was carried out at 80 °C to replicate the temperature straight from the pilot processing line. Figure 6.4 shows the extraction yields of oil, protein and solids from slurry versus the number of treatments at 100 MPa. The control sample (0 passes) represents slurry heated to 80 °C and separated under the same conditions as the treated samples. The extraction yield of protein was approximately 65% without homogenisation. The optimum number of passes for the extraction of oil, protein and solids already occurred for a single pass at the pressure investigated. Extraction yields improved by 21%, 16% & 12% for oil, protein and solids respectively after 1 pass through the homogeniser. After each subsequent pass through the homogeniser, a stepwise reduction in extraction of all components studied was observed.

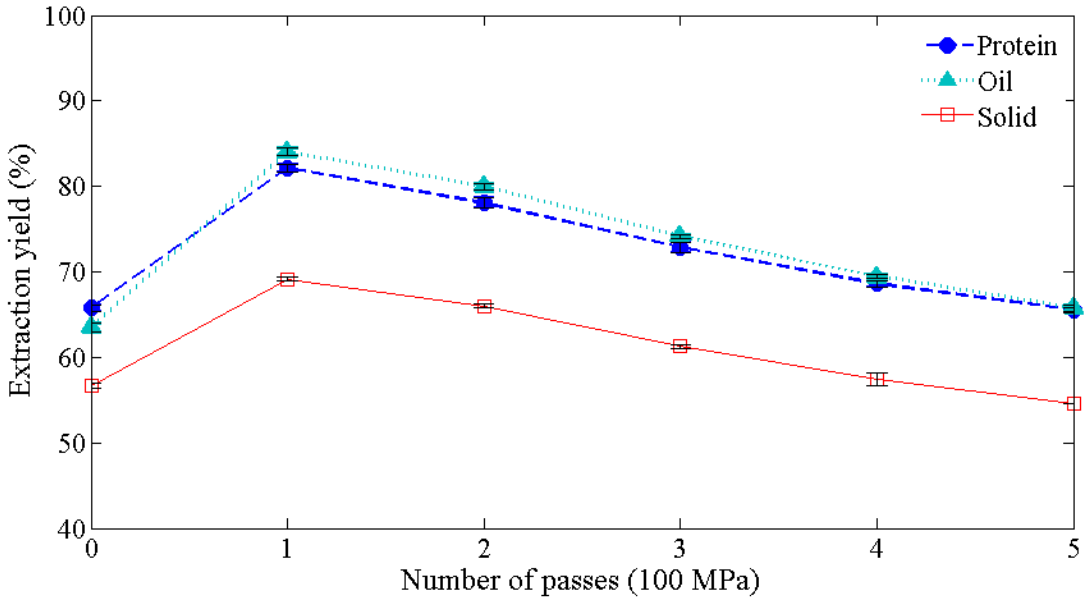


Figure 6.4. Extraction yields ($Y_I$) of oil, protein and solids from slurry as a function of number of passes through the homogeniser at 100 MPa at 80 °C. Error bars represent standard deviation calculated from 3 experiments analysed in duplicate. Each experiment was carried out on a different fresh batch of slurry.

### *6.3.1.2 Okara solution*

The effects of homogenisation were also tested on okara, the waste stream from soybase production ($O_I$; Stream 8, Figure 6.1). The extraction yields of oil, protein and solids were calculated considering the okara treatment only (no primary extraction yield considered) (Figure 6.5). From the control sample (0 passes), approximately 55% of oil and protein and 35% of solids were extracted. After 1 pass, oil protein and solid extraction yields were improved by 36%, 26% and 17%, respectively. Unlike soy slurry treatment, the subsequent extractions did not lead to a reduction in extraction yield: a plateau in extraction yields was reached after 1 pass through the homogeniser (1 pass, 100 MPa), with no significant change for higher numbers of passes.

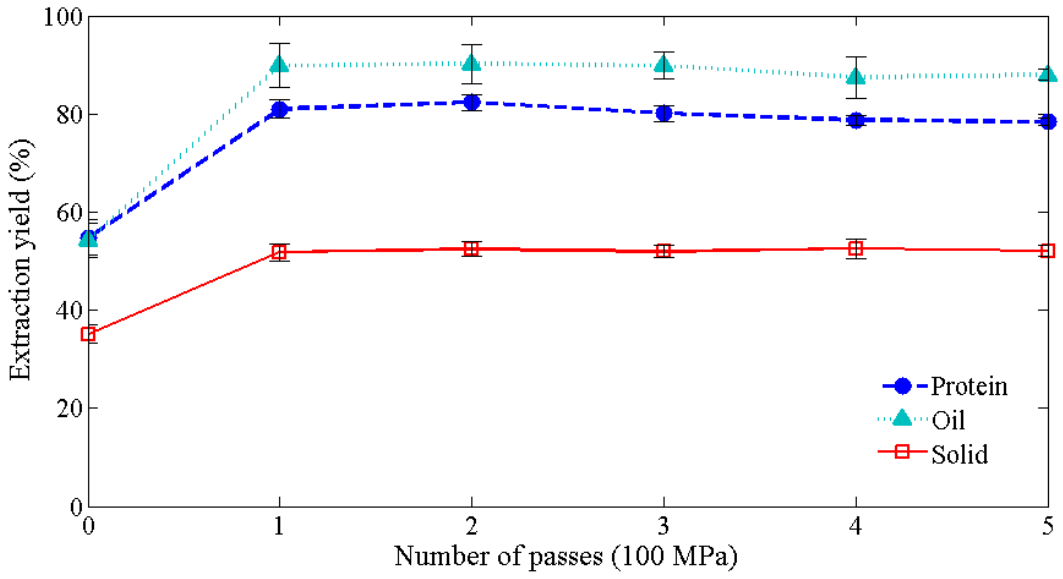


Figure 6.5. Effects of homogeniser passes on the extraction yields ($Y_{II}$) of oil, protein and solids from okara solution, the by-product of soymilk production. Error bars represent standard deviation calculated from 3 experiments analysed in duplicate. Each experiment was carried out on a fresh batch of slurry, prepared on different extractions from the pilot line.

### 6.3.2 Separation efficiencies and availability of protein

To understand how the homogenisation treatment affected the extraction yield, the separation efficiency and protein availability were calculated. Protein extraction yield is a function of the availability of protein and the separation efficiency (see Section 6.2.3). Figure 6.6 shows the effects of homogenisation treatment of both the slurry and okara feeds (Streams 4 and 8 ($O_{\mathrm{I}}$), Figure 6.1), compared to a control sample with heating but without HPH treatment.

Initially the availability of protein was considered: protein availability increased by approximately 18% and 30% (absolute values) during homogenisation of slurry and okara solutions, respectively. The increase in the availability of protein suggests that either intact cells were disrupted, or the solubility of protein was improved. After each subsequent pass of homogenisation treatment, there was no further change in solubility for either slurry or okara solution.

Separation efficiency was affected in both slurry and okara solution homogenisation. The largest effect of separation efficiency was observed for the slurry samples; after 1 pass, the separation efficiency was improved meaning less soluble protein was retained in the okara phase after homogenisation treatment ($O_{\mathrm{I,HPH}}$, Figure 6.1). After subsequent passes, a large reduction in separation efficiency of the slurry was observed (13% after 5 passes). This reduction in separation efficiency of slurry provides good correlation with the stepwise reduction in extraction yields from soy slurry after more than 1 HPH pass as shown in Figure 6.4. In contrast, the okara solution observed little change in the separation efficiency after homogeniser passes, suggesting a similar mass of soluble protein resided in the okara after each HPH treatment, compared to the control sample ($O_{\mathrm{II}}$ and $O_{\mathrm{II,HPH}}$, Figure 6.1). This coincides well with the plateau in the extraction yield observed for okara solution after 1 HPH pass in Figure 6.5.

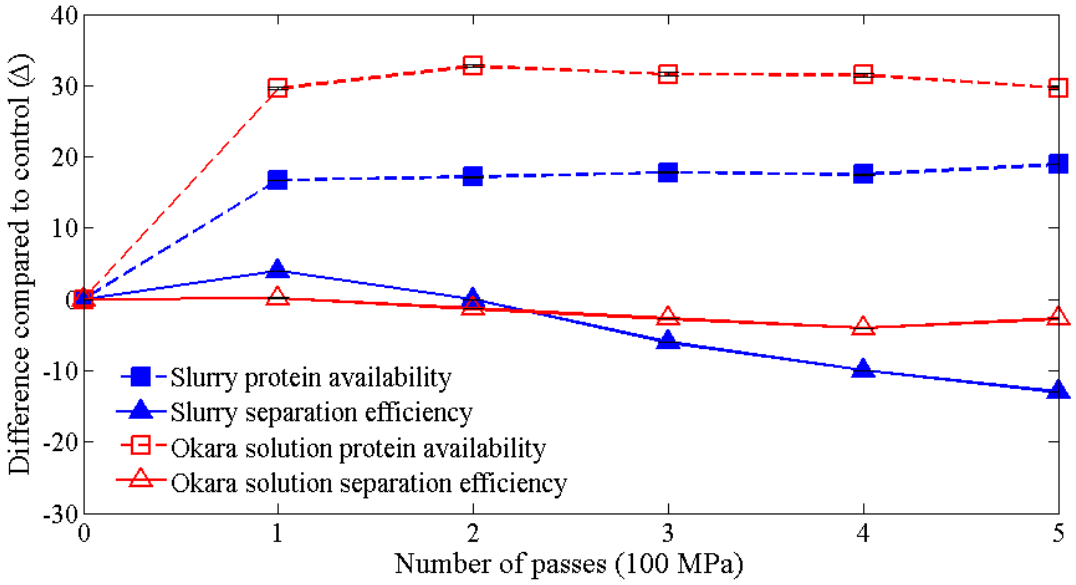


Figure 6.6. The effects of multiple homogeniser passes on availability of protein and separation efficiency for okara and slurry treatments. Error bars present the standard deviation for separation efficiency and availability of protein calculated from 3 separate experiments analysed in duplicate.

The sedimentation velocity in the centrifuge is influenced by several characteristics of the sample (Ballew, 1978):

$$v_c = d^2(\rho_s - \rho_l)\,\omega^2 r/18\eta \qquad (6.5)$$

where:

$v_c$ Sedimentation velocity in a centrifuge

$d$ Particle diameter

$\rho_s$ Particle density

$\rho_l$ Liquid density

$\omega$ Angular viscosity of the rotor

$r$ Radial position of the particle

$\eta$ Kinematic viscosity

As a result of HPH treatment in both soy slurry and okara solution samples, a reduction in the particle size, a smaller density difference between particles and the liquid, and an increase in viscosity were observed (see Sections 6.3.3 & 6.3.5). During the subsequent centrifugation step, the sedimentation velocity should be reduced with smaller particles and a higher viscosity, leading to a less efficient separation. This was the case for multiple passes of slurry through the homogeniser; however, a reduction in separation efficiency was not observed for the okara solution. This can be explained by the low solid content of the okara solution (2.85% w/w), resulting in a relatively minimal change in the viscosity with each consecutive pass through the homogeniser.

### 6.3.3 Particle size measurements

To understand the effects of homogenisation, it was important to study the effects of treatment on the resulting sample characteristics. Particle size measurements were carried out for soy slurry and okara solution samples to study the effects of homogenisation treatment. Figure 6.7 shows the effects of number of passes through the homogeniser on the resulting particle size of soy slurry. The control sample (0 passes) represents a soy slurry sample heated to 80 °C; all samples had the same pre-treatment. For soy slurry heated to 80 °C, the D90 value was approximately 760 µm with a D[4,3]) of ca. 350 µm and D[3,2] of 15 µm. After one high pressure treatment at 100 MPa, the biggest change can be observed in the D90 value; a reduction to a value in the region of 100 microns was observed. A reduction in D[4,3] was also observed; however, the D[3,2] appeared to increase slightly after one pass.

The slurry sample without HPH treatment consisted of particles ranging from submicron to 1 mm, seen in the PSD (0 passes, Figure 6.7B). The largest volume based reduction in particle size occurred after a single pass at 100 MPa compared to the control. The peak at 0.35-3 µm cannot be observed in any of the HPH treated soy samples, suggesting that oil droplets and other components, such as soluble proteins, reduced in volume (see also Section 6.2). After each subsequent pass of slurry, there was a small, stepwise increase in the particle size. The distribution of particles in the size range 2-200 µm, observed for the slurry sample after a single pass increased in broadness to 2-350 µm after 5 passes at 100 MPa.

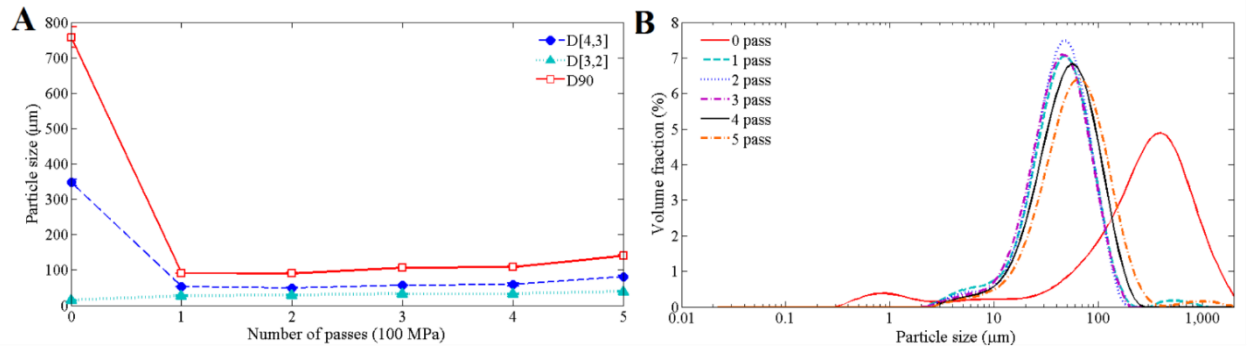


Figure 6.7. Soy slurry particle size variation (A) and PSDs (B) as a function of number of passes through the homogeniser geometry at 100 MPa. Each data point represents an average of 3 separate experiments carried out with different batches of slurry measured in duplicate, the error bars represent the standard deviation.

HPH treated okara solution was also analysed to examine the changes of particle size upon application of homogenisation. Figure 6.8A shows the effects of the number of passes through the homogeniser at 100 MPa on the particle sizes of the okara solution. The initial particle sizes for okara solution were greater than those of the soy slurry. After 1 pass through the homogeniser geometry: all particle sizes were reduced when compared to the control sample (0 passes, Figure 6.8A). Focusing on the particle size distribution of the control sample of okara solution (0 passes,

Figure 6.8B), there is a sharper, higher volume peak of particles in the range 100-1000 µm compared to the slurry control sample (0 passes, Figure 6.7B). Generally, the initial distributions are similar in size ranges. An initial reduction in the larger volume particles is seen upon a single pass, the peak shifts to the range 10-200 µm. There was also a loss of particles with a size of 0.35-6 µm with any number of passes with the homogeniser, as was also observed for the slurry sample (Figure 6.7B). This could be attributed to a reduction in size of the oil droplets. With each subsequent pass after a single pass, there was no stepwise increase in the particles size, contrary to the slurry after HPH with multiple passes.

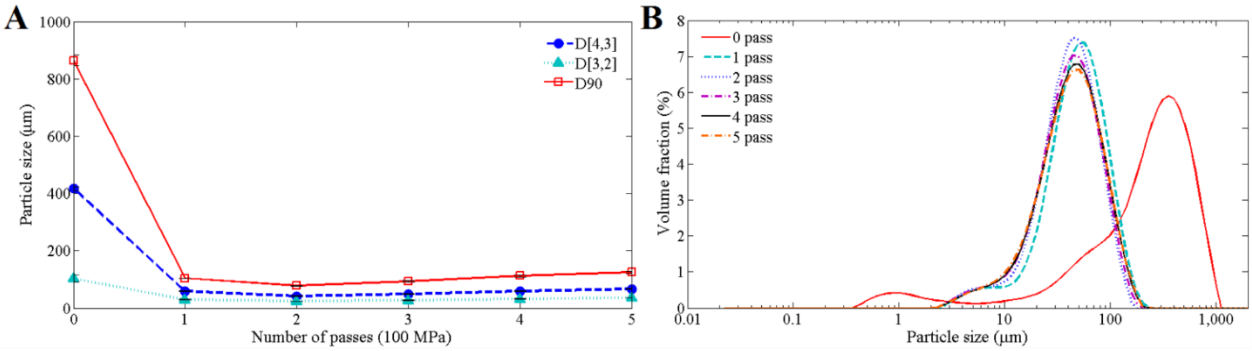


Figure 6.8. The effect of number of passes through the homogeniser geometry at 100 MPa on the particle sizes (A) and PSDs (B) of okara solution. Each point represents an average of 3 different samples from 3 separate batches of okara, with error bars representing the standard deviation.

### 6.3.4 CLSM

To investigate the effects of homogenisation treatment on slurry and okara solution samples further, CLSM was employed in the presence of nile blue for visualisation. Nile blue is a dye used to visualise apolar material (Preece *et al.*, 2015; **chapter 3**). In the system settings, oil appears green and other, less apolar materials, including protein and fibres, appear red. Initially, the microstructure of the control samples (0 passes) was investigated. Figure 6.9 shows the typical structures observed in the soy slurry after milling of soybeans at pilot scale with a thermal pre-treatment of 80 °C. Droplets of oil, depicted in green, were found throughout the continuous phase of the sample, with sizes up to 12 µm in diameter, which were larger compared to those located within soy slurry and were previously reported to be typically less than 0.5 µm (Preece *et al.*, 2015; **chapter 3**). Cell wall structures were visible in the soy slurry sample, without HPH treatment (red oblong structures, Figure 6.9A). In Figure 6.9B, intact cells are observed, and intact protein bodies are visible within these structures, visualised in red. Fibrous structures in red can also be seen, and these are empty cell wall structures from where the contents have been extracted.

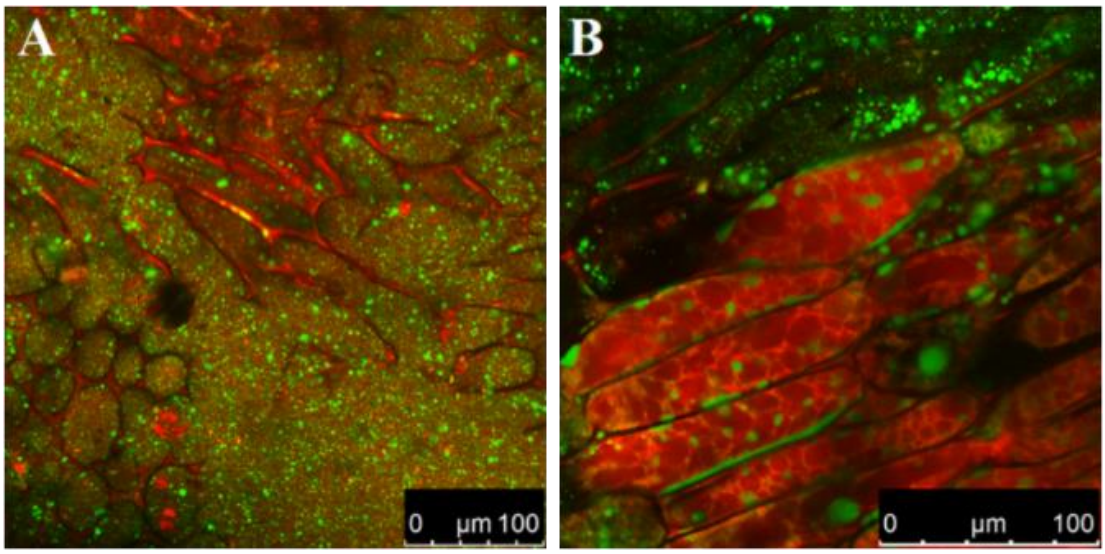


Figure 6.9. Microstructural images of soy slurry without homogenisation, visualised using CLSM and the fluorochrome nile blue. Oil is highlighted in green and other, less apolar materials (including protein and fibres) are presented in red.

After a homogenisation treatment at 100 MPa, a sample of slurry was visualised and the results are shown in Figure 6.10. The representative micrographs show changes in many of the aspects of the slurry sample. The oil droplets, green in these images, are significantly reduced in size. It is near impossible to distinguish the individual droplets in the continuous phase; the resolution of this technique makes the background of the image appear greener in comparison to the sample prior to treatment, measured using the same settings (Figure 6.9). This supports the reduction in particle size and loss of the volume based peak at 1 µm to submicron sizes (Figure 6.7B). Intact cells were not observed in any of the samples studied using CLSM, after one treatment at 100 MPa or for multiple passes. The fibrous structure observed in the control sample were made shorter by homogenisation treatment, which confirms the results seen in particle size examination (Section 6.3.3). The microstructure observed after 5 passes through the homogeniser using CLSM was similar compared to that seen after 1 pass (data not shown).

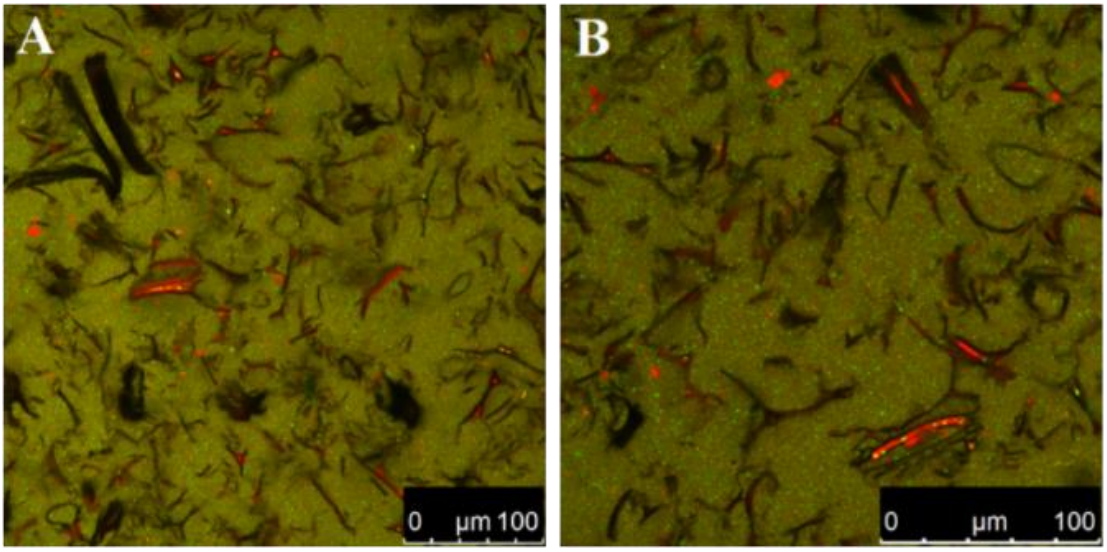


Figure 6.10. CLSM images of soy slurry after 1 pass through homogeniser at 100 MPa, highlighted using nile blue. Oil is highlighted in green & other apolar materials (including protein and fibres) are presented in red using Leica software settings.

The small increase in the particle size upon slurry homogenisation after a single pass (Figure 6.7) might be due to limited protein aggregation (Toro-Funes *et al.*, 2015), although we did not observe that using CLSM (data not shown). After 1 pass, the protein extraction yield from slurry increased to 82% (Figure 6.4). The D[4,3] was reduced to approximately 50 µm for all resultant samples, both slurry (53 ± 1 µm) and okara solution (59 ± 2 µm), after homogenisation. Apparently, most of the particles in this size range was still soluble or dispersible, and resided in the soybase during the extraction process. It has been shown previously using transmission electron microscopy (Rosenthal *et al.*, 1998) and CLSM (Preece *et al.*, 2015; **chapter 3**) that the size of hydrated soybean cotyledon cells vary in length from 70 to 80 µm and 20-30 µm in diameter. Assuming a spherical cotyledon cell, its average size is about 45-55 µm (average of length and diameter). The measured particle size data would suggest that homogenisation disrupted all intact cells (Figure 6-

7). That is confirmed by CLSM measurements in this study: after 1 pass through the homogeniser, no intact cells were present (see Figures 6.10).

### 6.3.5 Rheology-Flow behaviour

To shed more light on the differences observed between the slurry and okara solution separation efficiencies, a study of the flow behaviour was conducted (Figure 6.11). Focusing on the viscosity profiles of the control soy slurry (0 pass, Figure 6.11), it is possible to observe shear thinning behaviour: as the shear rate increased, the viscosity decreased. Upon 1 pass through the homogeniser, the slurry viscosity increased especially at the relatively lower shear rates, but at shear rates above 3 $s^{-1}$ the viscosity of slurry. With a single pass through the homogeniser, the greatest effect on the particle size of the slurry was observed of all treatments (Figure 6.7). Reducing the overall particle size results in a stepwise increase in viscosity, which can be observed for all of the homogenised samples. If we assume a constant volume fraction, than there are a greater number of particles, which results in a greater number of interactions. Upon 5 passes, the viscosity increased at all shear rates investigated compared to the control sample. This viscosity increase as well as the slight increase in particle size of the slurry (see Figure 6.7) upon subsequent HPH passes might be the reason why the slurry particle became increasingly difficult to separate from the bulk solution (see Figure 6.6).

Focusing on the okara solution viscosity profile (Figure 6.11B), the first obvious difference compared to the slurry curves is the lower viscosity for all okara samples, treated and non-treated. This was caused by the reduced solid content of the okara solution, i.e. 2.5 ± 0.1% versus the slurry samples; the control slurry sample (0 pass) consisted of 12.6 ± 0.1% solids in comparison, which accounts for soluble solids and insoluble solids, such as oil, protein, cell wall fibres and intact cells.

The control okara solution (0 pass, Figure 6.11B) behaved as a Newtonian fluid. At shear rates below approximately 1 $s^{-1}$, a shallow plateau in the flow curve was observed. It is believed that this was caused by shear banding in the okara solution samples (Mewis & Wagner, 2012). This is an artefact and can be neglected. At a shear rate of approximately 100 $s^{-1}$, it was possible to see a small increase in the dynamic viscosity for all of the okara solution samples; however, this is also an artefact caused by the presence of turbulence within the measurement, which is not assumed during the calculation of viscosity. This can also be neglected in the interpretation. Upon 1 pass through the homogeniser of the okara solution, the behaviour changed from Newtonian behaviour to shear thinning, with an increase of viscosity versus the control (0 passes). After 5 HPH passes, a viscosity increase was observed compared to the control at all shear rates investigated. The same effects of particle size that were observed for soy slurry can also be applied to the okara solution.

The release of intracellular materials, such as proteins and smaller fibrous materials upon cell disruption led to interactions and build-up of structure, thus increasing the viscosity (Figure 6.11) (Lee *et al.*, 2012). This has also been observed previously by Lopez-Sanchez *et al.* (2011) for tomato cell suspensions. Such an increase in viscosity could be beneficial for producing a low solids product, with a similar viscosity profile to soy slurry without homogenisation treatment.

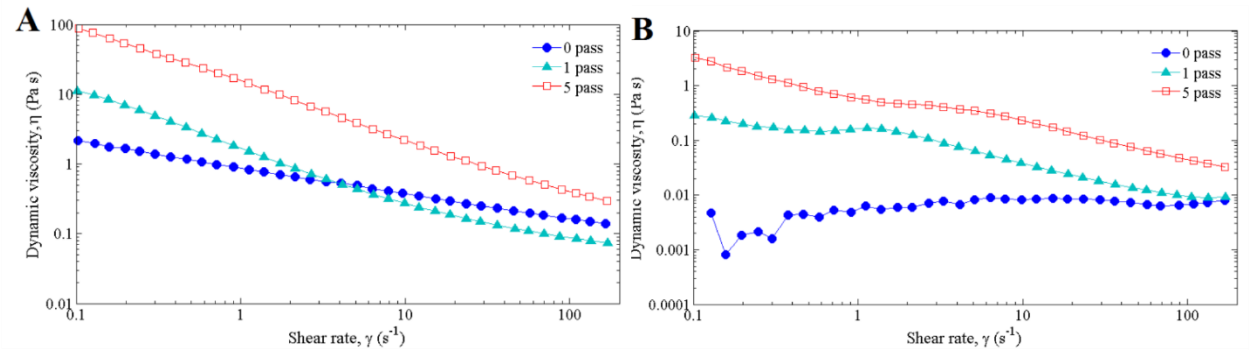


Figure 6.11. Viscosity profiles of slurry (A) and okara solution (13.7%) (B) with various homogenisation treatments (100 MPa) including a control sample without homogenisation. Each graph shows a sweep with increasing shear rate followed by a downwards sweep.

The viscosity of the starting material also affects the phenomena of cavitation during the application of HPH by influencing how readily the microbubbles grow within the liquid sample. Low viscosity solutions experience higher cavitational effects; microbubble growth can occur more readily as the energy applied can exceed the molecular forces occurring within the solution (Kiathevest *et al.*, 2009). This supports the fact that okara solution, which has a lower viscosity in comparison to the soy slurry starting material, would experience a greater cavitational effect, thus resulting in an increased extraction yield of protein and other intracellular materials.

### 6.3.6 Energy input and productivity of HPH treatment

To understand the feasibility of scale up for this promising technology, it was necessary to calculate the energy efficiency in comparison to other technologies. Energy input was calculated using the following equation (Bylund, 2003):

$$Power\ input\ (kW) = \frac{Q_{in} \times (P_1 - P_{in})}{36000 \times \eta_{pump} \times \eta_{elec.motor}} \quad (6.5)$$

Where $Q_{in}$ is the volumetric flow rate, $P_1$ and $P_{in}$ refer to the pressure of homogenisation treatment and the inlet pressure, respectively and $\eta_{pump}$ & $\eta_{elec.motor}$ are the efficiency of the pump and electric motor, respectively. Both were estimated as 75% (Peters *et al.*, 1968. For the investigated homogenisation pressures (50-125 MPa), the energy inputs ranged from 0.01-0.05 kWh $L^{-1}$. Previously Preece *et al.* (2017b; **chapter 5**) reported energy inputs in the range: 0.004-0.12 kWh $L^{-1}$ using a lab-scale probe system for sonication of similar soybean processing materials. Maximum yields of 70% and 65% were achieved at 0.12 kWh $L^{-1}$ for ultrasound-assisted extraction of protein from slurry and okara solution, respectively (Preece *et al.*, 2017b; **chapter 5**). Thus, the energy input during homogenisation was less than that quoted during sonication of soybean processing materials, while the protein extraction yield was greater for materials treated with homogenisation (see Figure 6.3-6.5). The differences in extraction yields can be attributed to the disruption of intact cells during homogenisation treatment – no intact cells were visualised after 1 pass through the homogeniser using CLSM (Figure 6.10), contrary to ultrasound.

Productivity is another important factor to consider when designing an industrial plant, giving an indication of the efficiency of processing. The definition of productivity is the ratio of the output to input for a specific process (Roger, 1998); in this chapter, it was calculated by dividing the mass fraction of protein in the soybase by the number of passes through the homogeniser. The 0 pass value represents the mass fraction of protein in control soybase, without HPH treatment. Figure 6.12 shows the effects of number of homogeniser passes at 100 MPa on the productivity. The greatest productivity was found for 1 HPH pass at 100 MPa for both slurry and okara solution (Figure 6.12). Comparing the productivity of slurry and okara solution after a single pass at 100 MPa, slurry treatment was found to be a more viable option. The low protein concentration in the

resultant soybase after okara solution treatment caused lower productivity in comparison to slurry. After each subsequent pass for both slurry and okara solution, the productivity reduced below that of the control sample, without homogenisation treatment.

Productivity was also calculated for pilot-scale ultrasound treatment of okara solution (Preece *et al.*, 2017b; **chapter 5**). The productivity for HPH treatment of okara solution (Figure 6.12) is lower than the productivity calculated for ultrasonic treatment (Figure 5.10). These two measurements of productivity cannot be directly compared since they are calculated using different assumptions.

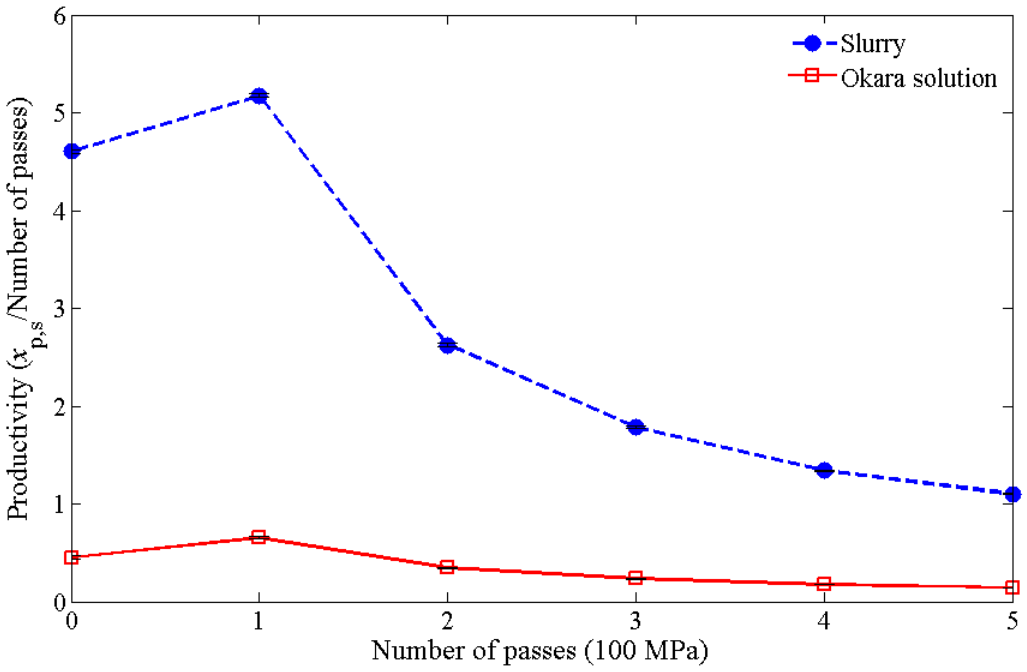


Figure 6.12. Productivity versus number of passes through HPH at 100 MPa. Each data point represents productivity calculated from an average of 3 separate experiments, with error bars representing the standard deviation.

Another means to compare the effectiveness of ultrasound and HPH includes the calculation of the energy input for each technique. A comparison of resultant protein extraction yields can be seen in Figure 6.13. Losses of energy, including temperature changes, sound and friction, are not

considered during the process, only the energy inputs are compared. The energy input of HPH is 3× greater than that supplied by ultrasound. 100 MPa was the pressure chosen for the HPH treatments, this was to ensure that the maximum improvement in yield could be obtained as a plateau in extraction yields had been reached. Treatments at lower pressures would result in a reduced energy input, and a similar protein extraction yield. The protein extraction yield achieved upon the application of ultrasound is similar to those of the control samples (0 kJ), whereas the improvement associated with HPH is more prominent.

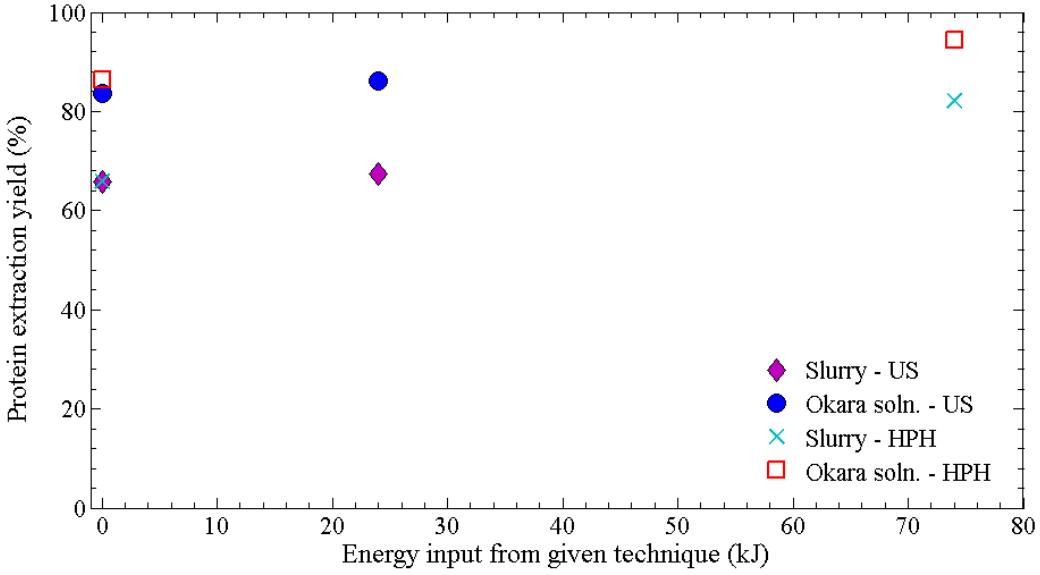


Figure 6.13. Plot of total protein extraction yield versus the energy input of ultrasound (US) & high pressure homogenisation (HPH). Energy input was calculated based on a single pass, 1 min lab-scale treatment of 100 mL of sample using the power input of the technique: 1.85 kW and 400 W for HPH and US, respectively. An okara concentration of 13.7% was used for the comparison.

Additional work is necessary to study the effects of lower pressure homogenisation with a higher number of passes. It was shown by Donsì *et al.* (2013) that microbial inactivation using 2 passes at 100 MPa was not equivalent to a single pass at 200 MPa. However, in Section 6.3.1 it was indeed possible to achieve a notable improvement in protein extraction yield of approximately 15% for

the treatment of slurry at 50 MPa, which is as high as the yield for 100 MPa treatment. A pressure of 100 MPa was chosen to ensure optimal protein extraction was achieved.

## 6.4 CONCLUSIONS

In conclusion, high pressure treatment (50-125 MPa) was found to improve the extraction of oil, protein and solids from soybean processing materials. The improvement for both slurry and okara solution treatment after one HPH pass (Figure 6.3) was found to be a result of availability of protein and separation efficiency (Figure 6.6). The improvement in availability can be attributed to the reduction in particle size and cell disruption, as confirmed by particle size measurements (Figures 6.7 and 6.8) and CLSM (Figures 6.9 and 6.10). A decrease in separation efficiency was observed for slurry treatment with increasing number of homogenisation passes (Figure 6.4, resulting in a reduction of protein extraction yield contrary to okara solution treatment (Figure 6.5). This reduction can be attributed to a slight increase in particle size (Figure 7) and increase in viscosity (Figure 6.11) upon subsequent HPH passes. High pressure treatment based on the phenomena of hydrodynamic cavitation offers a more viable route of extraction intensification from soybean processing materials in comparison to ultrasound. Based on the productivity of the technology, the best scenario includes the use of HPH on slurry rather than okara solution, for 1 pass at 100 MPa (Figure 6.12). Further work is required to optimise this processing technology, including scale up to determine the viability for implementation at factory scale as well as sensory evaluation and storage stability of the resulting soy based products. To reduce energy costs, it is also beneficial to study further the effects of lower pressures than 100 MPa.

## 6.5 REFERENCES

Apichartsrangkoon, A. (2003). Effects of high pressure on rheological properties of soy protein gels. *Food Chem, 80,* 55-60.

Ballew, H. W. (1978). *Basics of filtration and separation*. Nuclepore Corporation.

Bylund, G. (1995). *Dairy processing handbook*, Lund, Sweden: Tetra Pak Processing Systems AB, (Chapter 6.3).

Cruz, N., Capellas, M., Hernández, M., Trujillo, A.J., Guamis, B., Ferragut, V. (2007). Ultra high pressure homogenization of soymilk: Microbiological, physicochemical and microstructural characteristics. *Food Res Int, 40,* 725-732.

Donsì, F. G. Ferrari, E. Lenza, P. Maresca, (2009). Main factors regulating microbial inactivation by high-pressure homogenization: operating parameters and scale of operation. *Chem Eng Sci, 64,* 520-532.

Donsì, F., Annunziata, M., & Ferrari, G. (2013). Microbial inactivation by high pressure homogenization: effect of the disruption valve geometry. *Journal of Food Engineering*, *115*(3), 362-370.

Dumay, E., Chevalier-Lucia, D., Picart-Palmade, L.t., Benzaria, A., Grácia-Juliá, A., Blayo, C. (2013). Technological aspects and potential applications of (ultra) high-pressure homogenisation. *Trend Food Sci Tech, 31,* 13-26.

Floury, J., Desrumaux, A., Legrand, J. (2002). Effect of ultra-high-pressure homogenization on structure and on rheological properties of soy protein-stabilized emulsions. *J Food Sci, 67,* 3388-3395.

Gogate, P.R., Tayal, R.K., Pandit, A.B. (2006). Cavitation: a technology on the horizon. *Current Science, 91,* 35-46.

Gogate, P.R., Kabadi, A.M. (2009). A review of applications of cavitation in biochemical engineering/biotechnology. *Biochem Eng J, 44*, 60-72.

Gogate, P.R. (2011). Hydrodynamic Cavitation for Food and Water Processing. *Food Bioprocess Technol, 4,* 996-1011.

Kajiyama, N.O.B.O., Isobe, S.E.I.I., Uemura, K.U.N.I., Noguchi, A.K.I.N. (1995). Changes of soy protein under ultra-high hydraulic pressure. *Int J Food Sci Tech, 30,* 147-158.

Kiathevest, K., Goto, M., Sasaki, M., Pavasant, P., Shotipruk, A. (2009). Extraction and concentration of anthraquinones from roots of Morinda citrifolia by non-ionic surfactant solution. *Separation and purification technology*, *66*(1), 111-117.

Lee, A.K., Lewis, D.M., Ashman, P.J. (2012). Disruption of microalgal cells for the extraction of lipids for biofuels: Processes and specific energy requirements. *Biomass Bioenerg, 46,* 89-101.

Lee, I., Han, J.I. (2015). Simultaneous treatment (cell disruption and lipid extraction) of wet microalgae using hydrodynamic cavitation for enhancing the lipid yield. *Bioresource Technol, 186*, 246-251.

Lopez-Sanchez, P., Nijsse, J., Blonk, H.C.G., Bialek, L., Schumm, S., Langton, M. (2011). Effect of mechanical and thermal treatments on the microstructure and rheological properties of carrot, broccoli and tomato dispersions. *J Sci Food Agric, 91,* 207-217.

Mewis, J., Wagner, N.J. (2012). *Colloidal suspension rheology,* Cambridge: Cambridge University Press, (Chapter 9).

Okamoto, M., Kawamura, Y., Hayashi, R. (1990). Application of High Pressure to Food Processing: Textural Comparison of Pressure- and Heat-induced Gels of Food Proteins. *Agr Bio Chem Tokyo, 54,* 183-189.

Peters, M.S., Timmerhaus, K.D., West, R.E., Timmerhaus, K., West, R. (1968). *Plant design and economics for chemical engineers*, (pp. 478-579). New York: McGraw-Hill New York.

Poliseli-Scopel, F.H., Hernández-Herrero, M., Guamis, B., Ferragut, V. (2012). Comparison of ultra high pressure homogenization and conventional thermal treatments on the microbiological, physical and chemical quality of soymilk. *Food Chem, 46*, 42-48.

Preece, K.E., Drost, E,. Hooshyar, N., Krijgsman, A.J., Cox, P.W., Zuidam, N.J. (2015). Confocal imaging to reveal the microstructure of soybean processing materials. *J Food Eng, 147,* 8-13.

Preece, K. E., Hooshyar, N., Krijgsman, A., Fryer, P. J., Zuidam, N. J. (2017a). Intensified soy protein extraction by ultrasound. *Chem Eng Process*, *113*, 94-101.

Preece, K. E., Hooshyar, N., Krijgsman, A. J., Fryer, P. J., Zuidam, N. J. (2017b). Pilot-scale ultrasound-assisted extraction of protein from soybean processing materials shows it is not recommended for industrial usage. *J Food Eng*, *206*, 1-12.

Preece, K. E., Hooshyar, N., & Zuidam, N. J. (2016). Whole soybean protein extraction processes: A review. *Manuscript submitted for publication.*

Rastogi, N.K., Raghavarao, K.S.M.S., Balasubramaniam, V.M., Niranjan, K., Knorr, D. (2007). Opportunities and Challenges in High Pressure Processing of Foods. *Crit Rev Food Sci, 47,* 69-112.

Rosenthal, A., Pyle, D.L., Niranjan, K. (1998). Simultaneous aqueous extraction of oil and protein from soybean: Mechanisms for process design. *Food Bioprod Process, 76*, 224-230.

Save, S.S., Pandit, A.B., Joshi, J.B. (1997). Use of hydrodynamic cavitation for large scale microbial cell disruption. *Food Bioprod Process, 75*, 41-49.

Tobin, J., Heffernan, S.P., Mulvihill, D.M., Huppertz, T., Kelly, A.L. (2015). Applications of High-Pressure Homogenization and Microfluidization for Milk and Dairy Products. In: N. Datta, P.M. Tomasula (Eds.) *Emerging Dairy Processing Technologies: Opportunities for the Dairy Industry*, (pp. 93-114). John Wiley & Sons, Ltd.

Toro-Funes, N., Bosch-Fusté, J., Latorre-Moratalla, M.L., Veciana-Nogués, M.T., Vidal-Carou, M.C. (2015). Isoflavone profile and protein quality during storage of sterilised soymilk treated by ultra high pressure homogenisation. *Food Chem, 167*, 78-83.

Xi, J. (2006). Effect of High Pressure Processing on the Extraction of Lycopene in Tomato Paste Waste. *Chem Eng Technol, 29*, 736-739.

Zhu, X., Cheng, Y., Chen, P., Peng, P., Liu, S., Li, D., Ruan, R. (2016). Effect of alkaline and high-pressure homogenization on the extraction of phenolic acids from potato peels. *Innov Food Sci Emerg Technol, 37*, 91-97.

# CHAPTER 7

# CONCLUDING REMARKS & RECOMMENDATIONS

Every industry is keen to do more with less, and the food industry is no exception. During soybase production, currently a large fraction of protein is lost to the waste stream, okara, which is commonly utilised as animal feed. This thesis aimed to maximise the extraction of protein during the production of a soy-based extract for soymilk and tofu preparation. The objectives were:

- To gain a fundamental understanding of the complex microstructures of soybean processing materials of current soybase production processes
- Use this knowledge to identify the process limitations
- Identify technologies to improve the protein extraction yield
- Test the scalability of selected technologies by performing a pilot-scale study

The findings of this thesis is categorised into the following sections: 7.1 Deciphering limiting factors for protein extraction during soybase production and 7.2 Overcoming restraints to enhance protein extraction yield at various scales of treatment. Future recommendations will then be presented for succeeding work in this field.

## 7.1 DECIPHERING LIMITING FACTORS FOR PROTEIN EXTRACTION DURING SOYBASE PRODUCTION

To improve the utilisation of raw materials, it was necessary to determine the limiting factors for extraction of protein. Upon investigation of the literature (**chapter 2**), it became clear that whole soybean extraction can be divided into the following key steps:

- Mechanical disruption of soybeans by milling
- Solubilisation of compounds into the aqueous extract
- Separation of insoluble ingredients by filtration or decanting
- Ensuring sensorial quality by inactivation of trypsin inhibitors by heat treatment

High temperature is most often already applied in the first steps to inactivate LOX, an enzyme that catalyses oxidation of fatty acids, resulting in off-flavours. However, this also causes denaturation of the desirable soy proteins. The optimal, total extraction process for obtaining the final product might be a compromise between the optimal conditions of each individual step. The protein yield is dependent on all of the aforementioned steps and can be calculated by multiplying the protein availability (%) by the separation efficiency (%). The protein availability is dependent on the particle size of ground soybeans upon milling and the solubilisation into the aqueous bulk phase as a function of this particle size, extraction time and the properties of the aqueous bulk phase (pH, ionic strength, temperature, and protein concentration). The separation efficiency is controlled by the large amount of okara produced and its high moisture content (80%). Surprisingly, this has not been reported before and a novel extraction model based on this new insight is presented in **chapter 2**. This model also explains that extraction yields increase at higher L/Sol ratios due to higher

separation yields and not, as currently stated in the scientific literature, due to improved protein solubility.

Although the structure of soybeans is well known, the microstructural localisation of components of interest in soybean processing materials did not exist. Therefore, microstructures of soybean processing materials, slurry, okara and soybase were examined at lab-scale using a novel confocal laser scanning microscopy (CLSM) study in **chapter 3**. CLSM visualised various features, such as intact cells, oil droplets, protein (including protein aggregates) and cell wall structures. With heat treatment at 80 °C, protein was found to aggregate and as a result aggregated protein bodies in and outside of intact cells were visualised. These aggregated protein bodies were found to exit the process in the okara waste stream. This resulted in the reduction of protein extraction yield, compared to extraction carried out at ambient temperature.

To improve soybean extraction yields, the process limitations for protein availability and/or separation of the product and waste stream should be minimised. Process intensification is required to make protein more available than is currently accessible after standard, two-stage grinding, either by the disruption of more intact soybean cells, or aiding the solubilisation of protein. This could be achieved by introducing a new mill; it is known that replacing a worn mill with a new one increases the efficiency of cell disruption, resulting in an increase in yield. However, this is relatively short-lived and milling efficiency begins to decline with wear of the mills. Therefore, cavitation has been identified as an additional technology to aid soy protein extraction in this thesis. Cavitation includes the formation and growth of microscopic voids within a liquid, which collapse upon a sufficiently negative pressure. The resultant phenomena include local regions of high pressures and temperatures, in addition to liquid jets, leading to enhanced mass transfer. In this

thesis, we have evaluated both acoustic cavitation (ultrasound; **chapters 4 and 5**) and hydrodynamic cavitation (high pressure homogenisation (HPH), **chapter 6**) at lab-scale and at pilot-scale. We also studied the effect of these cavitational techniques on okara properties as this may affect the separation efficiency. Process intensification options to improve separation efficiency have been identified in **chapter 2** as well, i.e. the use of the Sedicanter® or belt press. However, there was no further time to evaluate these technologies in this thesis study.

## 7.2 OVERCOMING THE RESTRAINTS TO ENHANCE PROTEIN EXTRACTION YIELD AT VARIOUS SCALES OF TREATMENT

In **chapter 4,** ultrasound was presented as a technology that increased the extraction of oil, proteins and solids at lab-scale. Ultrasound has been applied to a number of food systems and its success is attributed to the disruption of intact cells and improved mass transfer caused by cavitation phenomena. In our investigations, the extraction yields of oil, protein and solids were indeed improved; upon milling at 80 °C, protein yield increased by 10% after only 1 min batch ultrasound treatment of soy slurry at 50 °C. Visualisation by CLSM indicated that the disruption of cells was not a significant reason for improved availability of protein, contrary to what has been stated in the literature by others. Availability of protein and the separation efficiency were calculated, assuming all water in the okara stream contained the same concentration of soluble protein as the soybase. Both availability of protein and separation efficiency were increased, even after as little as 30 seconds of ultrasonic treatment of soy slurry. The insoluble protein previously visualised in the continuous phase of the slurry and entering the okara stream had decreased in concentration after ultrasonic treatment, after 30 seconds of treatment. This finding was supported by particle size data based on number fractions; particles corresponding to the protein bodies' size range of 2-35 μm were reduced to the submicron range after any period of ultrasonic treatment that was investigated. Surprisingly, the reduction in insoluble protein bodies was not a stepwise decline in size, but a reduction in numbers. In conclusion, ultrasound treatment disrupted aggregated protein bodies outside cells, but not cells and protein bodies inside intact cells.

Once the effects of ultrasound had been investigated at lab-scale, the effects were examined on soybean processing materials produced in a pilot plant using lab-scale and pilot-scale ultrasonic probe systems (**chapter 5**). It is believed that materials produced in the pilot plant facilities have properties more similar to those found in a factory. The majority of studies of ultrasound published in the external literature were carried out at lab-scale, and rarely any consideration for the scale-up potential is offered. No other pilot-scale studies were found detailing the effect of ultrasound for extraction assistance of proteins from whole soybeans. In **chapter 5** of this thesis, ultrasound was applied to both soy slurry (milled soybeans in water) and the okara solution made at pilot-scale. As more than 9 passes of soy slurry through the flow cell were required at the operating flow rate to achieve similar energy inputs at pilot-scale to lab-scale, ultrasound treatment of slurry was considered unfeasible. The lab-scale probe system supplied an energy intensity 300 times greater than that of the pilot-scale probe. Ultrasound-assistance was found to improve the extraction of protein significantly at pilot-scale by 4.2% versus a control sample (no ultrasound, all other conditions unchanged). Using a response surface methodology, okara solution flow rate and okara concentration were found to also have a significant impact on the protein extraction yield during okara treatment. However, when considering the maximal increase in total extraction yield (5%) that could be achieved under the tested conditions, ultrasound is not a viable option during industrial processing.

CLSM revealed the microstructure of the soy slurry produced at pilot-scale using the standard process (without ultrasonic treatment) differed from that prepared at lab-scale. Aggregation of protein as found at lab-scale (see **chapter 3**) was not found in the continuous phase of the pilot-scale sample at the elevated temperature, thought to be a result of reduced processing time. The

primary protein extraction yields from the pilot-plant were elevated in comparison to those found for lab-scale production (66 ± 2% versus 36 ± 2%, respectively), therefore there was less protein available for subsequent extraction from okara and thus less opportunity to improve yield by okara treatment. More efficient milling during soybase preparation in the newly built pilot plant accounted for this greater primary extraction yield. In a factory, the mills are worn quickly and this results in lower yields and thus more opportunity for yield improvement by okara treatment. Intact cells were found within the okara after ultrasonic treatment using both probe systems, in line with the observation in **chapter 4** that ultrasound did not disrupt soybean cells. Minor improvements in extraction yield may therefore be attributed to the effects of ultrasound on the fibrous cell wall material.

Another method for implementing cavitation on a liquid sample is through constriction of fluid flow. High pressure homogenisation (HPH) is a unit operation typically employed to produce fine emulsions or the disruption of microbial cells via the actions of hydrodynamic cavitation. **Chapter 6** studied HPH and its effects on the extraction of components from soybean processing materials. An improvement in protein extraction yield was achieved from both slurry and okara solution treatment. A single pass of soy slurry at a pressure of 100 MPa was most effective for causing an improvement in extraction yield by 16%, and this was associated with improvements in protein availability and separation efficiency. The protein availability was increased by the disruption of intact cells (a result in contrast to ultrasound treatment), confirmed by CLSM and particle size measurements. Considering okara solution treatment, a single pass (100 MPa) caused a protein yield increase of 26%. However, multiple passes did not cause detrimental effects to the protein extraction yield, in contrast to soy slurry HPH treatment. This is explained by the reduction in

separation efficiency accompanying multiple passes of slurry due to slightly increased particle size and increased viscosity, which was not observed for okara solution to the same extent. Comparing the productivity of slurry and okara solution after a single pass at 100 MPa, slurry treatment was found to be a more viable option. When comparing the energy input from HPH compared to ultrasound, a smaller range of low energies were introduced using HPH with more promising results.

Based on the results obtained in **chapter 6**, applying a single pass homogenisation treatment to slurry is most productive and desirable for industry. Figure 7.1 shows a potential design for a soybase production plant, including the implementation of a high pressure homogeniser before the separation step. Financially, slurry treatment is more attractive than okara solution treatment due to the lack of a second separation unit, which is necessary for okara treatment shown in Figure 6.1, blue box. In the following section, points that require careful consideration when considering the potential implementation of HPH during soybase production will be presented as well as other process intensification options which might be used in addition to HPH as well.

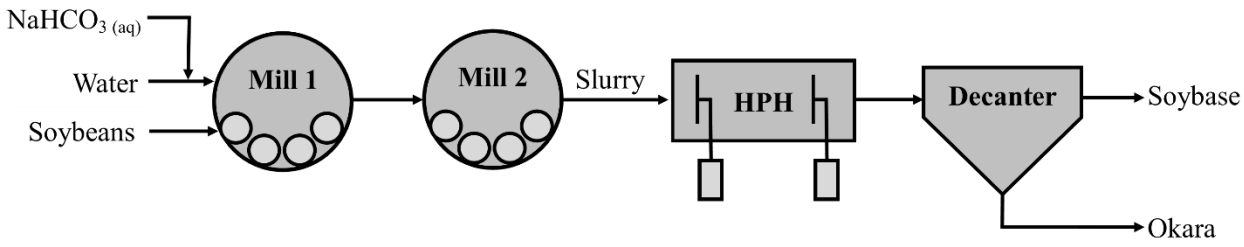


Figure 7.1. Potential design of a future process, with the addition of a high pressure homogenisation prior to the decanter centrifuge.

## 7.3 FUTURE RECOMMENDATIONS

### 7.3.1 Continuation of high pressure homogenisation

Further studies are necessary to understand the scalability of HPH treatment, for implementation at an industrial scale. This technology showed advantages in comparison to ultrasonic processing, with the disruption of intact cells being the main source of enhanced extraction yields with HPH treatment. The volumetric flow rate of the bench-scale homogeniser utilised for experiments in this thesis was 9 L $h^{-1}$. Considering that the soy slurry mass flow rate in the pilot plant, Unilever R&D Vlaardingen, was 200 kg $h^{-1}$, an approximate flow rate increase of 22 times is necessary through the homogeniser geometry. This is only considering the pilot plant facilities; the throughput would be much greater at an industrial scale. High pressure homogenisers are available for purchase, capable of pressures up to 70 MPa at a flow rate of 12,000 L $h^{-1}$ (GEA Niro Soavi, 2012). Careful consideration should be given to the resultant fluid dynamics when varying the flow rate of the sample and the gap opening of the homogenisation valve. For the implementation of HPH during an extraction process at industrial scale, cost analysis will be necessary to calculate the payback time for such equipment.

Furthermore, during HPH treatment at such high pressure (100 MPa) there are some other potential issues that have to be considered. Soy slurry is a fibrous material with a particle size of approximately 350 µm (D[4,3]) which is relatively large compared to the gap size which the liquid will be forced through. This can lead to potential issues with blockages of the sample in the equipment, leading to down time of the equipment, which is undesirable at production scale. However, this was not a problem when performing the experiments using a bench-scale homogeniser geometry. Complete cell disruption by homogenisation may also result in a more

challenging okara separation. However, with a single pass through the lab-scale homogeniser at 100 MPa, both slurry and okara solution had a similar separation efficiency in comparison to the control without homogenisation treatment. Sedimentation of solids during storage or changes in the sensory characteristics of the final soy-based product are other issues to keep in mind.

Finally yet importantly, one should carefully check that the soybase obtained with a new, more efficient process does not lead to negative changes in the storage stability and sensory perception of the resulting soy-based consumer product, as perceived by consumers.

### 7.3.2 Focusing on separation technologies

Another focus for enhancing protein extraction can be reducing the moisture content of the waste stream, okara. Currently a decanter centrifuge is employed within the industry to produce soybase and okara with a moisture content of about 80%. One may use a second decanter to wash in water 2x diluted okara, which commonly results in 10-15% extra yield (depending on the exact conditions used). Other identified process intensification options to obtain more yield by decreasing the okara moisture content (see **chapter 2**) include the Sedicanter® (which operates at a higher *g*-time than a decanter, but at higher costs) and a filter press system (but with an open, hygienic-risk design).

### 7.3.3 Measurement of the mechanical force required to disrupt a cotyledon cell

Cavitational techniques such as ultrasound and high pressure homogenisation introduce a large amount of energy during their application. Analytical techniques are available to measure the mechanical properties of single cells, which give an insight into the types of approaches necessary to disrupt all intact cells for a given type of cell. Atomic force microscopy (AFM) is a technique used by Lee *et al.* (2013) to measure the mechanical properties of single microbial cells. It was reported that on average, a disruption energy of 17.43 pJ was required to disrupt a single microalga

cell (Lee *et al.*, 2013). In order to assess the efficiency of the processing technology, a technique such as AFM should be employed on a cotyledon cell to understand the system more fully.

## 7.4 CONCLUDING REMARKS

This thesis has studied cavitation-based technologies, with the objective of improving the protein extraction yield during soybase production. Initially, a microstructural investigation highlighted insolubility of protein and inefficient milling as causes for a suboptimal extraction yield during the production of soybase. Ultrasound is a technology that has been studied in this thesis at lab-scale with promising extraction results; diminishing the presence of aggregated protein in the continuous phase of soybean processing materials improved the yield. Upon treatment at pilot-scale, ultrasound was less effective due to the lack of insoluble proteins within the soybean processing materials and efficient milling. High pressure homogenisation has been identified as a promising technology for scale-up based on lab-scale treatments detailed in this thesis.

## 7.5 REFERENCES

GEA Niro Soavi. (2012). *GEA Niro Soavi Homogenizers, Technical Leaflet: Ariete NS5355*. Retrieved from http://www.gea.com/global/en/binaries/Ariete_NS5355_ENG_tcm11-24532.pdf

# CHAPTER 8

# APPENDICES

## 8.1 PUBLICATION & PRESENTATIONS LIST

### 8.1.1 Journal publications

**Chapter 2**: Preece, K. E., Hooshyar, N., & Zuidam, N. J. (2016). Whole soybean protein extraction processes: A review. *Manuscript submitted for publication in Innov Food Sci Emerg Technol.*

**Chapter 3**: Preece, K. E., Drost, E., Hooshyar, N., Krijgsman, A. J., Cox, P. W., Zuidam, N. J. (2015). Confocal imaging to reveal the microstructure of soybean processing materials. *J Food Eng*, *147*, 8-13.

**Chapter 4**: Preece, K. E., Hooshyar, N., Krijgsman, A., Fryer, P. J., Zuidam, N. J. (2017). Intensified soy protein extraction by ultrasound. *Chem Eng Process*, *113*, 94-101.

**Chapter 5**: Preece, K. E., Hooshyar, N., Krijgsman, A. J., Fryer, P. J., Zuidam, N. J. (2017). Pilot-scale ultrasound-assisted extraction of protein from soybean processing materials shows it is not recommended for industrial usage. *J Food Eng*, *206*, 1-12.

**Chapter 6**: Preece, K. E., Hooshyar, N., Krijgsman, A. J., Fryer, P. J., Zuidam, N. J. (2017). Intensification of protein extraction from soybean processing materials using hydrodynamic cavitation. *Innov Food Sci Emerg Technol., 41, 47-55.*

### 8.1.2 Poster presentations

Preece, K. E., Marshman, C., Cox, P. W., Krijgsman, A. J., Zuidam, N. J. Valorisation of food processing waste streams, 10$^{th}$ Annual Formulation Conference, 2013, Birmingham, UK.

Preece, K. E., Drost, E., Hooshyar, N., Krijgsman, A. J., Cox, P. W., Zuidam, N. J. Visualisation of soybean processing materials, 12$^{th}$ International Congress on Engineering and Food (ICEF12), June 2015, Quebec City, Canada.

### 8.1.3 Oral presentations

The speaker for each presentation is highlighted in bold:

**Preece**, **K**. **E.**, Krijgsman, A. J., Hooshyar, N., Zuidam, N. J., Cox, P. W., Marshman, C. Fundamental investigation of soymilk processing materials, 11th Annual Formulation Engineering Conference, 2014, Birmingham, UK.

**Preece, K. E.,** Hooshyar, N., Marshman, C., Krijgsman, A. J., Cox, P. W., Zuidam, N. J. Intensification of protein extraction for soymilk production, 12th Annual Formulation Engineering Conference, 2015, Birmingham, UK.

**Preece, K. E.,** Hooshyar, N., Cox, P. W., Krijgsman, A. J., Zuidam, N. J. Process intensification during soymilk production, Process Intensification Network Netherlands (PIN-NL), 2015, Vlaardingen, The Netherlands.

**Preece, K. E.,** Hooshyar, N., Cox, P. W., Krijgsman, A. J., Zuidam, N. J. Intensifying soy protein extraction by ultrasound: A microstructural approach, 5th European Process Intensification Conference (EPIC5), 2015, Nice, France.

**Preece, K. E.**, Hooshyar, N., Marshman, C., Krijgsman, A. J., Fryer, P. J., Zuidam, N. J. Upscaling of soybase production with intensification by ultrasound: From lab- to pilot-scale, 1st Annual Centre For Doctoral Training (CDT) in Formulation Engineering Conference, 2016, Birmingham, UK.

## 8.2 MICROSCOPIC ANALYSIS BY CONFOCAL LASER SCANNING MICROSCOPY (CLSM)

### 8.2.1 Theory of CLSM (Dürrenberger *et al.*, 2001)

Confocal laser scanning microscopy (CLSM) is chosen over conventional wide field microscopy due to a better resolution and contrast via selection of the region of the sample from which the emitted light is collected. Figure 8.1 shows the path of the excitation and emission signals found within a confocal microscope. The excitation laser passes through a pinhole aperture, which blocks other wavelengths that are not required, and the light is deflected by a dichromatic mirror. The excitation source passes through the objective prior to focusing onto the sample on the glass slide. There are three specific focal planes which are excited by the excitation source. Only the lower focal plane is focused, therefore only the emission from this point is of interest at the photomultiplier detector. The pinhole aperture before the photomultiplier guarantees that only emission signal from the required focal plane is detected, which is a unique feature of confocal microscopy. This reduces the out of focus detection from different regions in the sample. To scan across a sample to produce an image point by point, the excitation laser beam is deflected in the x- and y-direction by a scanning unit before deflection by the dichromatic mirror.

The preparation of samples for visualisation using CLSM for this work was very easy and quick; samples only required homogenisation via shaking and stirring and addition of the fluorochrome. Thick samples can be imaged using CLSM, which was ideal for imaging of slurry and okara samples.

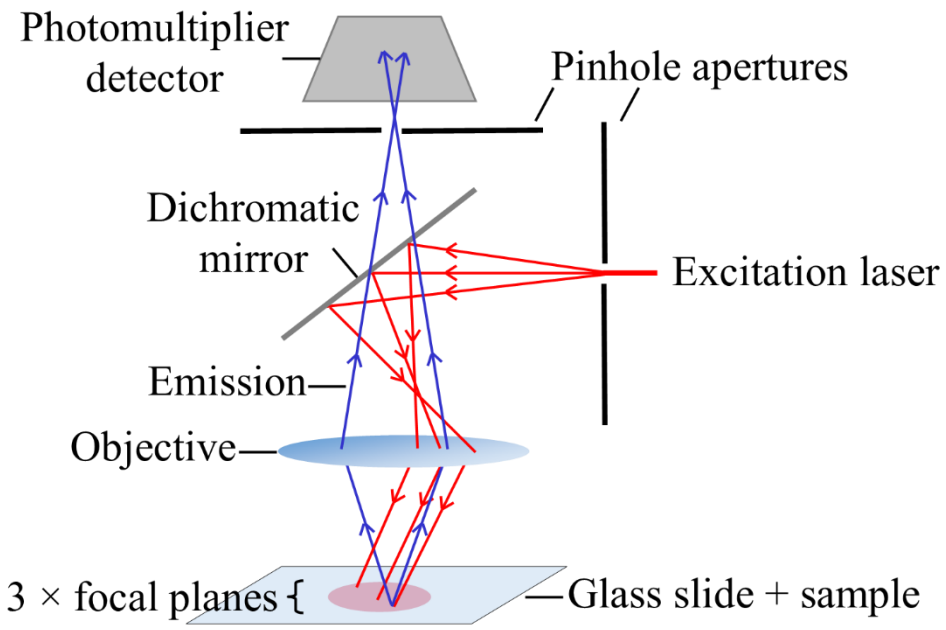


Figure 8.1. Schematic diagram of confocal laser scanning microscope.

### 8.2.2 Additional micrographs

In **chapter 3**, a series of micrographs were presented to give an overview of the structures observed in soybean processing materials. Additional micrographs were also collected and will be added here to give more insights into the structures observed in soy slurry, soybase and okara.

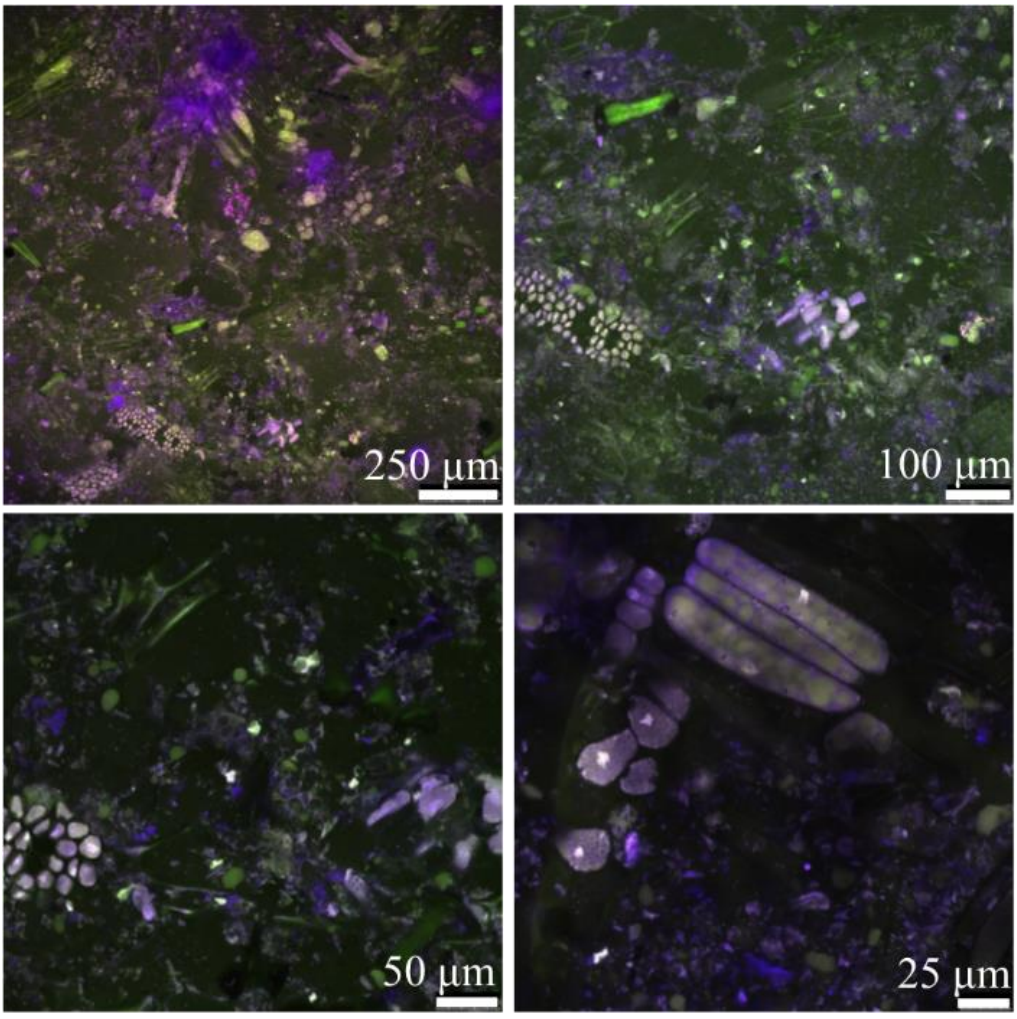


Figure 8.2. A selection of confocal laser scanning micrographs of soy slurry prepared at 80 °C, lab-scale imaged at different magnifications. The fluorochrome acridine orange was employed for visualisation.

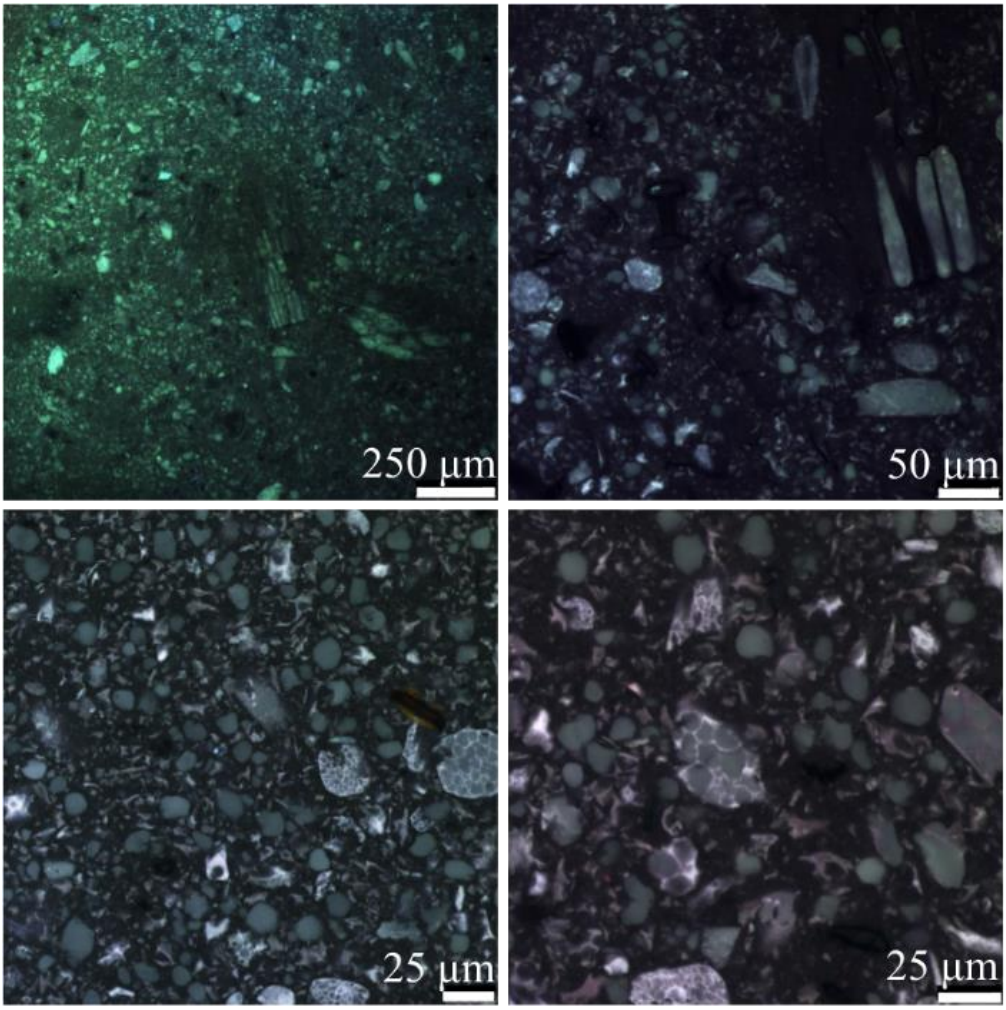


Figure 8.3. Confocal laser scanning micrographs of soy slurry prepared at 80 °C, lab-scale, visualised at various magnifications. Fluorochrome: rhodamine B.

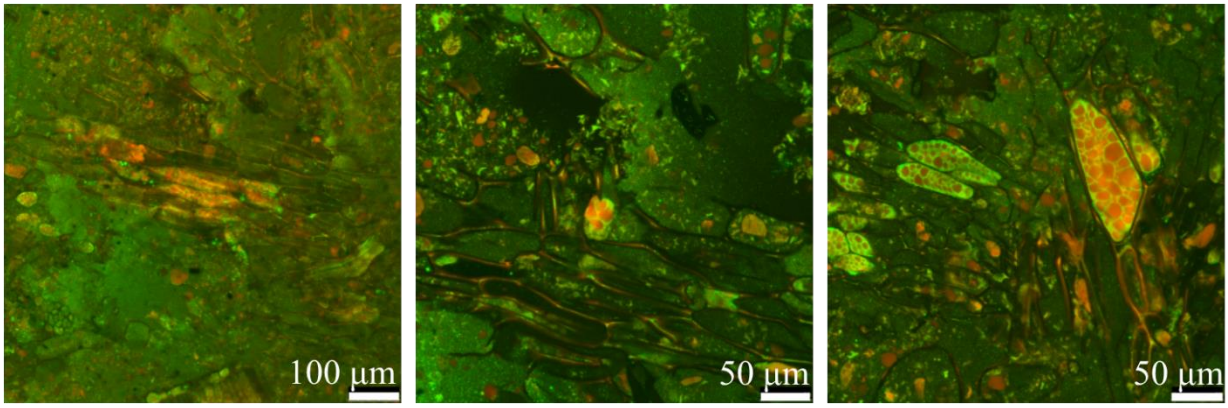


Figure 8.4. Soy slurry micrographs visualised using CLSM at various magnifications. Fluorochrome: nile blue.

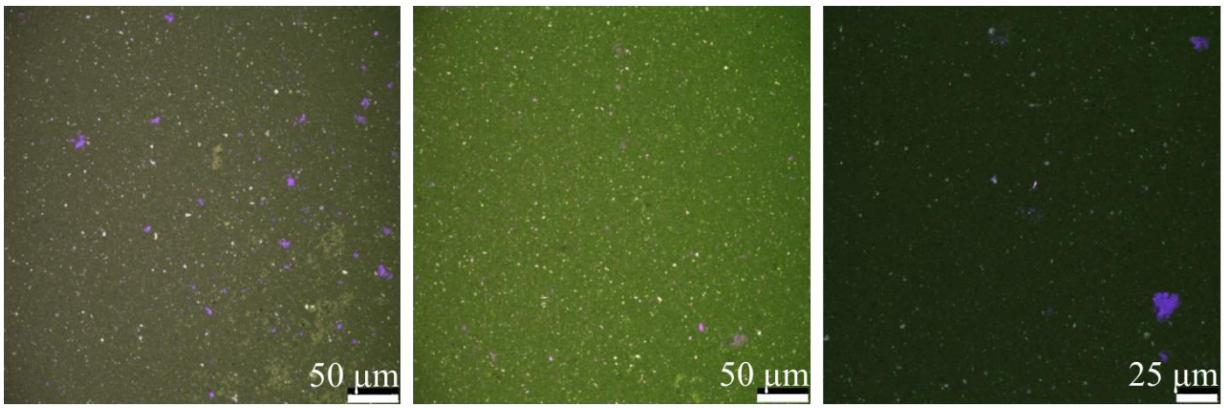


Figure 8.5. Confocal laser scanning micrographs of soybase prepared at 80 °C, lab-scale at various magnifications. Visualised with the fluorochrome acridine orange.

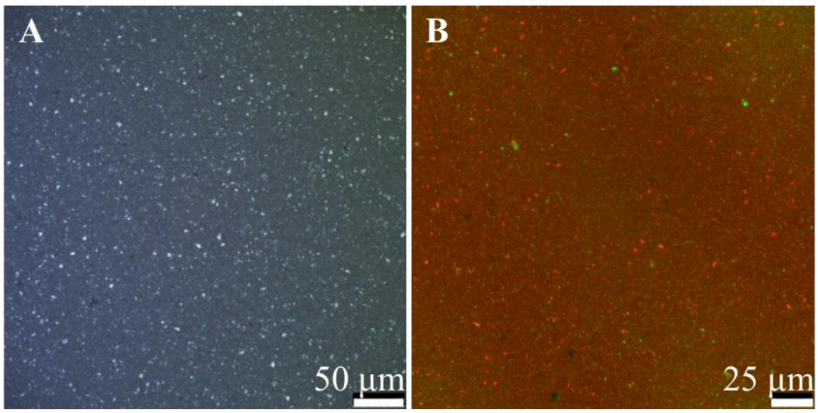


Figure 8.6. CLSM micrographs of soybase visualised using rhodamine B (A) and nile blue (A). Soybase was prepared using thermal treatment (80 °C) at lab-scale.

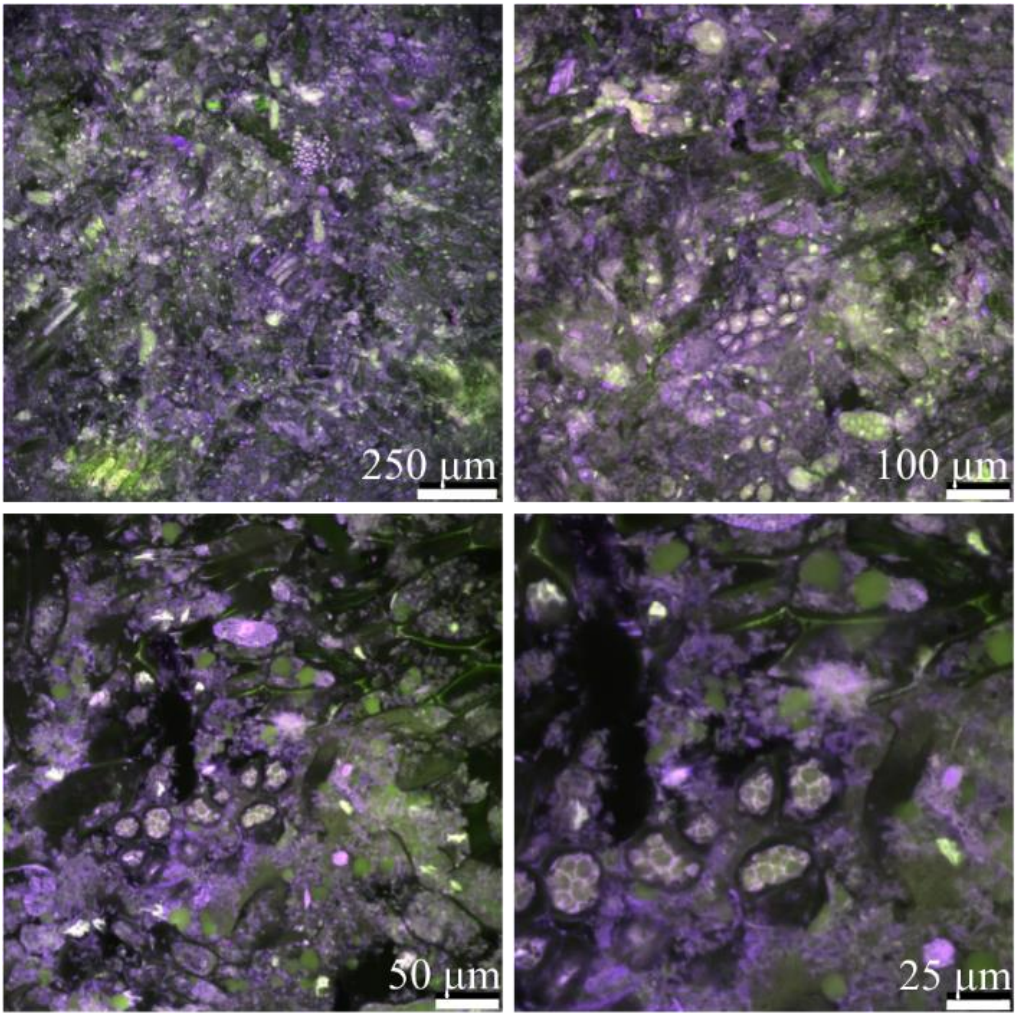


Figure 8.7. A selection of CLSM micrographs of okara visualised using acridine orange. Okara was prepared at lab-scale, at 80 °C.

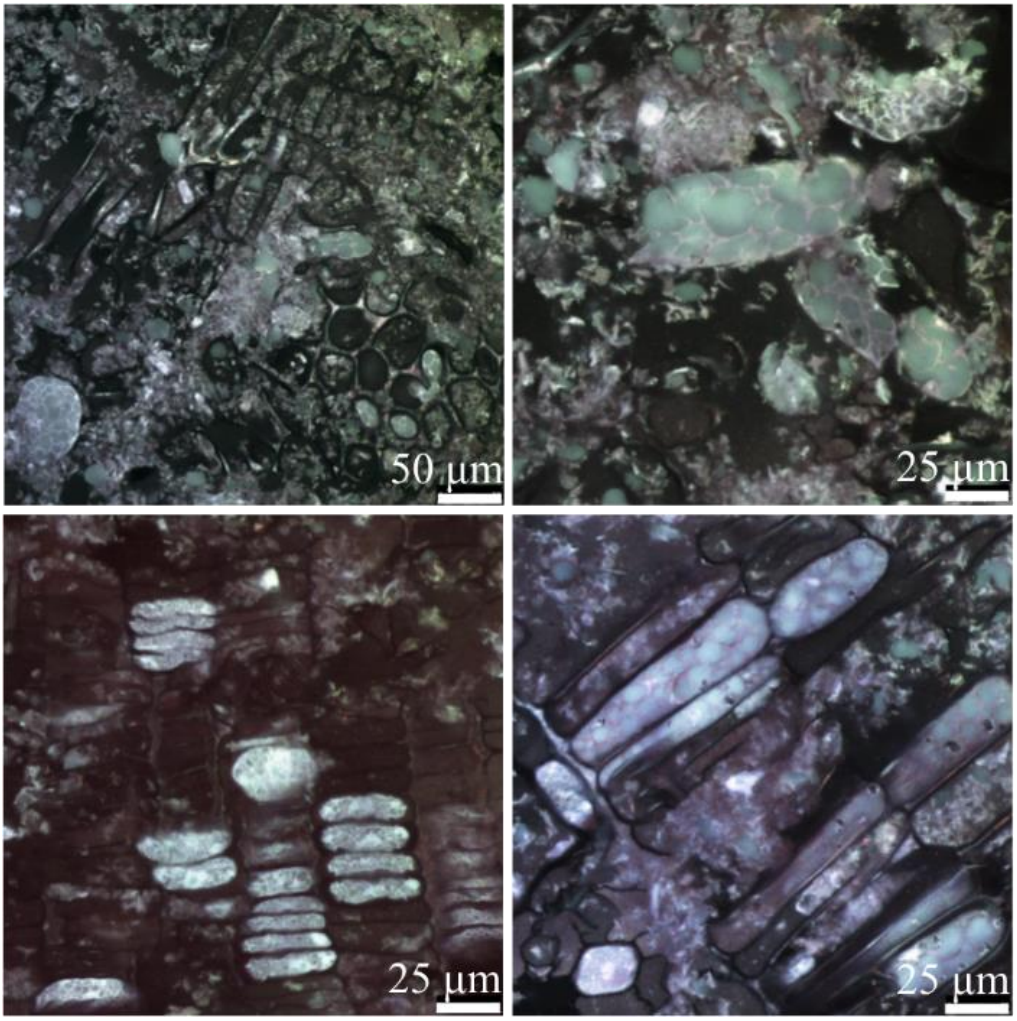


Figure 8.8. Micrographs of okara visualised using the fluorochrome rhodamine B. Sample was prepared at 80 °C, lab-scale.

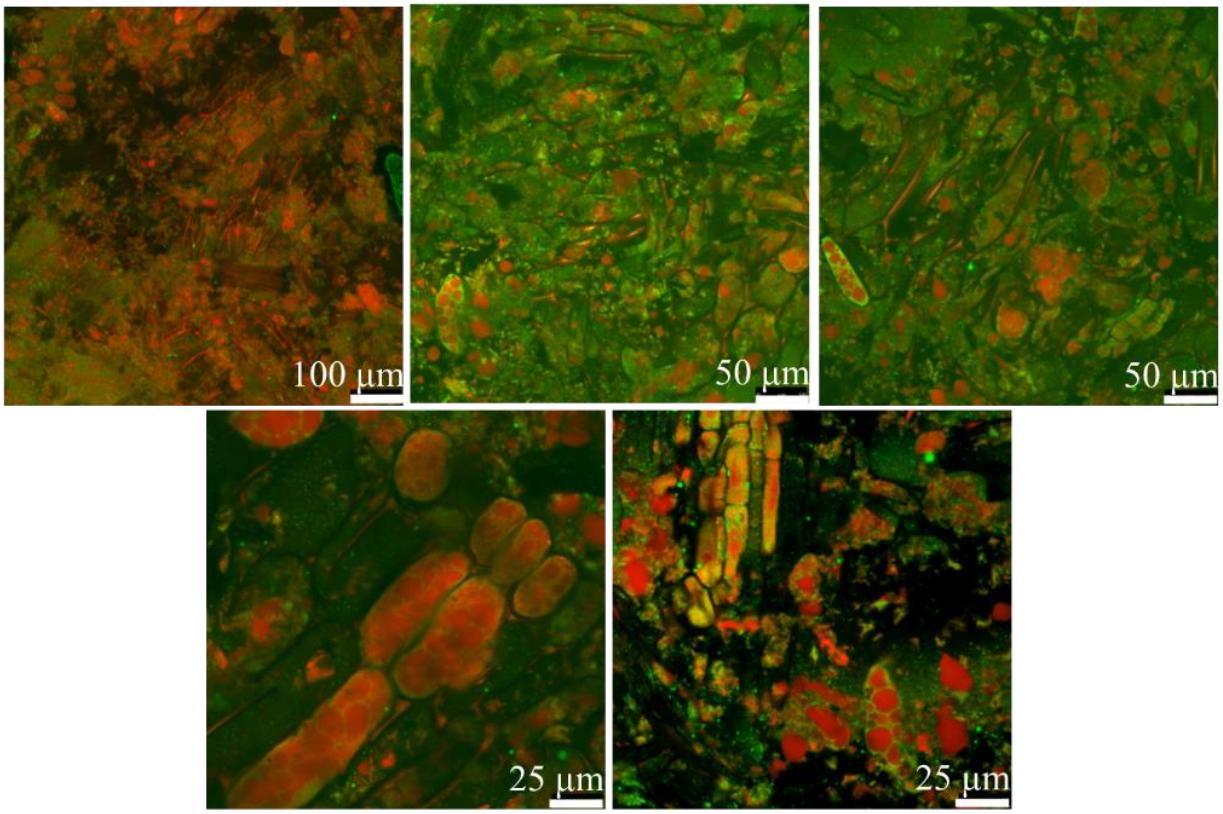


Figure 8.9. CLSM micrographs of okara visualised using nile blue. Sample prepared at lab-scale, 80 °C.

### 8.2.3 References

Dürrenberger, M. B., Handschin, S., Conde-Petit, B., Escher, F. (2001). Visualization of food structure by confocal laser scanning microscopy (CLSM). *LWT-Food Science and Technology*, *34*(1), 11-17.

## 8.3 PILOT PLANT PROCESSING EQUIPMENT

Figure 8.10 shows the set-up of the soy line at Unilever Research & Development, Vlaardingen. These facilities were utilised to prepare soy slurry, soybase and okara for experiments discussed in **chapters 5 & 6**.


Figure 8.10. A photograph of the soybase production facilities at Unilever R&D, Vlaardingen. Soybeans were introduced to the line by a bean hopper (A) before entering the milling units (B). The resultant soy slurry was fed into the decanter centrifuge (C), where fibrous materials (okara) were separated from the soybase.

An ultrasonic probe system was also utilised in the pilot plant facilities for pilot-scale sonication discussed in Section 5.2.3 of **chapter 5**. The set-up of the equipment can be seen in Figure 8.11.


Figure 8.11. A photograph of the set-up of the ultrasonic processing system within the pilot plant facilities at Unilever R&D, Vlaardingen. Okara solution was prepared at the desired temperature in a heated stirred tank (A), the solution was pumped through piping using a positive displacement pump (B), before entering the ultrasonic flow cell (C). Once the okara solution had been pumped through at the desired flow rate, the treated okara solution was collected (D) and stored for further analysis.